PB-227 021

CORRELATION BETWEEN CYCLE-BY-CYCLE CYLINDER GAS MOTION AND COMBUSTION VARIATIONS OF AN SI ENGINE

R. K. Barton

Pennsylvania State University
University Park, Pennsylvania

August 1970

DISTRIBUTED BY:

NTIS
National Technical Information Service
U. S. DEPARTMENT OF COMMERCE
5285 Port Royal Road, Springfield Va. 22151

PB 227 021

AUTOMOTIVE SAFETY RESEARCH PROGRAM

Director: W. E. Meyer
Professor of Mechanical Engineering
Head, Traffic Safety Division
Pennsylvania Transportation and Traffic Safety Center

Report No. S45

CORRELATION BETWEEN CYCLE-BY-CYCLE CYLINDER GAS MOTION AND COMBUSTION VARIATIONS OF AN SI ENGINE

by

R. K. Barton

Research Assistant in Mechanical Engineering

August 1970

The Pennsylvania State University
Department of Mechanical Engineering
University Park, Pennsylvania

Ref: PHS-NCAPC Grant AP-00560

Reproduced by
NATIONAL TECHNICAL
INFORMATION SERVICE
U S Department of Commerce
Springfield VA 22151

ia

REFERENCE: CORRELATION BETWEEN CYCLE-BY-CYCLE CYLINDER GAS MOTION AND COMBUSTION VARIATIONS OF AN SI ENGINE, by R. K. Barton; The Pennsylvania State University, Automotive Safety Research Program, Report No.S45 (1970) 136 p.

ABSTRACT: Cycle-by-cycle combustion process variations of a spark ignition engine result in cycle-by-cycle cylinder pressure development variations. Investigators have hypothesized that the combustion variations are caused by cycle-by-cycle variations of the gas motion in the vicinity of the spark plug at the time of ignition. This investigation was undertaken to determine if such a correlation does in fact exist.

The extent of cycle-by-cycle combustion variations of a single cylinder spark ignition engine were determined for specific characteristics of the cylinder pressure development histories. The extent of cycle-by-cycle gas velocity variations were determined in the vicinity of the spark plug of the motored engine using a hot film sensor.

The sample standard deviation of the cylinder velocity in the vicinity of the spark plug and the crank angle at which maximum cylinder pressure occurred were correlated for different engine operating variables. The correlation was made using a model which assumed the time required to burn approximately the first five percent of the fuel was dependent only on the velocity.

The results led to the conclusion that cycle-by-cycle combustion variations are caused by cycle-by-cycle variations of the gas velocity in the vicinity of the spark plug at the time of ignition. Additionally a quantitative measure of the phasing of the combustion process allows the effects of these velocity variations on maximum cylinder pressure to be evaluated for different engine variables.

ACKNOWLEDGEMENT: The work reported here represents the research carried out by the author for his Doctor of Philosophy degree in Mechanical Engineering.

The author wishes to acknowledge the assistance and advice of Professors S. S. Lestz and W. E. Meyer, Research Assistants P. K. Kenemuth, L. C. Duke and G. L. Winkler, all associated with the Department of Mechanical Engineering during the course of this investigation.

This investigation was made possible by U.S. Public Health Service Research Grant AP 00560, with Professors Meyer and Lestz as co-principal investigators.

KEY TERMS: Spark Ignition Engines, Cyclic Variations, Velocity Measurements

ABSTRACT

Cycle-by-cycle combustion process variations of a spark ignition engine result in cycle-by-cycle cylinder pressure development variations. Investigators have hypothesized that the combustion variations are caused by cycle-by-cycle variations of the gas motion in the vicinity of the spark plug at the time of ignition. This investigation was undertaken to determine if such a correlation does in fact exist.

The extent of cycle-by-cycle combustion variations of a single cylinder spark ignition engine were determined for specific characteristics of the cylinder pressure development histories. The extent of cycle-by-cycle gas velocity variations were determined in the vicinity of the spark plug of the motored engine using a hot film sensor.

The sample standard deviations of the cylinder velocity in the vicinity of the spark plug and the crank angle at which maximum cylinder pressure occurred were correlated for different engine operating variables. The correlation was made using a model which assumed the time required to burn approximately the first five percent of the fuel was dependent only on this velocity.

The results led to the conclusion that cycle-by-cycle combustion variations are caused by cycle-by-cycle variations of the gas velocity in the vicinity of the spark plug at the time of ignition. Additionally a quantitative measure of the phasing of the combustion process allows the effects of these velocity variations on maximum cylinder pressure to be evaluated for different engine variables.

ACKNOWLEDGEMENT

The author wishes to acknowledge the advice and encouragement of Associate Professor S. S. Lestz, his thesis advisor and co-chairman of his committee. The author also wishes to acknowledge the advice and help of Professor W. E. Meyer, Research Assistants D. K. Kenemuth, L. C. Duke, and G. L. Winkler, all associated with the Department of Mechanical Engineering.

This investigation was made possible by U.S. Public Health Service Research Grant AP00560, with Professors Meyer and Lestz as co-principal investigators.

TABLE OF CONTENTS

Chapter | Page

ACKNOWLEDGEMENT ii

LIST OF TABLES. v

LIST OF FIGURES vii

NOMENCLATURE. ix

1 INTRODUCTION. 1

1.1 General Statement of the Problem 1
1.2 Relevance of the Problem 2
1.2.1 Engine Surge. 2
1.2.2 Knocking Combustion 3
1.2.3 C.B.C. Exhaust Emission Variations. 4
1.3 Specific Thesis Objectives 4

2 PREVIOUS INVESTIGATIONS OF C.B.C. VARIATIONS. 6

2.1 Combustion Process Variations. 6
2.1.1 Physical Manifestations 6
2.1.2 Statistics of Variations. 8
2.1.3 Extent of Variations. 10
2.2 Effect of Engine Variables on C.B.C. Variations. . . 10
2.3 Effect of Engine Modifications on C.B.C. Variations 17
2.3.1 Possible Causes of C.B.C. Variations. 17
2.3.2 Direct Effects on C.B.C. Variations 19
2.4 Measurements of C.B.C. Gas Motion Variations . . . 20
2.5 Effect of Mixture Motion on Flame Front Speed. . . 21
2.6 Literature Summary 23

3 EXPERIMENTAL EQUIPMENT AND INSTRUMENTATION. 25

3.1 Combustion Equipment 25
3.1.1 Combustion Chamber. 25
3.1.2 Air-Fuel System 29
3.1.3 Ignition System 29
3.1.4 Dynamometer 32
3.1.5 Exhaust Gas Measurements. 32
3.2 Combustion Instrumentation 32
3.2.1 Pressure Transducer 33
3.2.2 Pressure Development Analog Signals 33
3.2.3 Timing Mark Analog Signal 35
3.3 Gas Motion Measurements. 35
3.3.1 Sensor Description. 38
3.3.2 Anemometer System 38
3.3.3 Sensor Calibration. 40
3.3.4 Cylinder Air Temperature and Pressure 47

TABLE OF CONTENTS (Continued)

Chapter Page

3 3.4 Data Collection and Analysis. 48
3.4.1 Real Time Data Acquisition System. 48
3.4.2 Data Analysis. 49
3.4.2.1 Combustion Data 50
3.4.2.2 Velocity Data 51
3.5 Experimental Procedure. 56

4 PRELIMINARY EXPERIMENTAL RESULTS 61

4.1 Experimental Accuracy 61
4.1.1 Absolute Measurements. 61
4.1.2 Repeatability of Experiments 63
4.1.3 C.B.C. Variations of Engine Variables. . . . 66
4.1.4 Frequency Distribution Characteristics . . . 67
4.1.5 Sampling Interval Effects. 71
4.1.6 Sample Size Effects. 72
4.2 Pressure Development Characteristics. 73
4.3 Gas Motion Characteristics. 78

5 EMPIRICAL MODELS USED TO CORRELATE CAUSE AND EFFECT OF C.B.C. VARIATIONS. 84

5.1 Model Relating C.B.C. Initial Burn Duration and Velocity Variations 84
5.2 Maximum Pressure and Torque C.B.C. Variations . . . 94

6 DISCUSSION OF RESULTS. 97

6.1 Spark Advance Effects 97
6.2 Air-Fuel Ratio Effects. 98
6.3 Speed Effects 99
6.4 Compression Ratio Effects 100
6.5 Relevance of the Results. 101

7 SUMMARY AND CONCLUSIONS. 102

7.1 Restatement of the Problem. 102
7.2 Conclusions 102
7.3 Recommendations for Future Work 103

REFERENCES 105

APPENDIX A - STATISTICAL DEFINITIONS 108
B - EQUATIONS USED TO CALCULATE VELOCITY. . . . 112
C - COMBUSTION DATA 115
D - VELOCITY DATA 121

LIST OF TABLES

Table Page

2.1 Combustion Variables and Statistics Used by Investigators of C.B.C. Variations. 7

2.2 Extent of C.B.C. Variation Found by the Investigators Listed in Table 2.1 14

2.3 Range of Engine Variables Used by Investigators of C.B.C. Variations. 15

2.4 Effects of Engine Modifications on C.B.C. Variations. . . . 18

3.1 Combustion Chamber Dimensions 26

3.2 Dimensions and Timing of Intake and Exhaust Valves. 26

3.3 Range of Variables Used for Sensor Calibration. 45

3.4 Calibration Constants Used in King's Law. 47

3.5 Sampling Rates and Voltage Resolution of Analog to Digital Data Acquisition System 49

3.6 Resolution of Parameters Digitized by Analog to Digital Data Acquisition System 49

3.7 Engine Variables Used to Construct Model Relating Motored Velocity Data to Combustion Data. 57

3.8 Engine Variables Used to Test Model Constructed from Engine Variables in Table 3.7 58

4.1 Accuracy of Engine Variables and Measured Combustion and Gas Motion Variables. 62

4.2 Repeatability of Similar Engine Operating Conditions. . . . 65

4.3 Coefficients of Skewness and Kurtosis for P_{max}. 68

6.1 Effect of Spark Advance on C.B.C. Variations. 97

6.2 Effect of Air-Fuel Ratio on C.B.C. Variations. 98

6.3 Effect of Speed on C.B.C. Variations. 99

6.4 Effect of Compression Ratio on C.B.C. Variations. 100

C.1 Combustion Data-Average Values of Pressure Development. . . 116

C.2 Combustion Data - Sample Standard Deviations of Pressure Development 118

LIST OF TABLES (Continued)

Table | Page

C.3 Combustion Data - Correlation Coefficients of Pressure Development 120

D.1 Velocity Data - Averages and Sample Standard Deviations . . 122

LIST OF FIGURES

Figure Page

2.1 Cylinder pressure of four selected engine cycles for steady state engine operating conditions. (After Troutman and Lestz [10]). 11

2.2 Rate of cylinder pressure change of four selected cycles for steady state operating conditions. (After Troutman and Lestz [10]) 12

2.3 Calculated cumulative energy release of four selected cycles for steady state operating conditions. (After Troutman and Lestz [10]). 13

3.1 CFR engine cross section through intake and exhaust valve center lines. 27

3.2 CFR engine cross section through center lines of spark plug and pressure transducer. 28

3.3 Intake valve lift as a function of crank angle. 30

3.4 Schematic of engine instrumentation 31

3.5 Schematic of analog circuit used to provide voltage signals proportional to cylinder rate of pressure change and pressure. 34

3.6 Schematic of analog circuit used to provide a timing mark which indicates tdc of compression stroke 36

3.7 Combustion signals recorded by analog to digital data acquisition system. (After Kenemuth and Lestz [5]) . . . 37

3.8 Schematic of TSI Model 1125 calibrator used to calibrate velocity sensor 43

3.9 Sensor calibration results for determining constant, C_1, in King's law at zero Reynold s number. 44

3.10 Sensor calibration results used to determine the constants C_2 and n in King's law. 46

3.11 Anemometer bridge voltage digitized and reproduced as an analog signal by PDP-9 computer 52

3.12 Cylinder pressure of motored engine digitized and reproduced as an analog signal by PDP-9 computer. 53

3.13 Cylinder volume calculated from timing mark and reproduced as an analog signal by PDP-9 computer. 54

LIST OF FIGURES (Continued)

Figure Page

3.14 Calculated cylinder air temperature and reproduced as an analog signal by PDP-9 computer. 55

3.15 Sensor location in combustion chamber where air velocity was measured 60

4.1 Average velocity of 30 engine cycles for two sensor temperatures 64

4.2 Cumulative frequency distribution of maximum cylinder pressure plotted on normal probability coordinates 69

4.3 Auto correlation of maximum cylinder pressure as a function of cycle difference 70

4.4 Average maximum cylinder pressure as a function of its average crank angle of occurrence produced by different spark advances 74

4.5 Correlation between estimated values of $S(P_{max})$ and experimentally determined values of $S(P_{max})$. 75

4.6 Spark advances which produced changes in the average values of the crank angle at which maximum pressure occurred 77

4.7 Velocity for one revolution of the crank 79

4.8 Conceptual schematic of velocity pattern in the combustion chamber after intake valve closure 80

4.9 Correlation between the velocity at crank angles corresponding to ignition and the velocity occurring $\Delta\theta$ degrees after ignition 82

5.1 Flame front position after ignition used to divide cylinder volume into burned and unburned regions 85

5.2 Experimental results used to confirm model relating C.B.C initial burn duration variations to C.B.C. velocity variations at crank angles corresponding to ignition . . . 92

5.3 Experimental results used to test model. 93

NOMENCLATURE

Symbol	Description of Engine Nomenclature	Units
A/F	Air-fuel ratio	-
atdc	After top dead center	-
BDC, bdc	Bottom dead center	-
btdc	Before top dead center	-
C.B.C.	Cycle-by-cycle	-
CR	Compression ratio	-
D	Cylinder bore	in.
L	Connecting rod length	in.
MBT	Maximum brake torque spark advance	-
MV	Manifold vacuum	in. Hg
rpm	Crank speed	rev/min
s	Stroke	in.
SA	Spark advance	deg
T_d	Dynamometer scale torque	ft-lbf
TDC, tdc	Top dead center	-
	Description of Statistical Nomenclature	
CA(x,K)	Sample auto correlation as a function of K for the variable x	-
CC(x,y)	Sample cross correlation of the variables x and y	-
CK(x)	Sample coefficient of kurtosis for the variable x	-
CS(x)	Sample coefficient of skewness for the variable x	-
CV(x)	Sample coefficient of variation for the variable x	-
$\overline{D}(x)$	Sample mean deviation of the variable x	x

NOMENCLATURE (Continued)

Symbol		Units
$IV(x)$	Sample index of variation for the variable x	-
N	Number of samples	-
$Pr(x_1<x<x_2)$	Probability that x is between x_1 and x_2	-
$PR(x)$	Sample percentile range of the variable x	-
$S^2(x)$	Sample variance of the variable x	x^2
$S(x)$	Sample standard deviation of the variable x	x
$SR(x)$	Sample range of the variable x	x
x,y	Arbitrary sample variables	-
$\overline{x}$	Sample mean of the variable x	x
σ	Standard deviation of a known frequency distribution	-
μ	Average of a known frequency distribution	-

Description of General Nomenclature

A	Area	ft^2
b'	Sensitivity of maximum pressure variations to initial burn duration variations	psi/deg
C_1,C_2	Constants in King's Law	-
C_3,C_4,C_5	Constants	-
$D\theta$	Crank angle resolution of analog to digital data acquisition system	deg
d_s	Velocity sensor's diameter	ft
E	Expansion ratio = $T_b M_u / T_u M_b$	-
$F(O.V.)$	Function of the operating variables $F(O.V.) = \frac{h(A/F)}{\rho_{ic}^{0.4}\ A/F^{0.33}}$	-

NOMENCLATURE (Continued)

Symbol		Units
$f(U)$	Increase in burning velocity due to velocity U	-
$g(U)$	Function of the velocity, U	1/sec
$h(A/F)$	Function of air-fuel ratio $h(A/F) = 16.25 - 0.22(A/F - 14.35)^2$	-
imep	Indicated mean effective pressure	psi
K	Cycle difference	-
k	Thermal conductivity	btu/hr-ft-F
M	Molecular weight	lbm/lb-mole
m	Mass	lbm
m_{in}	Mass ingested per cycle	lbm
NS	Number of samples between timing marks	-
n	Exponent in King's law	-
P	Cylinder pressure	psi
$\dot{P}$	Cylinder rate of pressure change	psi/sec
$\dot{Q}$	Rate of heat release	btu/deg
Q_{rel}	Cumulative heat release	btu
Q_s	Sensor heat loss	watt
Q_t	Total heat release per cycle	btu
R	Gas constant of air	lbf-ft/lbm-R
Re	Reynold's number	-
R_s	Velocity sensor's resistance	ohm
r	Radius	ft
S_b	Laminar burning velocity	ft/sec
SFP	Pressure scale factor	psi/volt
$s_{T_d}(P_{max})$	Sensitivity of torque to P_{max} variations	ft-lbf/psi

NOMENCLATURE (Continued)

Symbol		Units
$s_{T_d}(\theta(P_{max}))$	Sensitivity of torque to $\theta(P_{max})$ variations	ft-lbf/deg
T	Temperature	F,R
T_d	Dynamometer absorption torque	ft-lbf
t	Time	sec
t_b	Initial burn duration	sec
U	Velocity	ft/sec
U_f	Flame front velocity	ft/sec
V	Volume	ft^3
V_B	Bridge voltage	volt
VD	Piston displacement volume	ft^3
v	Analog pressure voltage	volt
α_o	Temperature coefficient of resistance at 32F	ohm/F
$\Delta\theta$	Crank angle difference between ignition and velocity measurement	deg
μ	Dynamic viscosity	lbm/ft-sec
ρ	Density	lbm/ft^3
θ	Crank angle	deg, rad

Subscripts

a	Air
b	Burned gases
ec	Conditions when exhaust valve closes
eo	Conditions when exhaust valve opens
i	Conditions at ignition
ic	Conditions when intake valve closes
io	Conditions when intake valve opens

NOMENCLATURE (Continued)

m	Mean
max	Maximum value in a cycle
md	Intake manifold
r	Relative value of burned gases to unburned gases at ignition
s	Velocity sensor
u	Unburned gases

Chapter 1

INTRODUCTION

1.1 General Statement of the Problem

The combustion process in a spark ignition (SI) internal combustion (IC) engine exhibits cycle-by-cycle (C.B.C) variations. These C.B.C. variations exist under apparent invariant engine operating variables such as spark timing and air-fuel ratio. Physical manifestations of the combustion process variations have been observed in the cylinder pressure development histories (1-14)[a], experimentally measured flame speeds (2,8,12), computed rates of heat release (9,11,14), and indicated mean effective pressures (9,14). Herein, the combustion variations are defined in terms of the variations from cycle to cycle of the pressure development histories.

The C.B.C. pressure development variations are a result of variations in the combustion process. The extent of C.B.C. pressure variations is thus influenced by engine operating variables such as spark advance and compression ratio because these variables also influence the combustion process. The problem is to delineate the pressure development variations so that specific characteristics can be identified and related to the combustion process.

In the past, the effects of combustion process variations on engine performance were circumvented by judicious engine design and choice of operating variables. These practices resulted in increased brake torque and qualitative measures of engine performance such as vehicle "surge" or driveability were thus improved. Presently, automotive exhaust emissions must be lower than federal standards. The past design practices which resulted in increased brake torque and improved driveability are not compatiable with lower emission levels. Sacrifices in driveability may be necessary to meet federal exhaust emission standards. Hence there is a need for a better understanding of the combustion process, a part of which is understanding the C.B.C. combustion process variations. Improved understanding of the cause of the combustion process variations could lead to their reduction and thereby substantially benefit present day engine designers in meeting both performance criteria as well as exhaust emission standards.

---

[a] Numbers refer to entries in Reference list.

1.2 Revelance of the Problem

The increased attention in meeting federal exhaust emission standards has resulted in engines which are operated at conditions other than maximum torque. This "detuning" of engines could results in decreased driveability. Three areas in which controlling the cause of C.B.C. combustion variations could reduce exhaust emissions and improve engine performance are:

1. Engine surge,
2. Knocking combustion,
3. Cycle-by-cycle exhaust variations.

1.2.1 - Engine Surge - The brake torque of an engine is increased by increasing the compression ratio and operating with an air-fuel ratio richer than the stoichiometric air-fuel ratio. However, increasing the compression ratio results in increased levels of unburned hydrocarbons and nitric oxides in the exhaust gas. Operation with a fuel rich mixture results in levels of carbon monoxide and unburned hydrocarbons which are greater than fuel lean mixture operation.

In meeting the exhaust emission standards, lower compression ratios and leaner air fuel mixtures are used than those which produce higher brake torques. The effect of these modifications made to meet emission standards is to increase engine surge or torque variations relative to the average torque. In order to reduce this surge, C.B.C. combustion process variations must be reduced. In addition, extremely lean mixtures, which further reduce nitric oxide emissions, have been avoided because of increased C.B.C. variations to the point of occasional misfires. Reduction of the variations would permit examination of emission levels for extremely lean mixtures without significantly sacrificing engine performance.

1.2.2 - Knocking Combustion - The C.B.C. combustion variations cause extremes which must be avoided to prevent engine knock (2,8,12). The detrimental effects of knock dictate engine design and fuel requirements that eliminate knock when extreme but infrequent combustion process variations exist. Lead additives help to reduce knock under these extreme conditions (12). However current practice has limited and might eventually eliminate the use of lead as a fuel additive. Lead additives hinder efforts to reduce exhaust emissions and represent a pollution health hazard. Engine design and fuel requirements must be effected so as to reduce engine knock potential. Both a lowering of compression ratio, and higher natural "octane" ratings through petroleum refining will be required. These modifications will result in slight sacrifices of engine performance. Reducing C.B.C. combustion process variations could lead to less stringent fuel and design requirements if the extreme variations could be reduced.

1.2.3 - C.B.C. Exhaust Emission Variations - It has been hypothesized that elimination of combustion irregularities could result in a 20 percent reduction of nitric oxide emissions (3). Additionally it has been shown that the C.B.C. combustion process variations produce C.B.C. variations in the exhaust emissions (10). Thus stabilizing the combustion process to produce minimum exhaust emissions would satisfy engine performance and emission reduction criteria.

1.3 Specific Thesis Objectives

In the past, investigators (1-14) have examined the combustion variations for different operating conditions and engine component configurations. Some of these investigators (1,3,7) have hypothesized that the principal cause of the combustion variations is the C.B.C. variations in the cylinder gas motion. However, no quantitative measurements of C.B.C. cylinder gas motion variations have been related to the C.B.C. combustion process variations.

The hypothesis of this work is that the gas motion variations from cycle to cycle are the principal cause of C.B.C. combustion process variations. It is also hypothesized that specific characteristics of the gas motion can be identified and related to the combustion process variations.

An experimental program consisting of velocity measurements ahead of the intake valve and in the cylinder of a motored CFR engine was developed to test the validity of the hypothesis. Also statistical measurements of various combustion parameters, which reflect the C.B.C. combustion process variations, were made to determine their extent.

Specifically, then, the objective of this work is to determine if and how the C.B.C. gas motion variations are related to the C.B.C. combustion process variations. This objective will be accomplished by:

1. Identifying a physical manifestation of the combustion process whose C.B.C. variations are dependent primarily on C.B.C. variations of the gas motion.
2. Developing statistical measures of the C.B.C. variations in the gas motion and the combustion process.
3. Determining which gas motion characteristics are the principal cause of combustion variations.
4. Developing a model which allows gas motion variations under motoring conditions to be related to the variations of combustion process characteristic.
5. Developing a means of relating the effects of engine operating variables on the C.B.C. combustion process variations.

Chapter 2

PREVIOUS INVESTIGATIONS OF C.B.C. VARIATIONS

The literature concerning C.B.C. combustion variations in SI engines is not exhaustive in that particular aspects of the problem have been studied independently. No direct relationship between the cause of C.B.C. combustion variations and C.B.C. pressure variations has been established. Also the interrelationships between the variations of various parameters of the combustion process have not been established. For this reason, the literature is used here to establish and provide the following:

1. The statistical parameters which best describe C.B.C. combustion variations,
2. Those characteristics of the combustion process variations which might be indicative of cause and effect,
3. Identification of possible causes which have been shown not to affect the variations.

The literature is discussed relative to the above points.

2.1 Combustion Process Variations

2.1.1 - Physical Manifestations - The measurable and calculated quantities which are physical manifestation of the combustion process exhibit C.B.C. variations. The physical manifestations used by previous investigators are summarized in Table 2.1.

The first five variables were experimentally measured while the last three were calculated from experimental measurements. All eight variables exhibit C.B.C. variations.

Table 2.1

Combustion Variables and Statistics Used by Investigators of C.B.C. Variations

	Combustion Variable							
Investigator	P_{max}	$\dot{P}_{max}$	$\theta(P_{max})$	$\theta(\dot{P}_{max})$	U_f	Q_t	$\dot{Q}_{max}$	imep
Averette (1)	$\overline{D}$[1]							
Harrow (2)					PR			
Karim (3)	CV							
Barton (4) and Kenemuth (5)	S	S	S	S				
Land (6)	IV							
Patterson (7)	PR	PR						
Curry (8)					PR			
Soltau (9)	CV					SR	SR	CV
Troutman (10)	SR	SR	SR	SR		SR	SR	
Vichnievsky (11)	S							
Warren (12)					PR			
Stivender (13)	SR							
Peters (14)	SR					SR		

[1] See Appendix A for definition of the statistics, $\overline{D}$, mean deviation, PR, percentile range, CV, coefficient of variation, S, standard deviation, IV, index of variation, and SR, sample range.

The maximum cylinder pressure (P_{max}) was chosen by most investigators to determine the extent of C.B.C. combustion variation. The maximum pressure was chosen for two reasons; 1) ease of measurement and 2) P_{max} is very sensitive to C.B.C. combustion variations. The same is true of the maximum rate of pressure change ($\dot{P}_{max}$). The disadvantage of using only P_{max} or $\dot{P}_{max}$ is that it depends on the entire combustion process up to its occurrence. Thus P_{max} and $\dot{P}_{max}$ do not provide specific information of the combustion process variations.

The calculated quantities such as the cumulative heat release or rate of heat release also depend on the entire combustion process. They do indicate the cycle to cycle variations in the fuel consumed and the rate at which the fuel is consumed (10).

Calculated imep of each cycle permits a quantitative evaluation of the effects of C.B.C. combustions variations on engine brake torque variations (9). The imep allows one to determine the importance of C.B.C. variations relative to engine output variations.

The combustion process characteristics which seem to be closely associated with the cause are flame front speed (2,8,12) and the crank angles of occurrence of P_{max} and $\dot{P}_{max}$ (4). Although flame front speeds and their extent of variation have been experimentally determined (2,12), their relationship to the cause or to cylinder pressure variations has not been related to maximum pressure variations (4) but their relationship to a specific combustion process characteristic has not been established.

2.1.2 - Statistics of Variations - There exist numerous possible statistical measures of the C.B.C. variations. The statistical measures used in previous investigations are summarized in Table 2.1.

The definitions of the measures of dispersion are found in Appendix A.

The six statistical measures used to indicate the extent of C.B.C. variations were useful depending on the investigators purpose. The coefficient of variation was useful to indicate the deviations of imep relative to the average imep (9) as it allows one to judge the overall effect of C.B.C. combustion variations. When the coefficient of variation of P_{max} of $\dot{P}_{max}$ is used with respect to effects of engine variable changes, it is difficult to separate dispersion changes from changes in the average.

The index of variation is only a measure of dispersion in the case of a normal frequency distribution. It also is a measure of departures from a normal frequency distribution. Small changes in the index of variation could be attributed to either changes in the dispersion or shape of the frequency distribution. Thus the index of variation is not suitable to measure the extent of C.B.C. combustion variations.

The sample variance, sample range and percentile range indicate the extent of C.B.C. dispersion. However, only the sample variance or standard deviation is commonly used as a statistical measure of dispersion. For these reasons it appears that the sample standard deviation is the most suitable indication of C.B.C. variations.

The sample size used by the investigators listed in Table 2.1 varied from 12 engine cycles to over 2000 engine cycles. Statistical tests of significance were not used except by Barton (4) and Kenemuth (5). The other investigators used their judgement in determining what was or was not significant.

2.1.3 - Extent of Variations - The extent of C.B.C. combustion variations are illustrated by four cycles of a sample population. The cylinder pressure histories in terms of pressure versus crank angle and rate of pressure change versus crank angle are shown in Figs. 2.1 and 2.2. Each cycle corresponds to maximum rates of pressure change of 11.0, 15.9, 19.2 and 22.8 psi/deg.

Calculated values of the cumulative heat release versus crank angle, for the same cycles, are shown in Fig. 2.3. The data are taken from Troutman (10) who used the same CFR engine as was used for the present experimental program. The figures illustrate the interrelationship of three manifestations of the combustion process as well as the extent of C.B.C. dispersion of each. The largest dispersion occurs in the maximum values of the pressure and rate of pressure (1,4,5,7,9). The total heat released for each cycle does not exhibit a large C.B.C. dispersion (9,10,14). The crank angles at which P_{max} occur also vary from cycle to cycle (4,5). The interrelationships between the variables are apparent, that is, high values of $\dot{P}_{max}$ are associated with high values of P_{max} (4,5).

Numerical values for the extent of dispersion found by the investigators listed in Table 2.1 are shown in Table 2.2.

2.2 Effect of Engine Variables on C.B.C. Variations

Engine variables are defined as those engine operating variables which can be changed without engine component modification. Examples of engine variables are air-fuel ratio, type of fuel, compression ratio, speed, water jacket temperatures, etc. Table 2.3 presents the range of engine variables used in other studies of C.B.C.

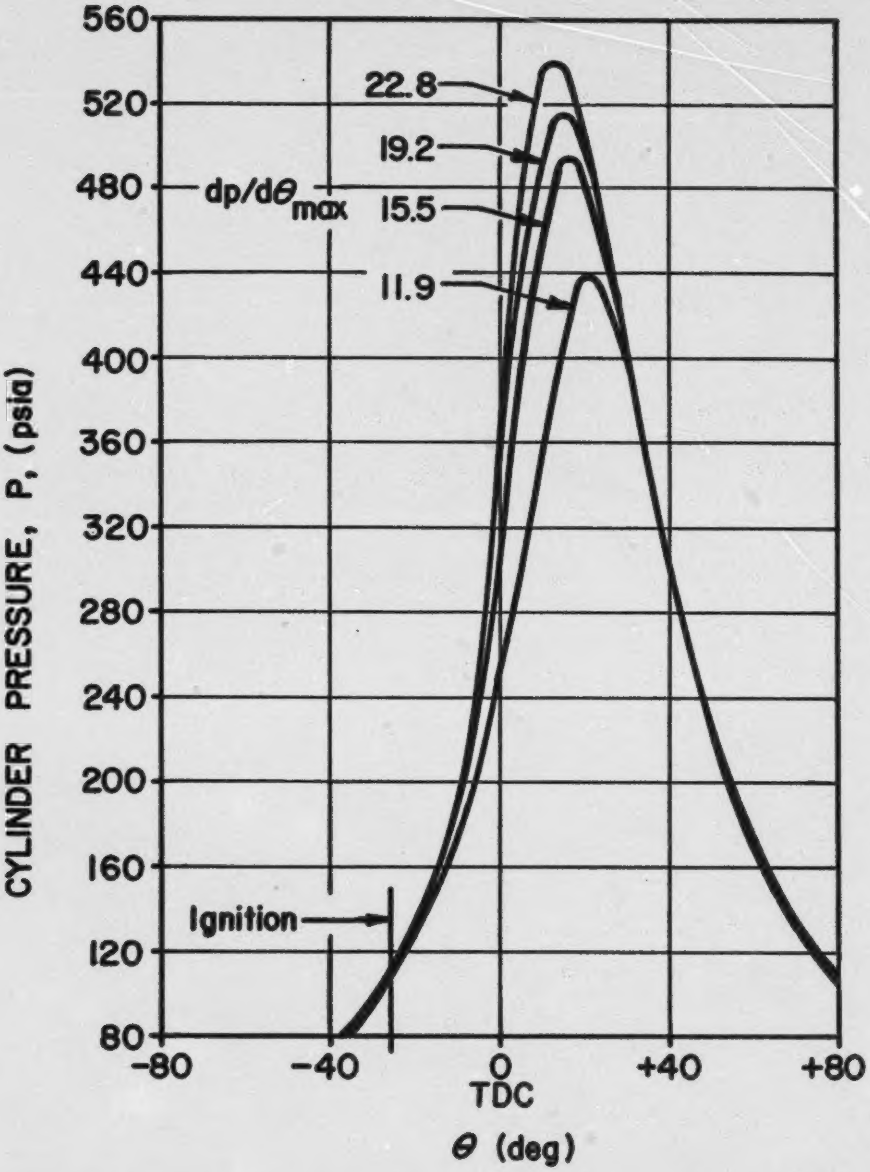

Figure 2.1. Cylinder pressure of four selected engine cycles for steady state engine operating conditions. (After Troutman and Lestz [10])

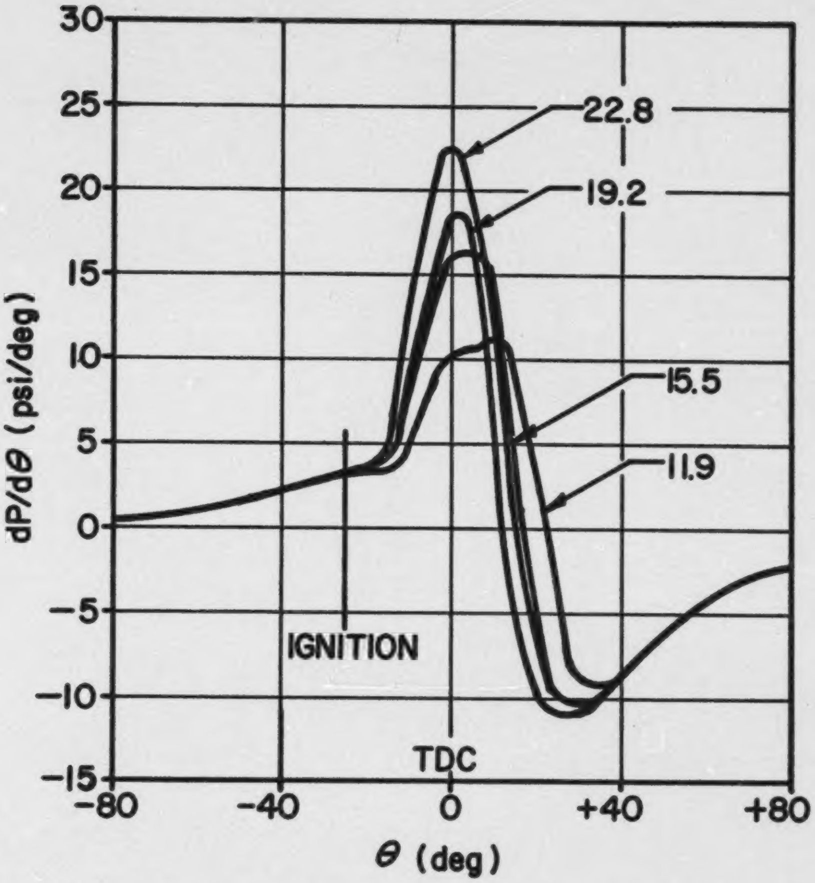

Figure 2.2. Rate of cylinder pressure change of four selected cycles for steady state operating conditions. (After Troutman and Lestz [10])

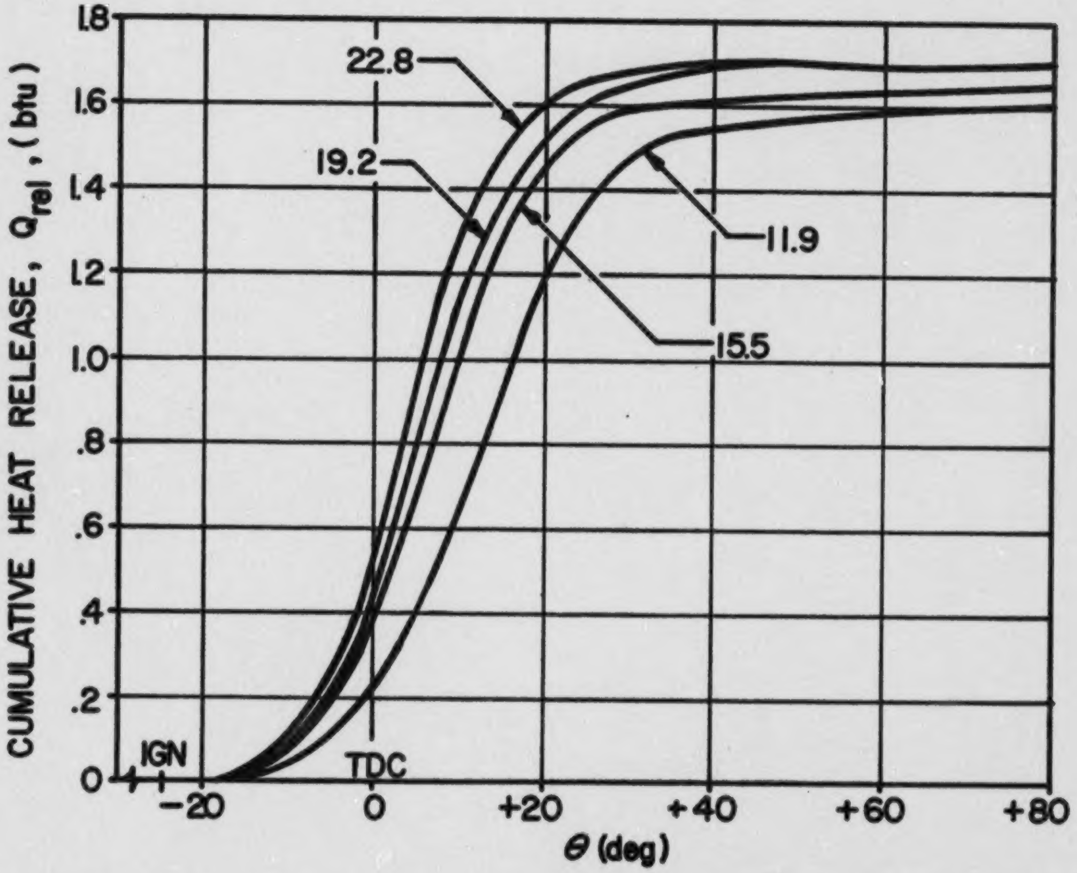

Figure 2.3. Calculated cumulative energy release of four selected cycles for steady state operating conditions. (After Troutman and Lestz [10])

Table 2.2.

Extent of C.B.C. Variations Found by the Investigators Listed in Table 2.1

Statistic	Range of Numerical Values
$S(P_{max})$	30-80 psi
$S(\dot{P}_{max})$	3-9 psi/deg
$S(\theta(P_{max}))$	3-10 degs
$S(\theta(\dot{P}_{max}))$	5-15 degs
$SR(\dot{Q}_{max})$	0.6-0.8 btu/deg
$CV(U_f)$	5%-20%
CV(imep)	1%-22%

Table 2.3

Range of Engine Variables used by Investigators of C.B.C. Variations

	Engine Variables						
Investigator	CR	A/F	rpm	Spark Timing	Fuel	Throttle	Water Jacket Temperature
Averette (1)	6.0	16.60	1200	15° btdc	-	66%-100%	170F
Harrow (2)	6.0	10-16	750-2500	15-25° btdc	Isooctane Di-isobutylene Benzene	100%	80C
Karim (3)	6.5-9.5	7-19	2000-3000	10-70° btdc	Isooctane	25%-100%	40-80C
Barton (4) and Kenemuth (5)	7.0-10.5	13-18	900-1800	MBT	Isooctane	100%	180F
Land (6)	-	15-18	-	-	Natural gas	-	-
Patterson (7)	10.0	10-20	1200-1400	MBT ± 5°	Idolene Propane	25%-100%	-
Curry (8)	9.0-10.5	12-14	1000-1200	15-20° btdc	Isooctane plus TEL	100%	212F
Soltau (9)	6.0-12.0	10-18	2000-4000	16-45° btdc	Petrol, Benzene Methanol, Methane Butane	100%	-
Troutman (10)	7.0	15.1	900	MBT	Isooctane	100%	180F
Vichnievsky (11)	4.0-7.0	13-20	900-3000	25-40° btdc	Isooctane, Benzene Heptane	-	-
Warren (12)	9.5	8-17	1200	40° btdc to 5° atdc	Isooctane plus 6.ml TEL per gal.	100%	-
Stivender (13)	10.0	20.2	1440	-	Indolene 30	-	-
Peters (14)	-	15-19	1000-3000	40° btdc to 5° atdc	Isobutylene	10%-100%	-

combustion variations.

The results of the investigators listed in Table 2.3 indicate effects of engine variables which are not consistent with respect to flame front speed. Of the engine variables investigated the following changes tend to increase the average flame front speed.

1. Decreasing the air-fuel ratio from a fuel lean value to slightly richer than stoichiometric (2).
2. Using fuels with faster burning velocities (2,7,11).
3. Increasing compression ratio (4).
4. Decreasing speed (4).
5. Increasing water jacket temperature (3).

These investigators have reported that 1, 2, and 5 decrease the C.B.C. dispersion of P_{max} (3,4,7,11), 3 increases the dispersion (4,9) and 4 does not affect the dispersion significantly (3). However, the P_{max} dispersion depends on the combustion process between ignition and its occurrence. This could be the reason all changes in engine variables which increase the average flame front speed do not result in lower P_{max} variations. Barton et al. (4) examined this point and separated the flame speed variations from the effects of the flame speed variations on P_{max} variations. They concluded that flame speed variations decreased for the changes indicated by one through five above. In general, those engine variables which increase the average flame front speed decrease flame front speed variations and could or could not decrease C.B.C. P_{max} variations.

The coefficient of variation of the imep is also affected by engine variable changes (9). The changes in engine variables which produce maximum brake torque generally decrease the coefficient of variation of the imep. Thus design practices which increase an engine's brake torque, also reduced engine "surge".

2.3 Effect of Engine Modifications on C.B.C. Variations

Engine modifications are hardware changes in engine components. Examples of engine modifications include changes in the intake, ignition, valve, etc. systems. Engine modifications are made to reduce the C.B.C. combustion variations. Table 2.4 summarizes the modifications used by various investigators, and their effect on C.B.C. combustion variations.

2.3.1 - Possible Causes of C.B.C. Variations - Possible causes of C.B.C. variations investigated and eliminated were ignition variations, air-fuel variations, exhaust residual variations and cylinder wall temperature variations.

Ignition variations, including timing variations, type and position of the spark plug, and spark energy were found to have no effect on C.B.C. combustion variations. The range of timing variations were found to be ± 1.0 crank angle degrees and these small variations were not large enough to cause the large C.B.C. variations observed (7,9). A range of spark energies from 0.2 to 200 millijoules (7,9) similarly had no effect on the combustion variation. The configuration, combustion chamber position and type of spark have little effect on the combustion variations (1,3,9). The use of multiple ignition sources (1,6,9,11) decreased the maximum pressure variations, however, they did not decrease imep variations (9).

Air-fuel variations from cycle to cycle were investigated using procedures to insure a homogeneous charge. These procedures

Table 2.4

Effects of Engine Modifications on C.B.C. Variations

Reference	(1)	(3)	(5)	(7)	(9)	(11)	(13)
A. Ignition Variations							
1. Spark Energy				NE	NE		
2. Number of Ignition Sources	RS				R	R	
3. Type and position of plug	NE	NE			NE		
B. A/F Variations							
1. Gaseous vs. Liquid Fuels				RS		R	
2. Mixture Preparation			NE		NE		
C. Exhaust Residual	NE	NE		NE	IS		
D. Mixture Motion Variations							
1. Valve Shrouds	I and R			I and R			
2. Manifold Disturbers			I		NE		
3. Sonic Valve							R
E. Cylinder Wall Temperature Variations		RS			NE		

Key:
R - Reduced variations
RS - Reduced variations slightly
NE - No effect on variations
IS - Increased variations slightly
I - Increased variations

included mixing tanks (5,9) and gaseous fuels (7,11). Neither procedure reduced significantly the C.B.C. combustion variations. Calculated values of the fuel burned each cycle (9,10,14) also indicate that air-fuel variations are not the cause of combustion variations.

The effect of exhaust residuals on C.B.C. variations were examined by comparing scavenged and unscavenged engine operation (1,3, 7,9). The exhaust residuals were found to have no effect on C.B.C. combustion variations except at low engine speeds and manifold vacuum where the effects of exhaust residual would be the greatest. Exhaust residuals were found to affect adversely the combustion process, but their C.B.C. variations are not the cause.

Cylinder wall temperature variations do not influence C.B.C. combustion variations (9). Increases in the average coolant temperature (3) reduced the variations slightly.

2.3.2 - Direct Effects on C.B.C. Variations - The engine modifications which significantly changed the C.B.C. combustion variations were those that altered the valves or the intake system directly ahead of the valve. Shrouded valves (1,6,7) and sonic valves (13) produce higher intake valve velocities and air swirl due to area restrictions. Flow straighteners (5,9), such as tube bundles, wire screens, and etc., cause increases in the small scale turbulence before the valve. Each of these engine modifications affect the mixture motion and resulted in a significant difference in the combustion variations compared to normal operation. Of all the causes investigated only those which produced changes in the mixture motion caused significant differences in the C.B.C. combustion variations. These results indicate that C.B.C. variations in the gas motion could be the major cause of C.B.C. combustion variations.

2.4 Measurements of C.B.C. Gas Motion Variations

The valve changes mentioned in Sec. 2.3.2 showed the effect of changing the mixture motion on C.B.C. combustion variations. However, quantitative measurements of the mixture motion variations have not been reported. Investigators have made quantitative gas velocity measurements in motored engine cylinders, water models, scaled engine models, etc., but data relating to combustion were not reported. In addition, the investigators who measured gas velocities were interested not in C.B.C. variations, but rather in determining characteristics of the velocity profiles that would allow evaluation of their effects on other phenomena. Qualitative information pertaining to gas velocity C.B.C. variations were reported incidently.

Semenov (15) measured velocities in the cylinder of a single cylinder CFR engine with a variable compression ratio and cylindrical combustion chamber. Velocity measurements were made with a constant temperature hot wire sensor. The main object of Semenov's investigation was the effect of engine operating variables on turbulence parameters. He averaged parameters over many cycles and was not concerned with C.B.C. variations but rather the effect of engine variables on these averages. Oscillograms (15) of the instantaneous velocity during the compression stroke indicates the C.B.C. variations in the velocity at a specific location in the cylinder. The velocity of five consecutive cycles at a crank angle of 30 degrees before tdc of the compression stroke ranged from 8 to 14 ft/sec about a mean of 10 ft/sec. The gas motion seems to exhibit large C.B.C. variations relative to its mean.

Velocity measurements in the cylinder of modified SI engines (16), water models (17) and compression ignition engines (18,19) all exhibit C.B.C. variations in the gas motion. These results were obtained using both paddle wheels (16) and hot wire anemometers (17,18, 19).

Patterson (7) accompanied his investigation with attempts to measure C.B.C. velocity variations in the cylinder. The results of his velocity measurements were unreported but he drew important conclusions from the results of his investigation.

"Our test results indicate that the major cause of cyclic combustion rate variation is the mixture velocity variations that exist within the cylinder near the spark plug at ignition" (7).

Patterson considered the above an assumed relationship. Nevertheless, it is based on unreported velocity and combustion measurements using the same engine and as such is unique. That is to say, measurements of both C.B.C. velocity variations and C.B.C. combustion variations were investigated and apparently resulted in a specific conclusion that other investigators could not make. For this reason, Patterson's assumed relationship provided the impetus for the project which supported the present research.

2.5 Effect of Mixture Motion on Flame Front Speed

The combustion literature is concerned with increases in the laminar burning velocities of homogeneous combustible mixtures due to turbulence. Turbulence can be generated by screens, turbulent pipe velocities, etc., and burning velocities under such turbulent conditions are compared to laminar burning velocities. The turbulent conditions are associated with well defined directional flows which permit measurement of well defined turbulence parameters such as scale and intensity. The effects of turbulence under these conditions can be summarized as follows (20),

1. Weak turbulence for which the increase in turublent burning velocity is proportional to the root mean square velocity of the turbulent fluctuations (turbulent intensity),
2. Strong turbulence for which the turbulent burning velocity is proportional to the square root of the turbulent intensity,
3. The burning velocity is inversely proportional to the scale of turbulence.

The difficulties in using combustion measurements of the turbulent burning velocity for estimation of engine flame front speeds are the measurement of the turbulent parameters, intensity and scale. In an engine during the compression stroke directional velocities are not defined, making measurements of these turbulent parameters difficult if not impossible. The effect of mixture motion in an engine is the same, in that it distorts the flame front area thereby increasing the flame front speed relative to a quiescent mixture. An estimate of the relative importance of mixture motion can be made.

Clerk (21) ignited an air-fuel mixture on the compression stroke immediately following intake and observed the normal combustion duration. He then modified the engine so that four compression strokes occurred without ignition or valve movement. On the fifth compression stroke the mixture was ignited. The combustion period was extended well into the expansion stroke and was still proceeding across the chamber when the exhaust valve opened some 200 crank angle degrees after ignition. Assuming that the mixture was fairly quiescent after the fourth non-firing compression stroke, as Semenov (20) has shown by his velocity measurements, these results illustrate the pronounced effect of mixture motion on flame front speeds or combustion duration.

2.6 Literature Summary

The literature has provided the following information:

1. The statistical parameter which best describes C.B.C. variations is the sample standard deviation,
2. Mixture motion variations from cycle to cycle appear to be the cause of C.B.C. combustion variations and warrants singular pursuit,
3. The C.B.C. gas motion variations directly influence C.B.C. variations in the flame front speed,
4. Velocities in the vicinity of the spark plug at the time of ignition are related to the variations,
5. The characteristics of the pressure development histories which are a direct indication of flame front speeds are the crank angles at which P_{max} and $\dot{P}_{max}$ occur.

The literature suggests that supplemental information is required from experimentation. The experimental information required to substantiate the hypothesis are:

1. Those characteristics of the mixture motion which cause C.B.C. variations must be identified and their extent statistically measured,

2. A measure of the flame speed variations must be identified from the pressure development histories,
3. A semi-empirical model must be constructed to relate gas motion C.B.C. variations in a motored engine to C.B.C. combustion process variations in a fired engine.

In the following chapter, the experiments and experimental equipment necessary to supply the supplemental empirical information are discussed.

Chapter 3

EXPERIMENTAL EQUIPMENT AND INSTRUMENTATION

An experimental program was required to test the validity of the hypothesis that C.B.C. combustion and velocity variations are related. Specifically, characteristics of the pressure development history and gas motion, whose C.B.C. variations are related, must be identified. The experimental program to obtain this information required the following equipment and instrumentation:

1. Combustion equipment,
2. Combustion instrumentation,
3. Measurement of a gas motion characteristic,
4. Experimental data recording and processing equipment.

Details concerning the equipment, instrumentation, and calibration procedures necessary for the experimental program are discussed within this chapter.

3.1 Combustion Equipment

3.1.1 - Combustion Chamber - The combustion of an air-fuel mixture was performed in the combustion chamber of a removable dome head (RDH) cooperative fuel research (CFR) engine manufactured by Waukesha Motor Co. This engine is constructed with a hemispherical head and is equipped with overhead valves. The clearance volume with respect to the piston is variable and allows compression ratios from 3 to 13 to be obtained. The engine assembly is mounted on a CFR-48 crank case. Two threaded access holes into the combustion chamber are provided in the cylinder head. This engine with intake and exhaust system is shown in Figs. 3.1 and 3.2. The combustion chamber and related dimensions are given in Table 3.1.

Table 3.1

Combustion Chamber Dimensions

Bore (D)	3.8125 inches
Stroke (s)	3.625 inches
Displacement volume (VD)	41.38 cubic inches
Connecting rod (L)	10.0 inches
Connecting rod to stroke (L/s)	2.758

The overhead valves are actuated by cams in the crank case. The valve mechanism train is constructed so that correct clearances can be maintained over a range of compression ratios. Dimensions and timing of the intake and exhaust valves are presented in Table 3.2.

Table 3.2

Dimensions and Timing of Intake and Exhaust Valves

Intake Valve	
Head Diameter	2.0 inches
Maximum Lift	0.235 inches
Opens	20° atdc
Closes	200° atdc
Exhaust Valve	
Head Diameter	1.75 inches
Maximum Lift	0.235 inches
Opens	512° atdc
Closes	3° atdc

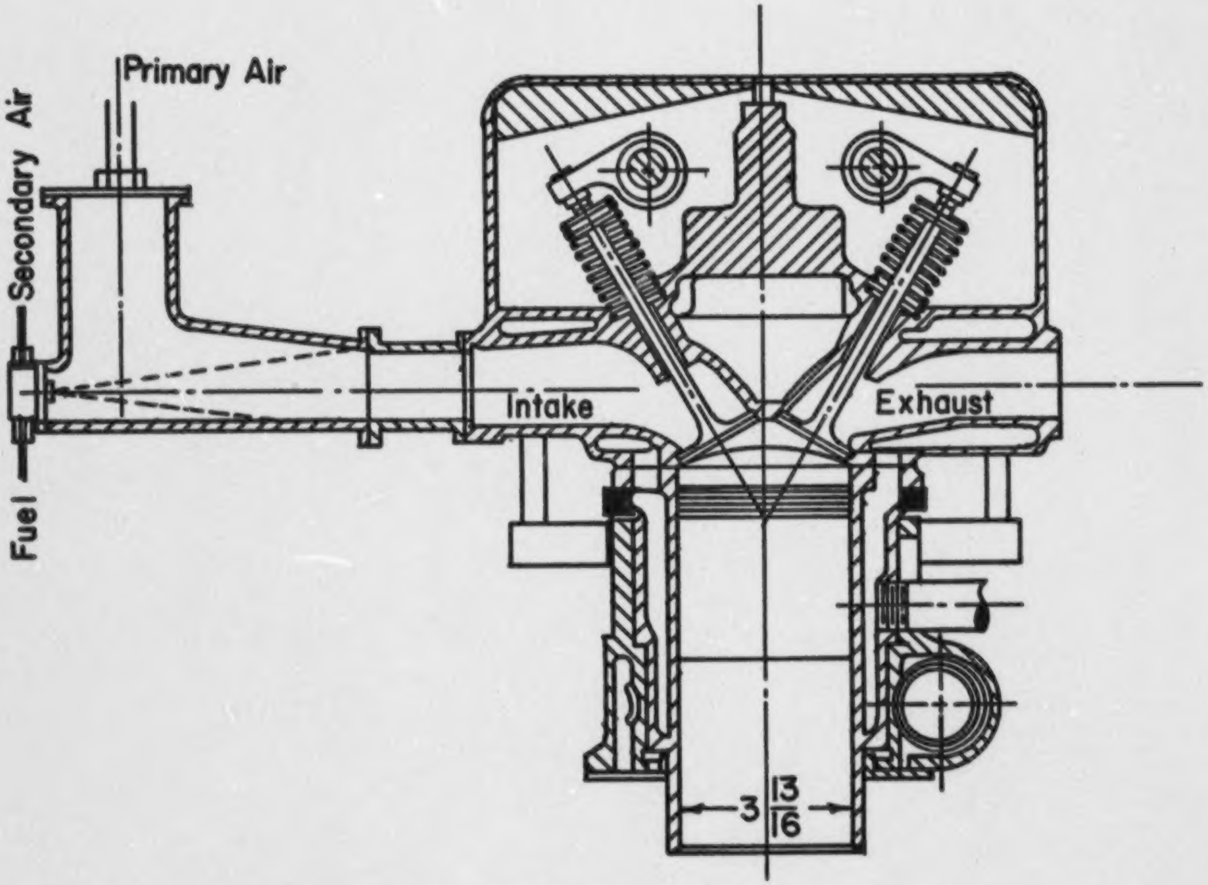
Primary Air
Secondary Air
Fuel
Intake
Exhaust
3 13/16

Figure 3.1. CRF engine cross section through intake and exhaust valve center lines.

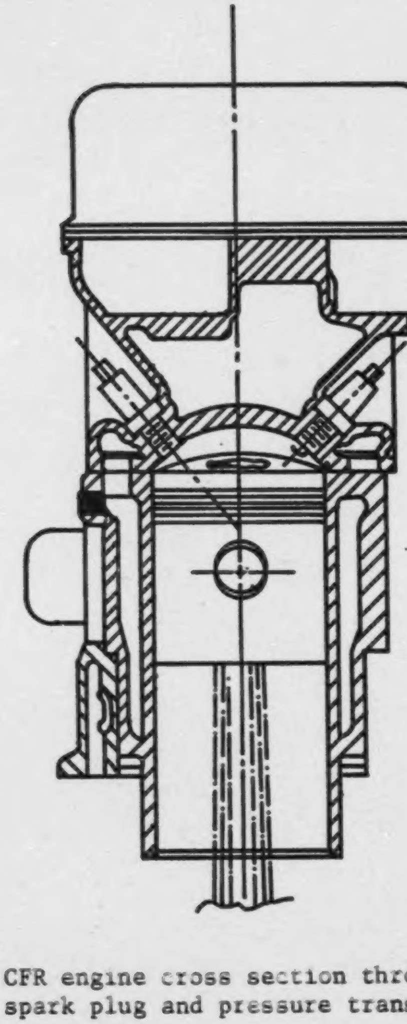

Figure 3.2. CFR engine cross section through center lines of spark plug and pressure transducer.

The intake valve lift versus crank angle relationship is shown in Fig. 3.3.

3.1.2 - Air-Fuel System - The air-fuel system consisted of a two fluid atomizer (air and fuel), metering equipment, surge tank, heaters, and intake manifold. A schematic of the air-fuel system is shown in Fig. 3.4.

The fuel, isooctane, was contained in a nitrogen pressurized fuel tank. The pressure forced the fuel through a calibrated rotameter, metering valve and atomizing nozzle into the intake manifold. The fuel rotometer was calibrated at room temperature using isooctane fuel. The air flow rate to the nozzle passed through a calibrated rotameter and metering valve. The air pressure at the rotameter was held constant at 40 psi. The nozzle air rotameter was calibrated and corrected to a standard temperature of 70F and pressure of 50 psi.

The primary air supply passed through a calibrated rotameter, metering valve, surge tank with heaters, and then mixed with the fuel in the intake manifold. The primary air temperature was maintained constant with thermostatically controlled electric heaters. Temperature measurements were made at the rotameter exit, surge tank, intake manifold entrance, and in the intake manifold. Pressure measurements were made at the exit of each rotameter and the intake manifold using vertical mercury manometers.

3.1.3 - Ignition System - The ignition system consisted of a six volt battery, points, condensor, ignition coil and spark plug. The points were opened and closed using a distributor driven by the crank case timing shaft. The spark plug was an automotive high resistance plug with a 0.25 inch gap. A high resistance plug was used to minimize

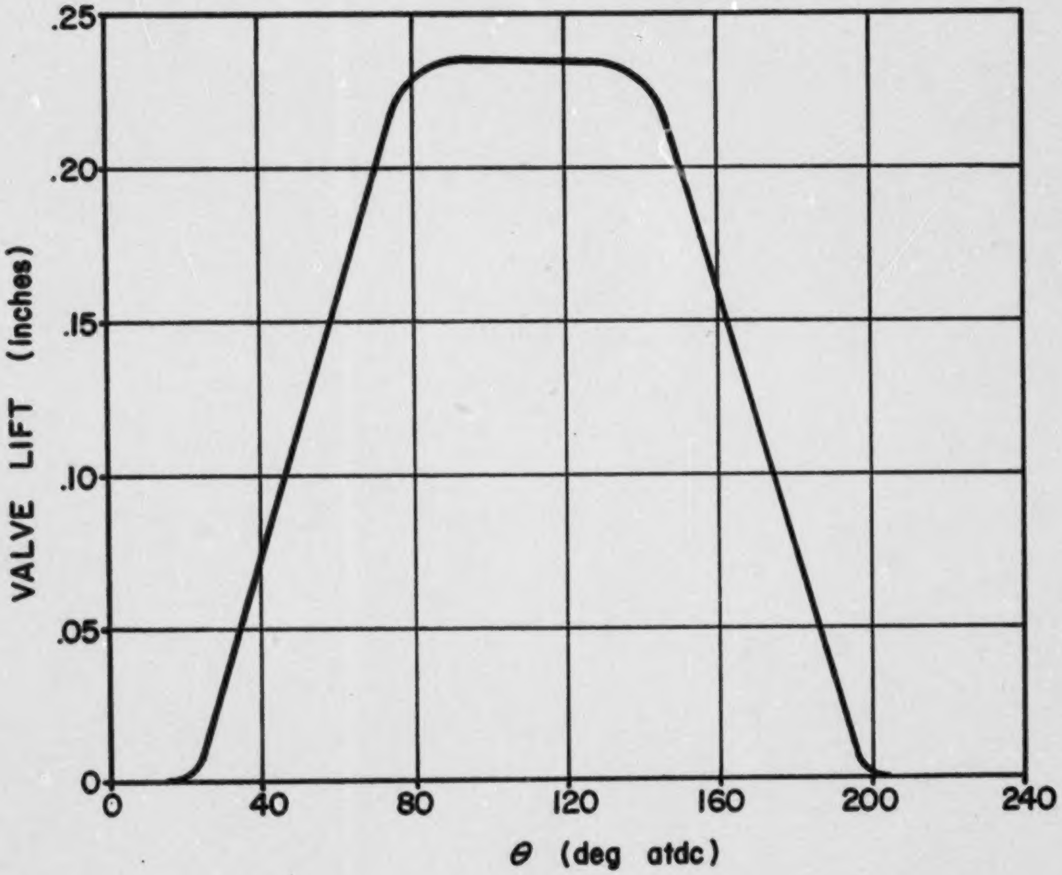

Figure 3.3. Intake valve lift as a function of crank angle.

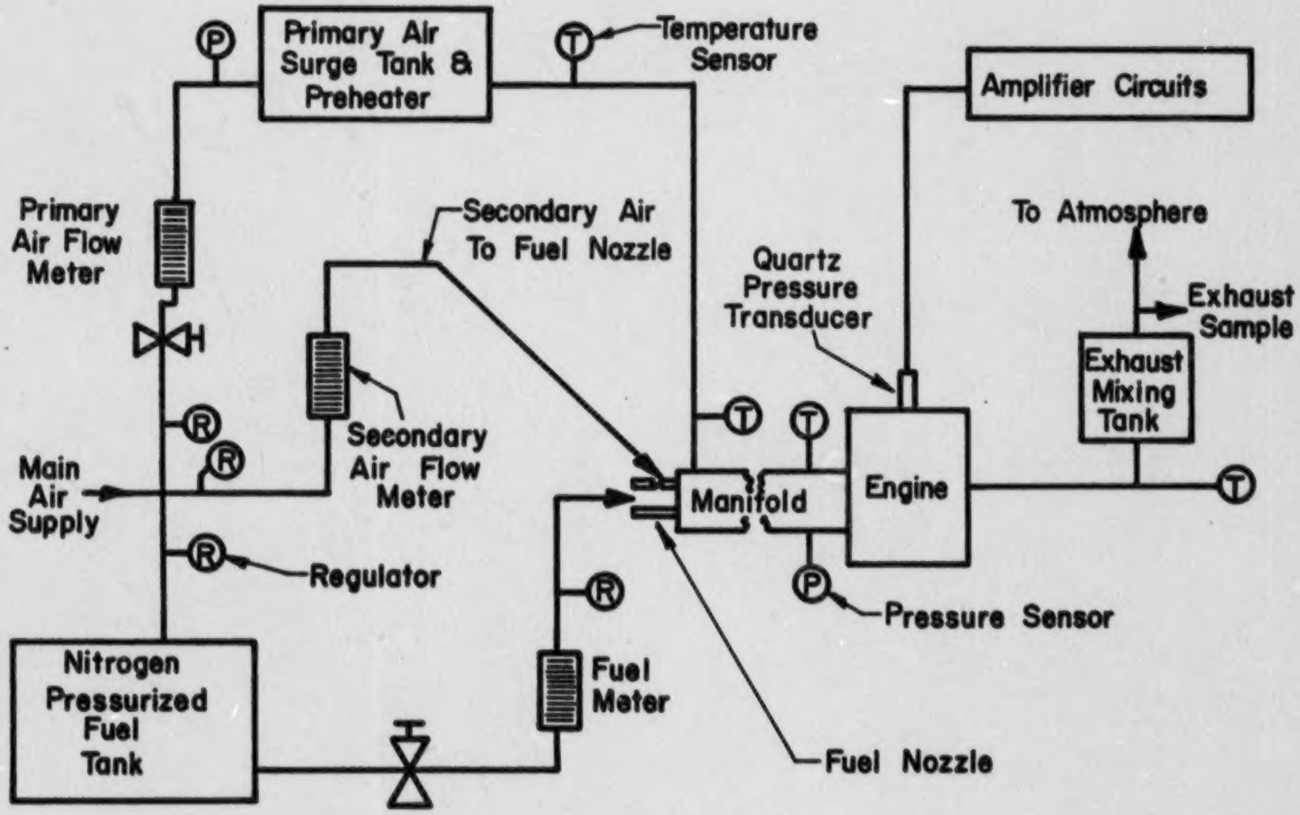
Primary Air Surge Tank & Preheater
Temperature Sensor
Amplifier Circuits
Primary Air Flow Meter
Secondary Air To Fuel Nozzle
To Atmosphere
Exhaust Sample
Quartz Pressure Transducer
Exhaust Mixing Tank
Secondary Air Flow Meter
Main Air Supply
Manifold
Engine
Regulator
Pressure Sensor
Nitrogen Pressurized Fuel Tank
Fuel Meter
Fuel Nozzle
P
T
R

Figure 3.4. Schematic of engine instrumentation.

interference of the ignition system on nearby electronic equipment. Ignition timing was determined by using a timing light which illuminated crank shaft degree markings on the flywheel. The distributor breaker plate was adjusted using a micrometer which was mounted between the breaker plate arm and the crank case base. The spark plug was placed in one of the two access holes provided. The grounded electrode was recessed 0.25 inches from the combustion chamber surface.

3.1.4 - Dynamometer - The cradled electric dynamometer used for motoring and absorbing operation was an A.C. induction type. The dynamometer and motor-generator system allowed nominal speeds of 600, 900, 1200 and 1800 rpm to be maintained. Engine torque output was measured with a balance beam scale. The balanced beam had one-tenth pound scale subdivisions.

3.1.5 - Exhaust Gas Measurements - Two exhaust gas constituents, carbon monoxide (CO) and carbon dioxide (CO_2), were measured using infrared detectors. The exhaust gas samples were drawn from an exhaust mixing tank, passed through water traps, a drying column, filter and the infrared detectors. Volumetric percent concentrations of CO and CO_2 in the exhaust gas were determined and used as a check on measured air-fuel ratios.

3.2 Combustion Instrumentation

The physical manifestations of the combustion process in terms of pressure and rate of pressure change histories were provided by a single transducer. The pressure development histories were related to tdc of the compression stroke by a timing mark. The transducers and associated instrumentation used to provide these signals are discussed below.

3.2.1 - Pressure Transducer - A Kistler SLM 253 quartz transducer was mounted in the access hole opposite the spark plug. The transducer's active face was flush with the combustion chamber wall. The current produced by the transducer is proportional to the rate of pressure change and the corresponding charge proportional to the cylinder pressure. The transducer was calibrated statically over a zero to 250 psi range using a charge amplifier and dead weight tester. The transducer sensitivity to pressure was 3.2 picocoulombs per psi.

3.2.2 - Pressure Development Analog Signals - The pressure transducer's current is amplified and then integrated. The voltage signals produced are proportional to the cylinder rate of pressure change and cylinder pressure respectively. The amplifier and integrating circuits are described by Winkler (22).

Figure 3.5 shows a schematic of the circuits used to obtain the desired voltage signals. The transducer's current was amplified and filtered with a high gain operational amplifier, resistors and capacitors. The filter passed frequencies below 10,000 Hz, thereby eliminating unwanted signals produced by engine vibrations and electrical noise. The resultant amplifier output voltage is proportional to the rate of pressure change. The constant of propotionality was 40,000 psi/sec/volt for all engine conditions.

The current amplifier signal was integrated using a high gain operational amplifier, capacitor, resistor, and reset switch. The reset switch was a magnetic reed switch mounted near the crank shaft. A rotating magnet closed the contact points every revolution near bdc.

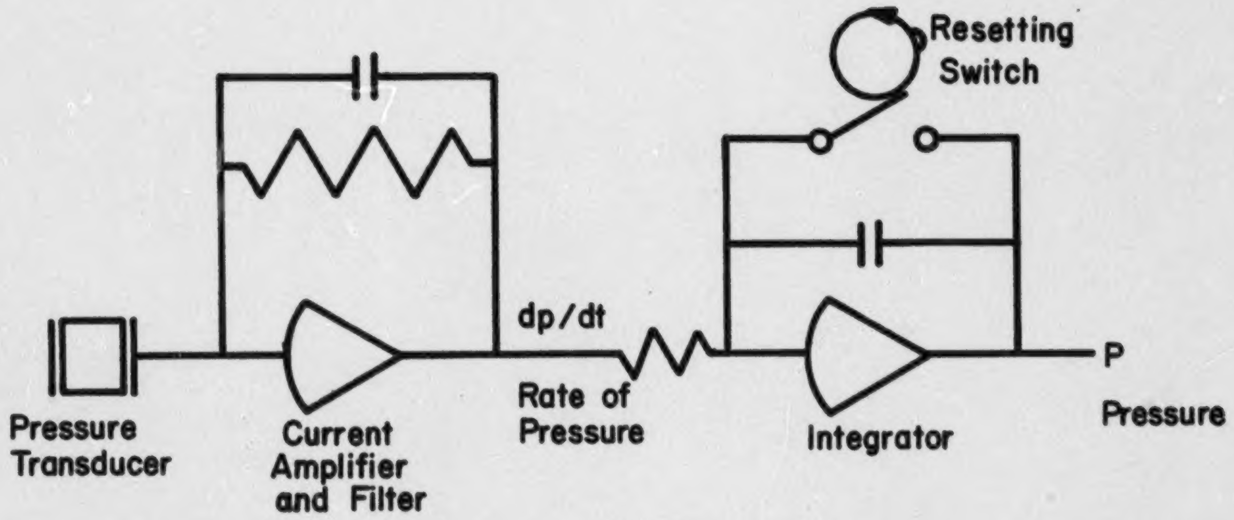
Resetting Switch
dp/dt
P
Pressure Transducer
Current Amplifier and Filter
Rate of Pressure
Integrator
Pressure

Figure 3.5. Schematic of analog circuit used to provide voltage signals proportional to cylinder rate of pressure change and pressure.

The reset switch permitted adjustments to the pressure signal that reflect changes in engine operating variables. The integrator's output voltage was proportional to cylinder pressure with a constant of proportionality of 100 psi/volt.

3.2.3 - Timing Mark Analog Signal - A timing mark indicating tdc of the compression stroke was generated using an operational amplifier, resistor, capacitor and reed switch. A schematic of the circuit is shown in Fig. 3.6. A constant voltage was integrated resulting in a ramp voltage. The ramp voltage was reset to zero at tdc of the compression stroke by a reed switch. The reed switch was closed by a rotating magnet mounted on the crank case timing shaft. The timing mark was generated in this manner to eliminate spurious signals.

The three voltage signals representing cylinder pressure, rate of cylinder pressure change and tdc of the compression stroke are shown in Fig. 3.7. These signals were recorded and subsequently used to determine the statistical extent of C.B.C. combustion variations.

3.3 Gas Motion Measurements

The gas motion's velocity was experimentally determined using a constant temperature hot film sensor. Constant temperature operation was provided by an anemometer whose output bridge voltage was proportional to the current required to maintain the sensor at a constant temperature. The anemometer's output signal was conditioned by filters and voltage suppressors. The anemometer bridge voltage was statically calibrated for velocity and temperature changes. The

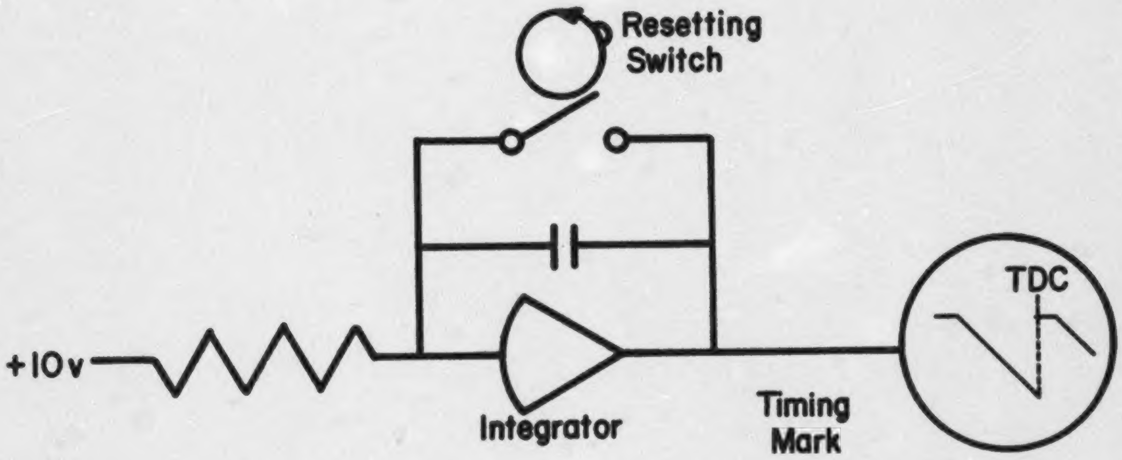
Resetting
Switch
+10v
Integrator
Timing
Mark
TDC

Figure 3.6. Schematic of analog circuit used to provide a timing mark which indicates tdc of compression stroke.

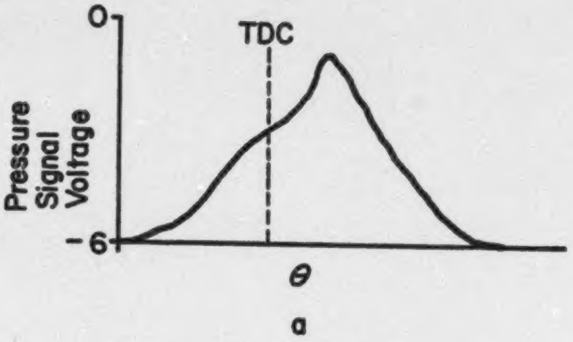

Pressure Signal

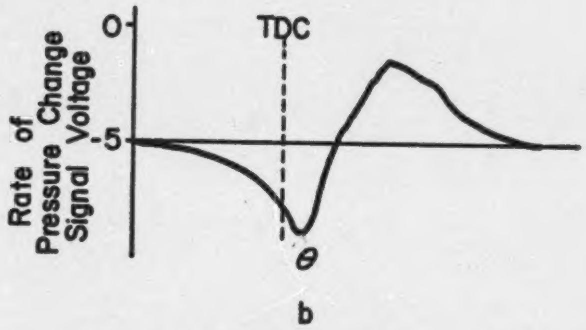

Rate of Pressure Change Signal

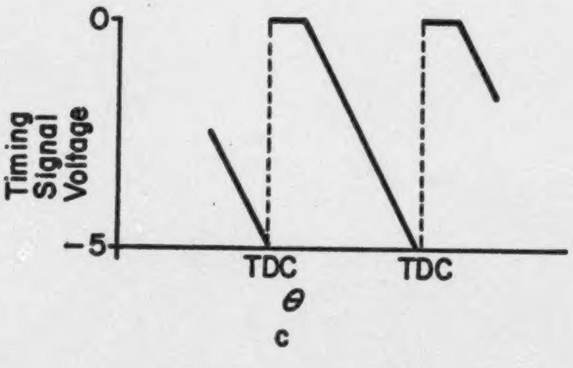

Timing Mark Signal

Figure 3.7. Combustion signals recorded by analog to digital data acquisition system. (After Kenemuth and Lestz [5].)

sensor was used to measure velocity in the intake manifold and in the combustion chamber of the CFR engine. The bridge voltage was compensated for the effects of temperature and pressure using King's law.

3.3.1 - Sensor Description - The hot film sensor used in this study was a 0.002 in. diameter quartz rod with a 1000 angstrom thick platinum film on the surface. The platinum film sensor is coated with a thin film of fused quartz. The film and substrate are supported by gold plated stainless steel supports. The sensor length is 0.04 inches.

The advantages of a hot film sensor over a hot wire sensor with respect to use for measurements in an engine are:

1. The film sensor is less susceptible to contaminants and surface corrosion, resulting in a calibration that is stable over a period of time,
2. The film sensor is supported on flexible supports and is therefore relatively insensitive to engine vibrations and other causes of breakage.

3.3.2 - Anemometer System - The anemometer system consists of a constant temperature anemometer, power supply, linearizer and signal conditioners. The system and probes were manufactured by Thermo Systems Inc. (TSI) of St. Paul, Minnesota. Detailed descriptions of the equipment are given in reference (23).

A brief description of the components follow, along with the manufacturer's model number.

1. TSI Model 1050 Anemometer - The model 1050 anemometer maintains the sensor at a constant temperature. The sensor operating temperature is determined by the sensor

resistance which is selected by variable resistance decades. The maximum sensor dissipation is 2.0 watts at a current of 0.45 amperes. The anemometer output is the voltage across a bridge leg and is proportional to the voltage drop across the sensor. The output bridge voltage range is 0-20 volts with a 50 ohm ouput impedance. The anemometer can also measure temperature (constant current operation) and resistance.

2. TSI Model 1051-6 Monitor and Power Supply - The power supply module provides power for the anemometers and accessory equipment. A 0.5% taut band voltmeter allows D.C. voltage measurements from 0 to 30 volts.
3. Model 1055 Linearizer - The linearizer provides a voltage which is proportional to the fluid velocity. The linearizer was used only when a constant ambient temperature existed. The linearizer is capable of matching ten points of a sensor calibration curve.
4. TSI Model 1057 Signal Conditioner - The signal conditioner was used as a voltage suppressor, low pass and high pass filter for the anemometer bridge voltage. Low pass frequency filters from 0.2 to 200 KHz with 12 db/octave attenuation are provided. High pass frequency filters from 5 to 1000 Hz with 12 db/octave attenuation are also provided. Zero voltage suppression from 0 to 20 volts in one volt increment can be used. The output voltage range is ± 20 volts with an output impedance of 20 ohms.

3.3.3 - Sensor Calibration - Sensors used for gas motion measurements must be calibrated. The sensor is exposed to a known velocity, and the bridge voltage required to maintain a constant sensor temperature is recorded. This calibration procedure is applicable for constant fluid properties, where only the fluid velocity affects the bridge voltage. The combustion chamber temperature and pressure during a motored compression stroke can vary from 560 to 1200R and 10 to 200 psi respectively. Calibration of a sensor for use in the combustion chamber must also include the effects of temperature and pressure on the bridge voltage as well as velocity. A relationship between the heat dissipated by the sensor, the fluid properties and velocity must be established. This relationship, confirmed by calibration, allows the velocity to be determined from the bridge voltage knowing the fluid properties.

The relationship used to relate sensor heat dissipation to fluid properties and velocity is known as King's law (24). King's law is given below.

$$Q_s = k_a \, [C_1 + C_2(Re)^n](T_s - T_a), \tag{3.1}$$

where C_1, C_2 and n are constants determined by calibration,

$$Re = \rho_a d_s \, U/\mu_a, \tag{3.2}$$

and

$$Q_s = V_B^2 \, R_s/(R_s + 40)^2. \tag{3.3}$$

Here, R_s is the sensor resistance and V_B is the bridge voltage. Substitution of Eq. 3.3. into Eq. 3.1 gives,

$$\frac{V_B^2 R_S}{(R_s + 40)^2} = k_a \, [C_1 + C_2(Re)^n](T_s - T_a), \tag{3.4}$$

which relates bridge voltage (V_B) to fluid properties and velocity. The fluid properties k_a, μ_a, and ρ_a are functions of the fluid temperature and pressure. The fluid properties are evaluated at the mean temperature $(T_s + T_a)/2$, between the sensor and fluid. The constants C_1, C_2, and n are determined by calibration in air at a known pressure, temperature and velocity. The sensor temperature, T_s, is determined by measuring the sensor resistance.

Since it is the operating temperature of the sensor that is of direct interest rather than the resistance, the relationship between the two must be established. The sensor resistance is related to the sensor temperature by the assumed linear relationship,

$$R_s(T) = R_s(T_o) + \alpha_o(T - T_o). \tag{3.5}$$

The temperature coefficient of resistance, α_o, at the reference temperature, T_o, was determined experimentally. The sensor was placed in an ice-water bath which provided the reference temperature, T_o, and resistance, $R_s(T_o)$. The sensor was then placed in boiling distilled water at atmospheric pressure and the sensor resistance measured. The coefficient of resistance was determined from the measured values of R_s at the boiling and ice point temperatures.

$$\alpha_o = \frac{R_s(210.5F) - R_s(32F)}{210.5F - 32F} \tag{3.6}$$

The experimental value of α_o together with Eq. 3.5 allowed the sensor temperature to be determined from the sensor resistance using the following relationship,

$$T_s = \frac{R_s(T_s) - R_s(T_o)}{\alpha_o} + T_o. \tag{3.7}$$

The sensor calibration with respect to velocity and fluid properties was accomplished using a TSI Model 1125 Calibrator. The calibrator consisted of three chambers for which the air velocity was determined by the manufacturer. The calibrator's air velocity range is 0.5 ft/sec to 1000 ft/sec. The calibrator is shown in Fig. 3.8. To calibrate the sensor at air temperatures other than ambient, a heat exchanger was added to the calibrator. The heat exchanger consisted of an electrical heating element inserted in a cylindrical mica tube. The tube was placed upstream to the calibrator and the air passed through the tube containing the heating element. Air temperatures from 70 to 200F were possible by controlling the heating element's current. Air temperatures were measured with mercury thermometers, thermocouples and the sensor itself. The calibrator, as modified, provided known velocities and temperatures for sensor calibration.

The constant, C_1, in Eq. 3.1 was determined by placing the sensor in the middle chamber with no flow passing through the chamber (zero Reynold s number). The air temperature was measured and the sensor temperature, T_s, was varied from 200 to 800F in increments of 100F. The bridge voltage corresponding to zero velocity and sensor temperature was recorded.

Equation 3.4 for zero Reynold s number gives the following relationship between C_1, V_B, and $k_a(T_s - T_a)$,

$$\frac{V_B^2 R_s}{(R_s + 40)^2} = C_1 \, k_a(T_s - T_a). \tag{3.8}$$

The constant, C_1, can be determined from the slope of the left hand side of Eq. 3.8 plotted versus $k_a(T_s - T_a)$. Figure 3.9 gives the experimental results from which C_1 was determined.

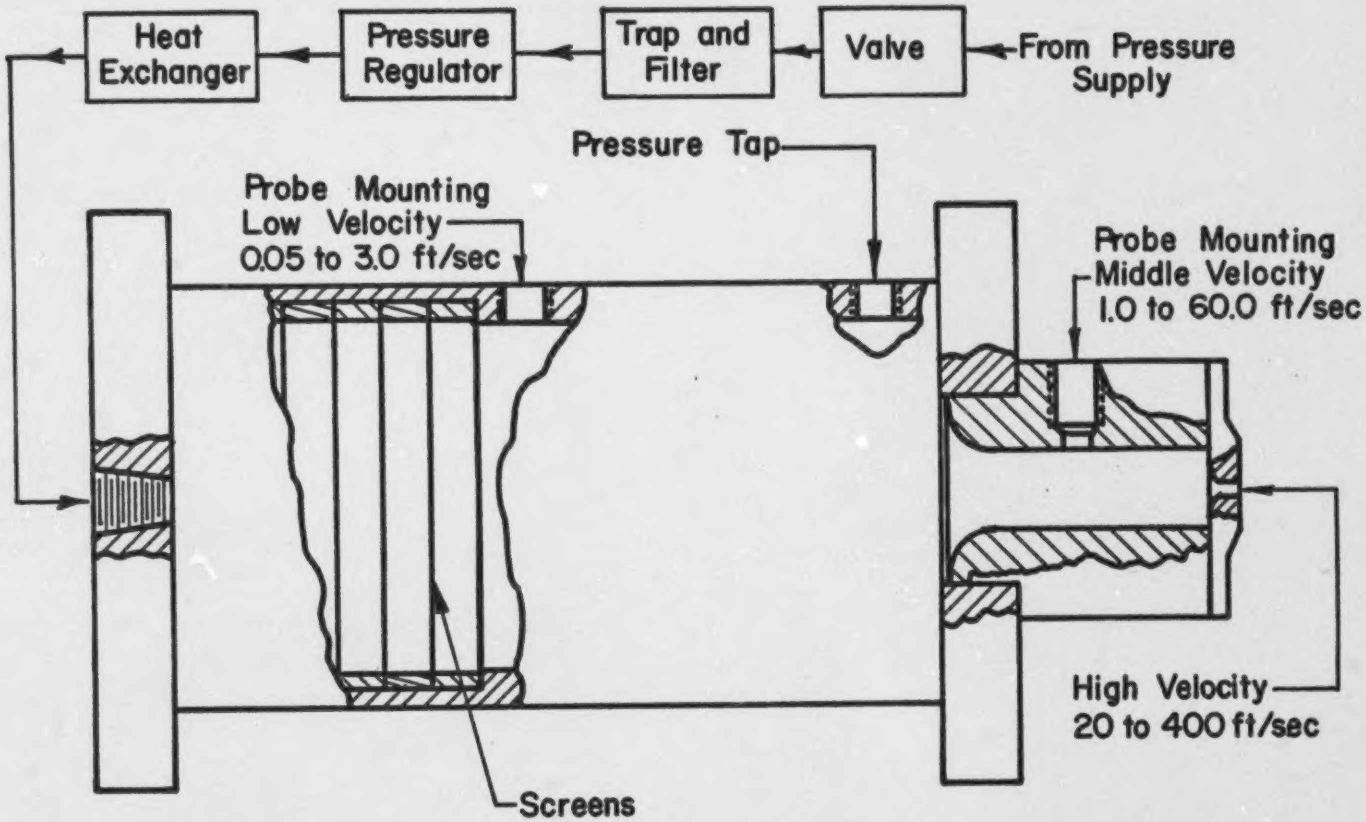
Heat Exchanger
Pressure Regulator
Trap and Filter
Valve
From Pressure Supply
Pressure Tap
Probe Mounting Low Velocity 0.05 to 3.0 ft/sec
Probe Mounting Middle Velocity 1.0 to 60.0 ft/sec
High Velocity 20 to 400 ft/sec
Screens

Figure 3.8. Schematic of TSI Model 1125 calibrator used to calibrate velocity sensor.

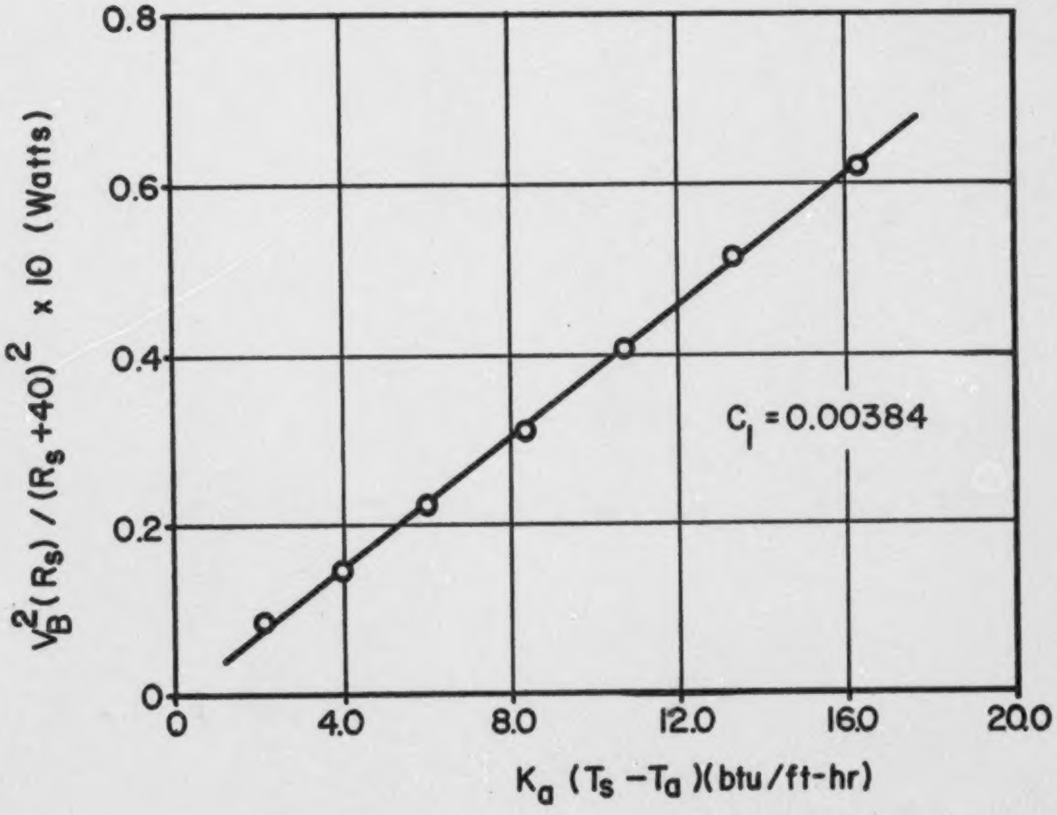

Figure 3.9. Sensor calibration results for determining constant, C_1, in King's law at zero Reynold's number.

The values of C_2 and n in Eq. 3.4 were determined using the following expression,

$$\frac{V_B^2 R_s}{(R_s + 40)^2 k_a (T_s - T_a)} - C_1 = C_2 Re^n. \qquad (3.9)$$

A logarithmic plot of measured values of the left hand side versus Reynold's number permits the constant C_2 and n to be evaluated. The constants C_2 and n were determined for the range of variables given in Table 3.3.

Table 3.3

Range of Variables Used
for Sensor Calibration

Variable	Range of Variable
Sensor Temperature	200-800F
Velocity	4.0 - 380 ft/sec
Reynolds Number	2.0 - 300

The logarithmic plots of the experimentally measured variables in Eq. 3.9 are shown in Fig. 3.10 for a sensor temperature of 700F and air temperatures of 67 and 167F. The calibration results indicate that King's law can be used to separate temperature and pressure effects on bridge voltage from velocity effects.

The constant, C_2, was found to depend on the sensor temperature and Reynolds number. The value of n, was dependent on Reynolds number only. Two sensor temperatures 700 and 800F were used for measuring air velocity in the combustion chamber. The values of the constants are tabulated in Table 3.4 for these sensor temperatures.

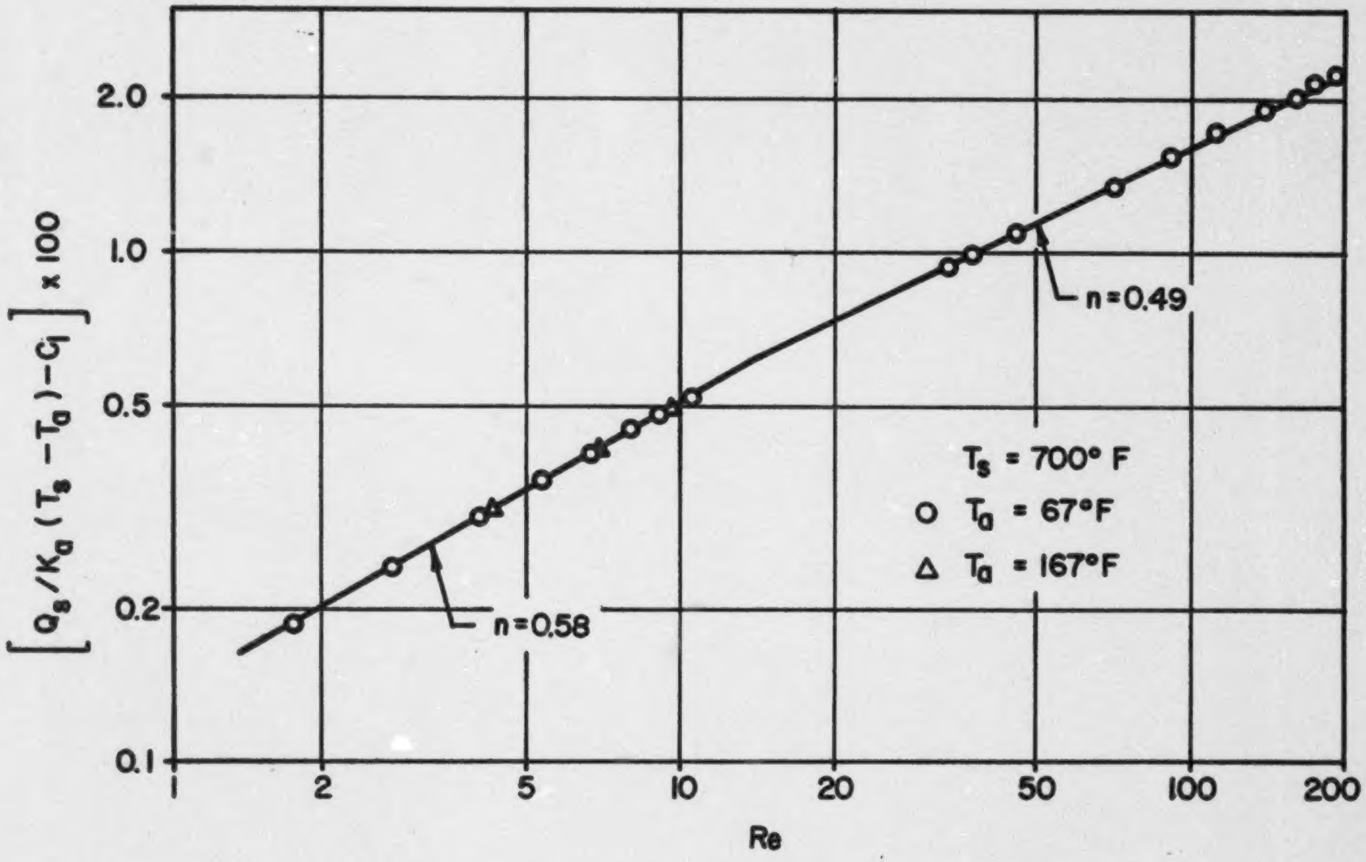

Figure 3.10. Sensor calibration results used to determine the constants C_2 and n in King's law.

Table 3.4

Calibration Constants Used in King's Law

T_s(F)	$\left[\frac{V_B^2 R_s}{(R_s + 40)^2 k_a (T_s - T_a)} - C_1\right]$	C_1	C_2	n
700	>0.0065	0.00384	0.00172	0.49
700	<0.0065	0.00384	0.00135	0.58
800	>0.0063	0.00384	0.00176	0.49
800	<0.0063	0.00384	0.00139	0.58

3.3.4 - Cylinder Air Temperature and Pressure - King's law requires the evaluation of the fluid properties ρ_a, k_a, and μ_a, and the temperature difference, $(T_s - T_a)$. The properties are in turn functions of the pressure and temperature existing within the cylinder. Pressure and temperature must either be measured or calculated using an equation of state. The bridge voltage is most sensitive to temperature and should be measured. Cylinder temperature is however difficult to measure as velocity affects its measurement. In addition temperature measurement at the probe location is physically impossible. Cylinder pressure was measured from which a mean cylinder air temperature was calculated using the ideal gas law.

Cylinder pressure was measured using a Kistler 606A transducer with a factory calibrated sensitivity of 4.75 picocoulumbs per psi. A Kistler electrostatic charge amplifier, Model 503, was used to produce a voltage proportional to pressure. The constant of proportionality was 20 psi/volt.

A timing mark which indicated tdc of the compression stroke was used to calculate cylinder volume. The description of the equipment used to generate the timing mark is described in the section dealing with combustion measurements.

The three signals used to determine the sensor velocity were the pressure signal, bridge voltage and a timing mark. The subsequent recording and equations used to obtain velocity are described in the following sections.

3.4 Data Collection and Analysis

The recording and subsequent analysis of the data was accomplished using a PDP-9[1] programmed data processing system. Three coaxial transmission lines were run from the engine facilities to the PDP-9 input terminals. The voltage signals were sampled, digitized and placed on magnetic tape using software programs written specifically for the PDP-9. Hardware description of the PDP-9 can be found in (25) and software programs are documented by Stone (26). Discussion of the real-time data acquisition system as it pertains to this work follows.

3.4.1 - Real-Time Data Aquisition System - Stone (26) wrote software programs to sample, digitize and place on magnetic tape real-time analog signals. The system's maximum capabilities permitted 24 separate channels to be sampled at a sampling rate of 20,000 samples per second in either a burst or continuous sampling mode.

The continuous sampling mode was chosen for this work which provided 30 seconds of continuous sampling. Nominal sampling rates and bit accuracy for the continuous mode are presented in Table 3.5.

---

[1] Trademark of the Digital Equipment Corp., Maynard, Mass.

Table 3.5

Sampling Rates and Voltage Resolution of Analog to Digital Data Acquisition System

Sample Rate (Samples/sec)	Voltage Resolution (Volts)
5,000	0.0025
10,000	0.02
15,000	0.16

The voltage resolution chosen was 0.02 volts and the sampling rate of 10,000 samples per second accompanying it was accepted. All experiments had three signals digitized at a sample rate of 10,000 samples/sec. This resulted in a sampling rate of 3300 samples per second per signal. The voltage resolution and sampling rate resulted in the resolution of the parameters shown in Table 3.6.

Table 3.6

Resolution of Parameters Digitized by Analog to Digital Data Acquisition System

		Combustion Parameter			Motored Parameter		
rpm	No. of engine cycles	P_{max} (psi)	$\dot{P}_{max}$ (psi/sec)	θ (deg)	P (psi)	V_B (volt)	θ (deg)
600	150	2	800	1.0	0.4	0.02	1.0
900	225	2	800	1.5	0.4	0.02	1.5
1200	300	2	800	2.0	0.4	0.02	2.0
1800	450	2	800	3.0	0.4	0.02	3.0

3.4.2 - Data Analysis - The experiments were divided into the two distinct sets, 1) combustion data and 2) cold cranking air velocity data. Statistics for the combustion data were calculated directly from the digitized data. The combustion chamber air velocity as a function crank angle was calculated from the bridge voltage, cylinder pressure and timing mark signals using King's law and placed on magnetic tape. The statistics were then calculated from the recorded velocities. The data reduction was accomplished with Fortran programs written for the PDP-9. A description of each Fortran program's function with respect to each data set follows.

3.4.2.1 - Combustion Data - A Fortran program was written to calculate the statistics of the following four characteristics of the pressure development history.

1. Maximum cylinder pressure (P_{max}).
2. Crank angle of occurrence of P_{max} relative to tdc of the compression stroke [$\theta(P_{max})$].
3. Maximum rate of pressure change ($\dot{P}_{max}$).
4. Crank angle of occurrence of $\dot{P}_{max}$ relative to tdc of the compression stroke [$\theta(\dot{P}_{max})$].

The maximum values, P_{max} and $\dot{P}_{max}$ were identified by comparing each digital signal of an engine cycle and storing the maximum values. The crank angles of occurrence were determined from the number of samples between the maximum values and the timing mark, the sampling rate and engine speed. The values of P_{max}, $\dot{P}_{max}$, $\theta(P_{max})$, and $\theta(\dot{P}_{max})$ were stored for each cycle.

Statistics for the four pressure development characteristics were calculated using running summations. The statistics calculated were:

1. Sample mean ($\overline{x}$),

2. Sample standard deviation [S(x)],
3. Cross correlation coefficients between,
   a. P_{max} and $\dot{P}_{max}$[CC(P_{max},$\dot{P}_{max}$)],
   b. P_{max} and $\theta(P_{max})$ (CC[P_{max},$\theta(P_{max})$]),
   c. $\dot{P}_{max}$ and $\theta(\dot{P}_{max})$ (CC[$\dot{P}_{max}$,$\theta(\dot{P}_{max})$]).

The summation formulas are given in Appendix A. The summations were then used to calculate the statistics defined in Appendix A.

The following statistics were also calculated for P_{max}:

1. Coefficient of Skewness (CS),
2. Coefficient of Kurtosis (CK),
3. Autocorrelation coefficient with respect to cycle difference (CA).

Maximum pressure values for each cycle were written onto magnetic tape. Fortran programs were used to calculate the summations used for each statistic as defined in Appendix A. Double precision was used to calculate the skewness and kurtosis values.

3.4.2.2 - Velocity Data - Three signals, cylinder pressure, bridge voltage and timing mark were recorded in digital form. Fortran programs were written to calculate the air velocity as a function of crank angle from these three signals. The volume and pressure corresponding to a recorded bridge voltage signal were computed. The cylinder air temperature was calculated using the ideal gas law. Knowing the temperature and pressure allowed calculation of the air properties, k_a, μ_a, and ρ_a, and then King's law was used to calculate the air velocity. Examples of the bridge voltage, cylinder pressure, volume, and temperature are shown in Figs. 3.11 to 3.14. A complete

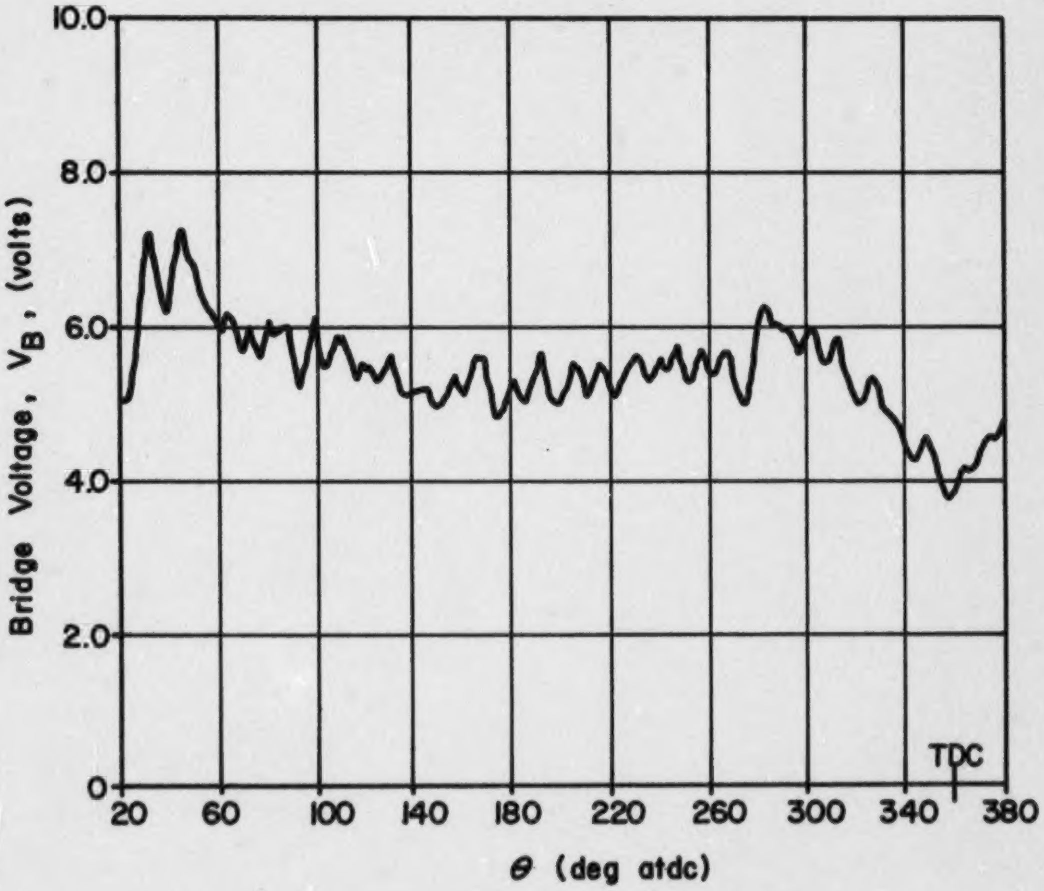

Figure 3.11. Anemometer bridge voltage digitized and reproduced as an analog signal by PDP-9 computer.

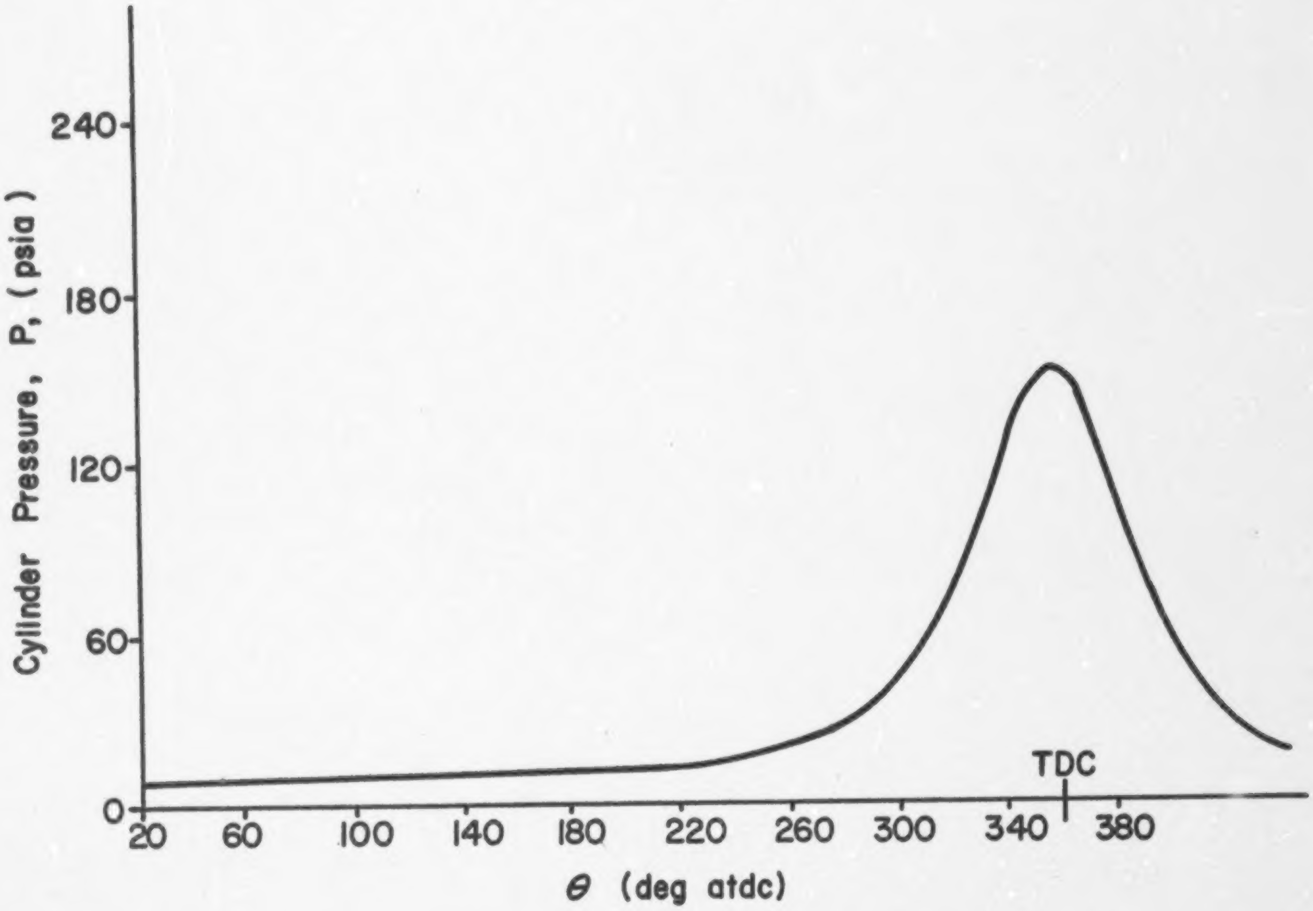

Figure 3.12. Cylinder pressure of motored engine digitized and reproduced as an analog signal by PDP-9 computer.

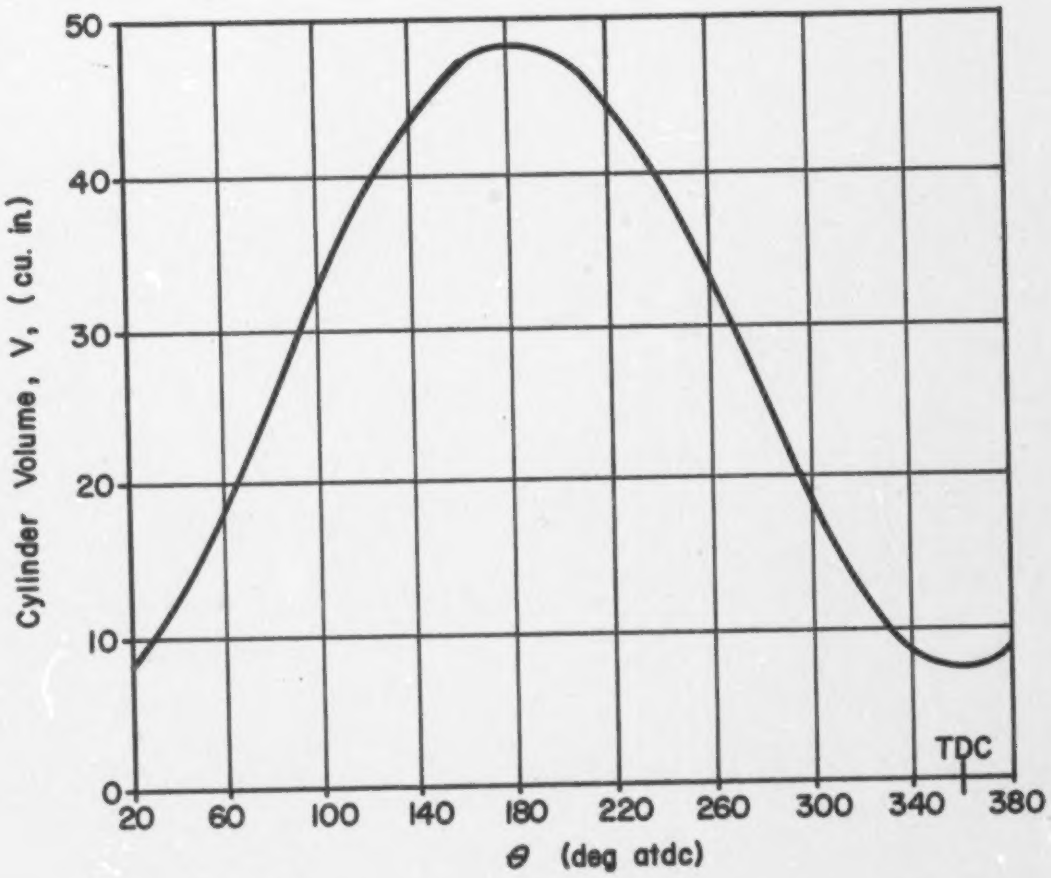

Figure 3.13. Cylinder volume calculated from timing mark and reproduced as an analog signal by PDP-9 computer.

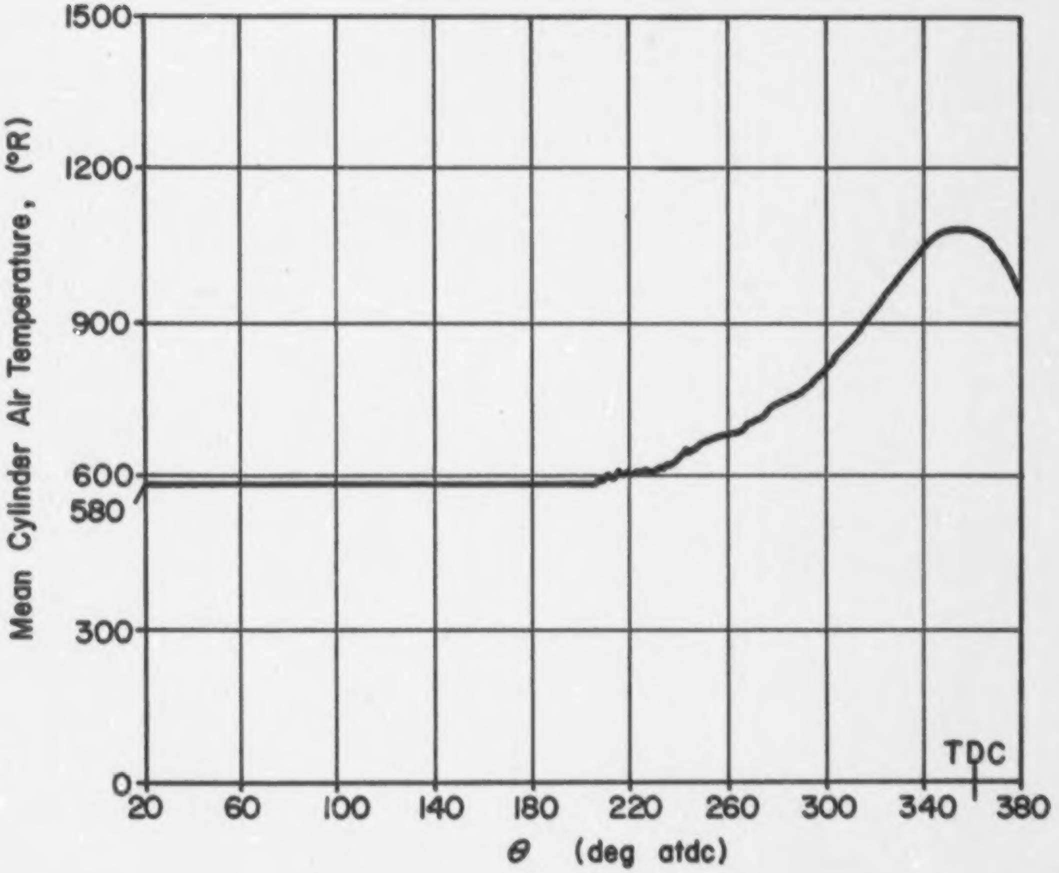

Figure 3.14. Calculated cylinder air temperature and reproduced as an analog signal by PDP-9 computer.

description of the equations used to compute the velocity from the three digitized signals can be found in Appendix B.

Initially the Fortran program was written to calculate velocity as a function of crank angle for each cycle between the opening of the intake valve to ten degrees after tdc of the compression stroke. The velocities between these limits were written on magnetic tape for thirty consecutive cycles. After a preliminary investigation, the Fortran program was rewritten to calculate the velocity between 60 deg btdc to 10 deg atdc for 200 consecutive cycles. The velocity statistics calculated as a function of crank angle for both sample sets were:

1. Sample mean $[\overline{U}(\theta)]$,
2. Sample standard deviation $[S(U(\theta))]$.
3. Cross correlation between the velocity at a crank angle corresponding to ignition and velocities occurring $\Delta\theta$ degrees from the crank angle corresponding to ignition.

These statistics were calculated in the same manner as those for combustion data using the summation formulas in Appendix A.

3.5 Experimental Procedure

An experimental program was designed to provide information not found in the literature and the experimental data for testing the validity of the hypothesis. Combustion and velocity data for the engine conditions shown in Table 3.7 were used to construct a model relating motored velocity data to combustion data. Once the model was formulated it was tested using the engine conditions shown in Table 3.8.

Table 3.7

Engine Variables Used to Construct Model Relating Motored Velocity Data to Combustion Data

Variable	Range
rpm	600, 900, 1200, 1800
Compression Ratio	7.0
Air-Fuel Ratio	~16.0
Spark Advance	MBT, 35°, 25°, 20°, 15°, 10°btdc
Manifold Vacuum	-4.0 to 4.0 in. Hg
Cooling Water Exit Temp.	
Combustion Data	180F
Motoring Data	120F
Lubricating Oil Temperature	115F
Intake Manifold Temperature	120F
Fuel	Isooctane
Stoichiometric Air-Fuel Ratio	15.12
Intake System	Fuel Atomizer
Base Conditions:	
rpm	900
Manifold Vacuum	0.0 in. Hg
Compression Ratio	7.0
Spark Advance	MBT (30°btdc)
Air-Fuel Ratio	~16.0

Table 3.8

Engine Variables Used to Test Model Constructed From Engine Variables in Table 3.7

Base Conditions:	Same as Table 3.7 except:
Air-Fuel Ratio:	17.7, 16.2, 14.5
Base Conditions:	Same as Table 3.7 except:
Air-Fuel Ratio:	15.3
Intake System:	Mixing Tank[1]

---

[1] See Kenemuth (5) for description of mixing tank.

The procedure established for the combustion data consisted of an initial period to allow the engine to reach steady state conditions. Steady state was reached when the oil, water and manifold temperatures remained constant at the desired levels for a five to ten minute interval. During the initial warm-up period, instruments and electronic equipment were turned on, and adjusted. Gas analysis equipment was zeroed and calibrated. The PDP-9 was then made ready to digitize signals. Having ascertained that the engine was at steady state and all signals were properly conditioned, data were recorded for 30 consecutive seconds of engine operation. Once the data were recorded, an engine variable was changed to another test condition and the procedure repeated.

The experiment using the velocity sensor required motoring the engine with no fuel addition at the manifold pressures and speeds for which the combustion data had been taken. The velocity sensor was located in the combustion chamber after engine warm-up. The sensor was positioned halfway between the piston crown and cylinder head wall with the piston at tdc. The angular position was such that the velocity passing through the intake valve opening was normal to the sensor length. Sensor location is shown in Fig. 3.15. All velocity data were taken with the same sensor location. The recorded data was subsequently analyzed using the Fortran programs described in section 3.4 and Appendix B.

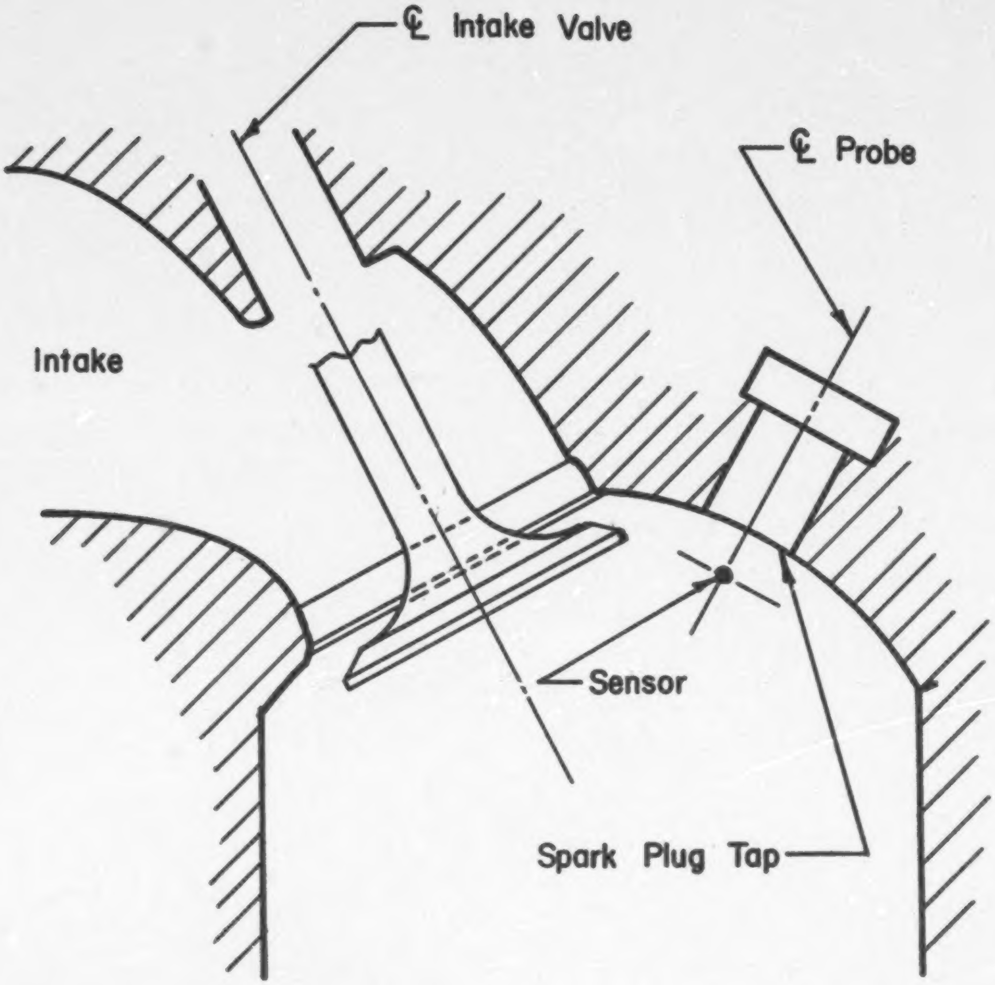
℄ Intake Valve
℄ Probe
Intake
Sensor
Spark Plug Tap

Figure 3.15. Sensor location in combustion chamber where air velocity was measured.

Chapter 4

PRELIMINARY EXPERIMENTAL RESULTS

Data were required to establish effects of experimental accuracy on describing C.B.C. variations, and to establish those criteria which were mentioned in the closing of Chapter 2. The preliminary data were used specifically to:

1. Establish effects of experimental accuracy,
2. Identify a pressure development characteristic which is directly related to the cause of C.B.C. variations,
3. Identify a gas motion characteristic whose C.B.C. variations can be related to C.B.C. combustion variations.

Each of these items are discussed relative to experimental results.

4.1 Experimental Accuracy

4.1.1 - Absolute Measurements - The absolute measurement of the engine variables air-fuel ratio, compression ratio, temperatures, cylinder volume, and pressure are a function of calibration and the ability to change one variable while the other variables are held constant. The range of the absolute values for each variable is given in Table 4.1. Absolute measurement of engine variables and manifestations of the combustion process are difficult. The relative differences between engine variables are more accurate if the errors relative to an absolute base are approximately constant. The purpose of the experimental program was not to determine effects of small differences from an absolute base, but rather the differences in C.B.C. variations for a range of engine variables. For this purpose the accuracies presented in Table 4.1 are adequate.

Table 4.1

Accuracy of Engine Variables and Measured Combustion and Gas Motion Variables

Engine Variables	Accuracy
Speed (rpm)	± 0.33%
Spark Advance	± 0.25 deg
Compression Ratio (7.0)	± 0.1
Air-Fuel Ratio (Calibration)	± 0.3
Air-Fuel Ratio (CO and CO_2)	± 0.2
Temperatures (Water, Oil)	± 2.5F
Pressure (Manifold)	± 0.1 in. Hg
Measured Variables	
Cylinder Pressure (Combustion Data)	± 5 psi
Cylinder Pressure (Motored Data)	± 1.0 psi
Timing Mark (tdc)	± 0.5 deg
Cylinder Rate of Pressure Change	± 1000 psi/sec
Velocity (Intake Stroke)	± 5%
Velocity (Compression Stroke)	± 5% - 20%

The absolute accuracy of velocity measurements in the combustion chamber are difficult to ascertain. A qualitative indication of the velocity measurement accuracy was made using two sensor operating temperatures, 700 and 800F. The average velocity for 30 cycles as a function of crank angle is shown in Fig. 4.1 for each sensor temperature. The results for each sensor temperature are similar except within 30 degrees of tdc of the compression stroke. Maximum cylinder temperatures occur close to tdc causing $T_s - T_a$ to be a minimum. Inaccuracies in determining the cylinder air temperature result in inaccurate velocity measurement. These inaccuracies in cylinder temperature are most pronounced for the small values of $(T_s - T_a)$ occurring near tdc of the compression stroke.

The sensitivity of bridge voltage to cylinder temperature was decreased by using the higher sensor temperature. The bridge voltage sensitivity to velocity was thereby increased. The reported velocity data were obtained using a sensor temperature of 800F.

4.1.2 - Repeatability of Experiments - The repeatability of the experiments at the same engine operating conditions is shown in Table 4.2. The controlled variables, spark advance, compression ratio, fuel rate, etc., were the same for both runs. The measured quantities, temperature, pressure, etc. indicate the repeatability of the experiment with respect to the controlled variables. The sample standard deviations $S(P_{max})$ and $S(\dot{P}_{max})$, are used to measure the extent of C.B.C. combustion variations. Both measured and controlled variables affect these values, however, the difference between two runs with identical controlled variables are seen to be less than the differences expected at the five percent level of significance due to a finite population

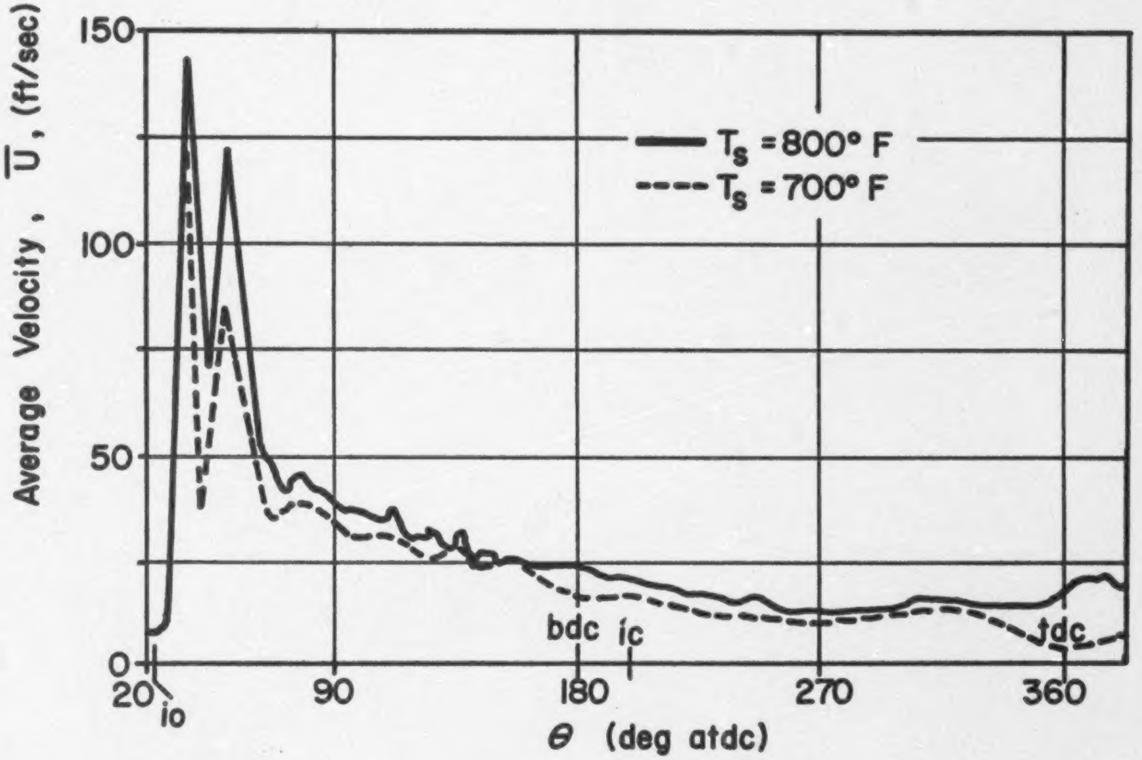

Figure 4.1. Average velocity of 30 engine cycles for two sensor temperatures.

Table 4.2

Repeatability of Similar Engine Operating Conditions

Engine Operating Conditions:
9.0 CR, 900 rpm, 23° Spark Advance

Measured Engine Operating Variables	Run No. 1	Run No. 2
Barometer (in. of Hg)	28.75	28.8
Dynamometer Load	22.9	23.0
Air-Fuel Ratio	14.7	14.6
Intake Manifold Temp. (F)	122	122
Intake Manifold Pressure (in. Hg)	-0.2	0.0
Exit Water Temperature (F)	180	180
Oil Temperature (F)	115	115
Exhaust Temperature (F)	780	800
Statistics		
$\overline{P}_{max}$ (psi)	467.0	470.0
$S(P_{max})$(psi)	48.3	45.4
$\overline{\dot{P}}_{max}$(psi/sec)	66,800.0	69,100.0
$S(\dot{P}_{max})$(psi/sec)	13,600.0	13,100.0
$CC(P_{max},\dot{P}_{max})$	0.916	0.885
Number of Cycles, N	227	228

Ratio of P_{max} variances = 1.129

Ratio of $\dot{P}_{max}$ variances = 1.075

Ratio of variances at 5% level of significance = 1.260

size. Identical runs were repeated after the engine was disassembled, and although their magnitude had changed, which was expected, the trends with respect to compression ratio, speed, and air-fuel ratio were identical to the runs before the engine was disassembled. This investigation is primarily concerned with the effects of engine variables on C.B.C. variations. In this context, the experiments were repeatable.

4.1.3 - C.B.C. Variations of Engine Variables - Cycle-by-cycle variations of engine components and measured variables could cause significant C.B.C. variations in the combustion process. The three most important variables whose C.B.C. variations would affect C.B.C. combustion variations are:

1. Variations in the ignition timing,
2. Variations in the fuel ingested per cycle,
3. Variations in the air-fuel mixture ingested per cycle.

The C.B.C. variations in ignition timing were qualitatively evaluated using a timing light. Observation of 50 to 100 cycles indicated that the ignition timing range was ± 0.5 crank angle degrees at 1800 rpm. These results are in agreement with Cheeseman (28), who evaluated the ignition C.B.C. variations of the engine used in this investigation.

Kenemuth et al. (5) used a hydrocarbon detector to observe time variations of the fuel in a sample air-fuel mixture drawn from the intake manifold. Kenemuth concluded that the small fuel variations observed could not cause more than 5% of the C.B.C. combustion variations.

The variations in the amount of charge ingested per cycle were investigated by measuring the air-fuel mixture velocity in the intake manifold. The velocity signal was integrated over the time interval the intake valve was open. The integrated velocity signal was then recorded and analyzed along with the cyinder pressure under firing conditions. The correlation coefficient between P_{max} variations and the integrated velocity variations was less than 0.08. This indicates that the association between variations in the amount of charge ingested per cycle and P_{max} variations is less than 10%. The variation of P_{max}, $S(P_{max})$, under motored conditions was 1.5 psi. This value indicates the C.B.C. variations of mass ingested per cycle to the average mass ingested is less than one percent.

The effect of the C.B.C. variations of spark timing, fuel ingested per cycle, and mixture mass ingested per cycle could not cause the large C.B.C. combustion variations that exist. In fact, the experimental evidence indicates that less than 10 percent of the combustion variations can be attributed to C.B.C. variations of the afore mentioned variables.

4.1.4 - Frequency Distribution Characteristics - Numerous statistical techniques, concerned with sampling, involve the use of a normal distribution. These statistical methods and tables derived for the normal distribution are a distinct advantage in evaluating whether significant differences occur in the sample standard devaitions. If the C.B.C. variations are approximately normally distributed, these statistical methods could be applied to this investigation. The frequency distribution of P_{max} under firing conditions was examined using the coefficients of skewness and kurtosis. These values are compared to a normal distribution in Table 4.3 for three engine speeds.

Table 4.3

Coefficients of Skewness and Kurtosis for P_{max}

Speed rpm	CR	A/F	$CS(P_{max})$	$CK(P_{max})$
900	9:1	15.9	-0.03	2.44
1200	9:1	16.5	+0.08	2.72
1800	9:1	15.7	+0.09	2.53
For a normal distribution			0.0	3.0

The skewness values indicate that the distributions are slightly positively or negatively skewed. Kurtosis values indicate the distributions are slightly flatter than a normal distribution. It is not evident if these values of skewness or kurtosis indicate a significant difference of the distribution from a normal distribution. For this reason, cumulative percentage frequency distributions were plotted on normal probability paper. A typical result is shown in Fig. 4.2. Figure 4.2 indicates that the values of skewness and kurtosis in Table 4.3 are not significant and an assumed normal distribution can be used to determine the cumulative distributions. The effect of previous cycles on P_{max} of a given cycle was determined using the autocorrelation of P_{max} as a function of cycle difference. Typical results are shown in Fig. 4.3. The autocorrelation never exceeded a value of 0.181 which is the critical value at the one percent significance level.

The conclusions based on the experimental evidence presented above are that the frequency distribution of the C.B.C. variations can

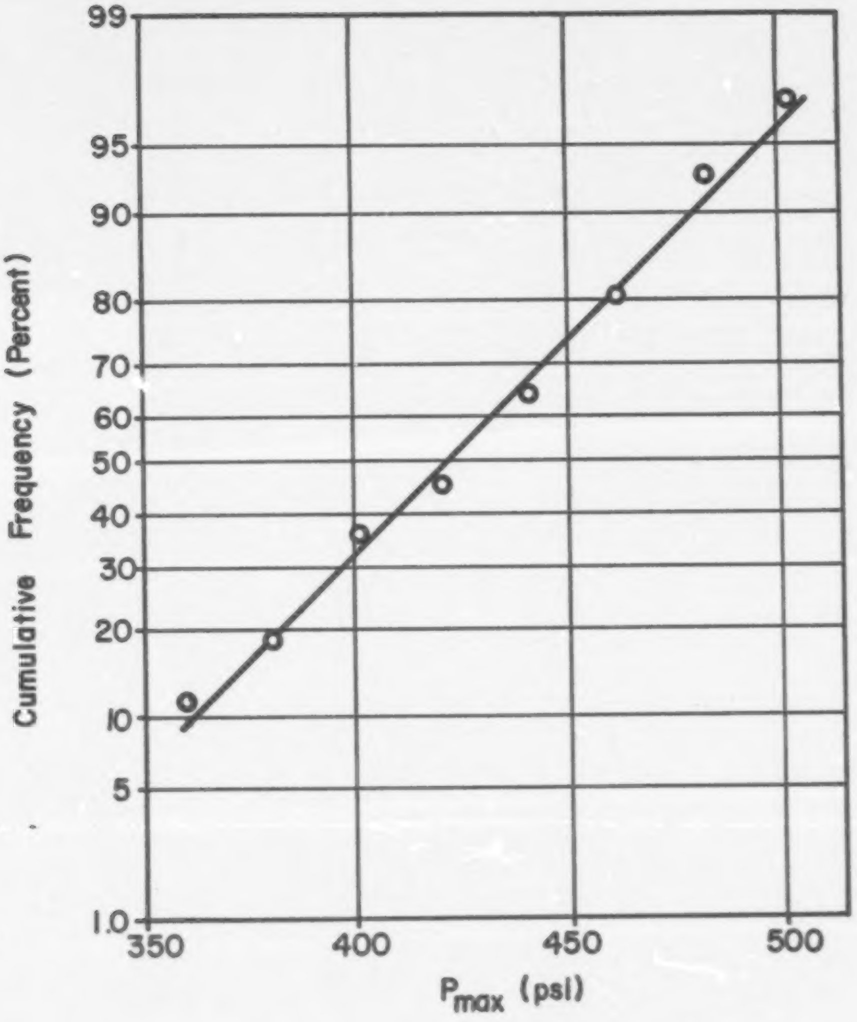

Figure 4.2. Cumulative frequency distribution of maximum cylinder pressure plotted on normal probability coordinates.

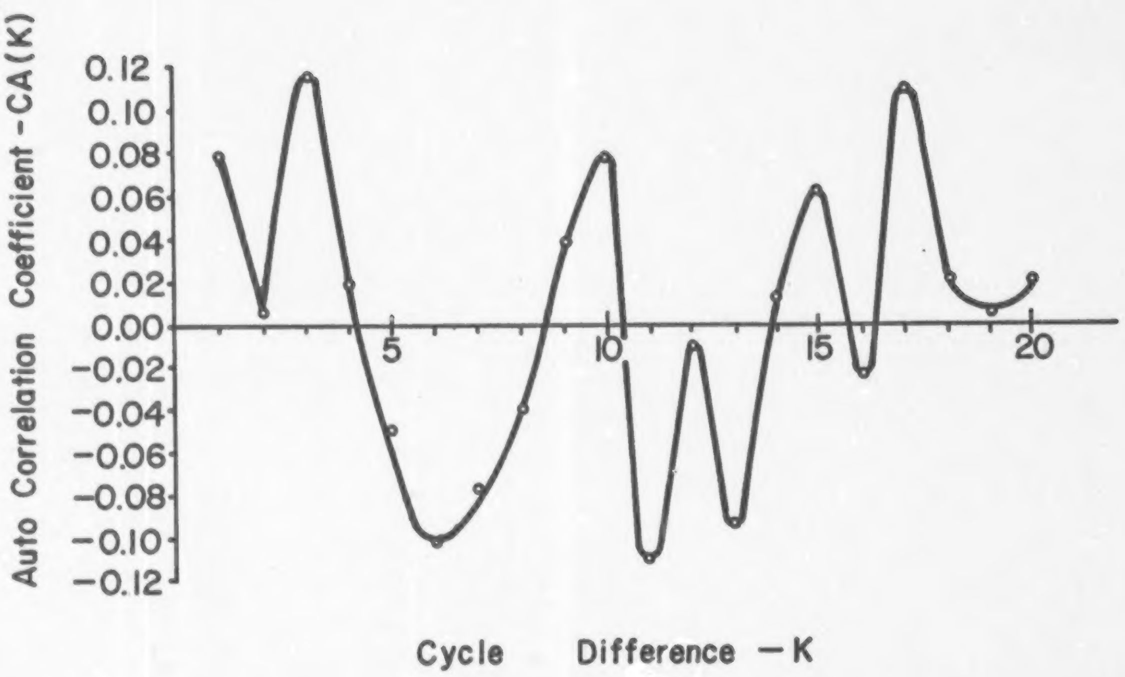

Figure 4.3. Auto correlation of maximum cylinder pressure as a function of cycle difference.

be approximated by a normal distribution and secondly, the combustion variations depend only on the events during intake and compression strokes of the same cycle.

4.1.5 - Sampling Interval Effects - Digitizing analog signals results in digital values which fall between two limits. The difference between these limits is the sampling resolution. For the combustion data the sampling resolution was 2 psi for P_{max} and 1.5 degrees of crank angle travel at 900 rpm. A finite sample resolution presents two problems: 1) sampling exactly when P_{max} occurs and 2) determining the sample standard deviation. An approximate solution for the first problem is obtained by assuming a Taylor series expansion for the cylinder pressure

$$(P - P_{max}) = \frac{(D\theta)^2}{2} \overline{\frac{d^2P}{d\theta^2}} [\theta(P_{max})]. \qquad (4.1)$$

The difference, $P - P_{max}$, with respect to the sampling resolution, $D\theta$, can be evaluated using Eq. 4.1. The value of $d^2P/d\theta^2$ at $\theta(P_{max})$ was estimated from $\bar{\dot{P}}_{max}$ and $\bar{\theta}(P_{max}) - \bar{\theta}(\dot{P}_{max})$,

$$\overline{\frac{d^2P}{d\theta^2}} [\theta(P_{max})] = \frac{\bar{\dot{P}}_{max}}{[\bar{\theta}(P_{max}) - \bar{\theta}(\dot{P}_{max})]}. \qquad (4.2)$$

At the base conditions presented in Table 3.7, the value of $(P - P_{max})$ was 1.5 psi, which is less than the sampling resolution of P_{max}.

The second problem can be solved by assuming a known normal distribution with a standard deviation, σ. The standard deviation of this known distribution, determined by numerical integration with a step size equal to the sample resolution, can be compared to the actual standard deviation. Using a step size equal to one half the actual standard deviation the distribution's numerically computed standard deviation is within 0.1 percent of the actual value.

The effects of sample resolution on the sample standard deviation are inconsequential compared to other considerations.

4.1.6 - Sample Size Effects - Sample size affects the accuracy with which a frequency distribution can be determined. In turn the higher the statistical moment is, the more accurately the frequency distribution must be determined to provide the same confidence interval. Statistical tests of significance are used primarily to determine the effects of sample size.

The 95 percent confidence intervals for the actual standard deviation, σ, relative to the sample standard deviation, S, for sample sizes of 200 and 450 are

$$0.915 \leq \frac{\sigma}{S} \leq 1.104 \quad N = 200,$$

$$0.94 \leq \frac{\sigma}{S} \leq 1.07 \quad N = 450.$$

For example, if the sample standard deviation for 200 samples was 50 psi, the 95 percent confidence interval for σ would be, 46 psi $< \sigma <$ 55 psi.

The ratio of two sample standard deviations S_1 and S_2, each from a 200 sample size must be greater than 1.12 to be considered significantly different at the 95 percent confidence level. These examples indicate that sample size has a significant effect on the sample standard deviation.

Kenemuth et al. (5) determined that engine variables caused significant differences in the C.B.C. combustion variations. The statistical tests used were the F test and Bartlett's test. Since engine variables have been shown to cause significant differences in C.B.C. variations, these tests will not be used herein. Rather, the variations will be compared for changes in engine variables, and reasons for the differences in the variations deduced, cognizant that 10 percent differences in two sample standard deviations are not statistically significant.

4.2 Pressure Development Characteristic

The literature indicated that a characteristic of the pressure development must be identified whose variation is directly related to C.B.C. variations. Also, the combustion variations appear to be due to large variations in the combustion process within 15 degrees of ignition (7,9,10). For these reasons experimental values of $\overline{P}_{max}$, $\overline{\dot{P}}_{max}$, $\overline{\theta}(P_{max})$ and $\overline{\theta}(\dot{P}_{max})$ were determined as a function of the spark advance. If the cause of the variations occurs during the first 15 crank angle degrees after ignition, then average values obtained by different spark advances should be similar to the C.B.C. combustion variations. The values of $\overline{P}_{max}$ as a function of $\overline{\theta}(P_{max})$, determined by advancing the spark are shown in Fig. 4.4. These average values are shown to be similar to C.B.C. variations by estimating $S(P_{max})$ from the experimental value of $S(\theta(P_{max}))$. The experimental value of $S(\theta(P_{max}))$ was used to determine an estimated value of $S(P_{max})$, using the average values obtained by advancing the spark. The method is shown in Fig. 4.4. The estimated values of $S(P_{max})$ are then compared to the experimental values of $S(P_{max})$ in Fig. 4.5. The estimated and experimental values of $S(P_{max})$ have a nearly one to one relationship. These results indicate quantitatively that the cause of combustion variations occurs within the first 15 degrees of crank angle travel after ignition. It appears that approximately 5% to 80% of the fuel

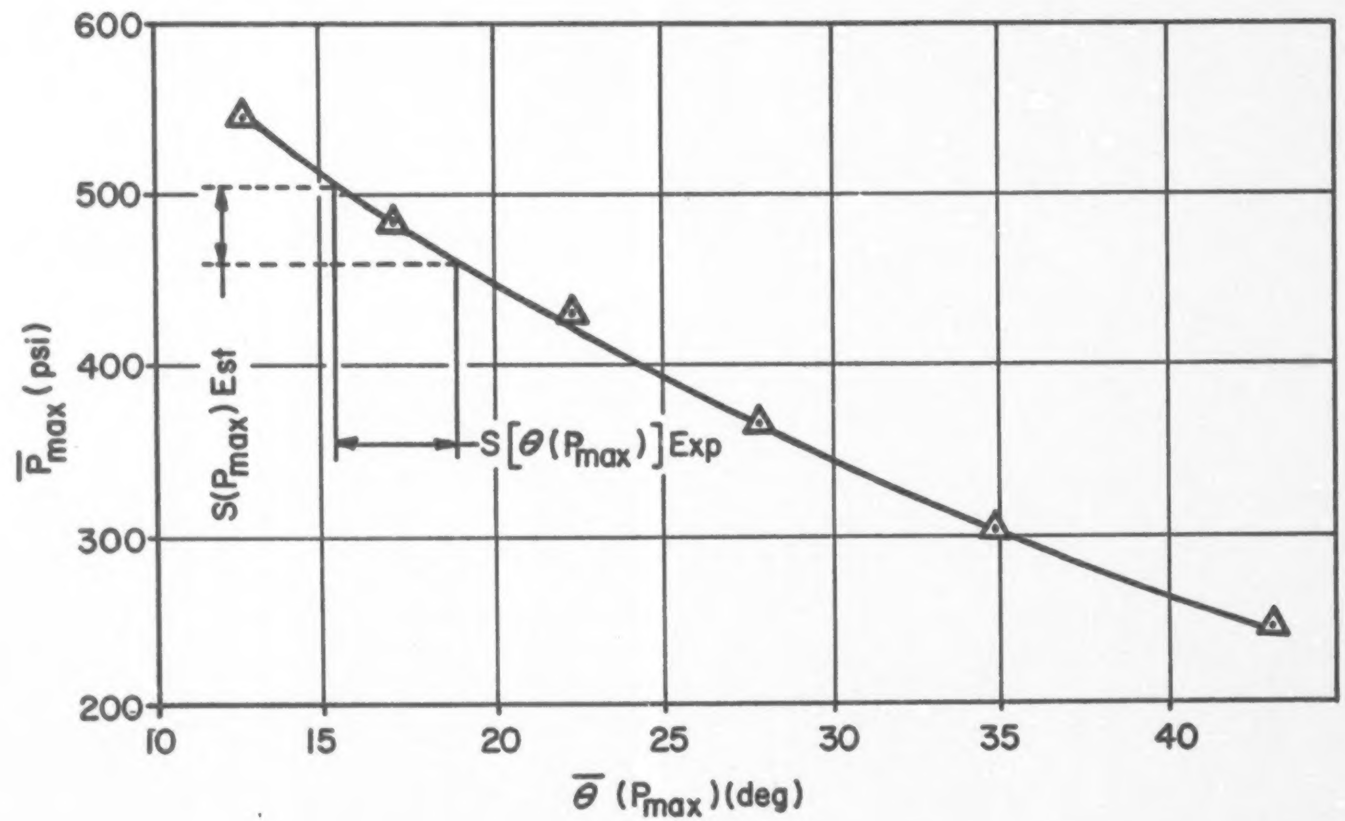

Figure 4.4. Average maximum cylinder pressure as a function of its average crank angle of occurrence produced by different spark advances.

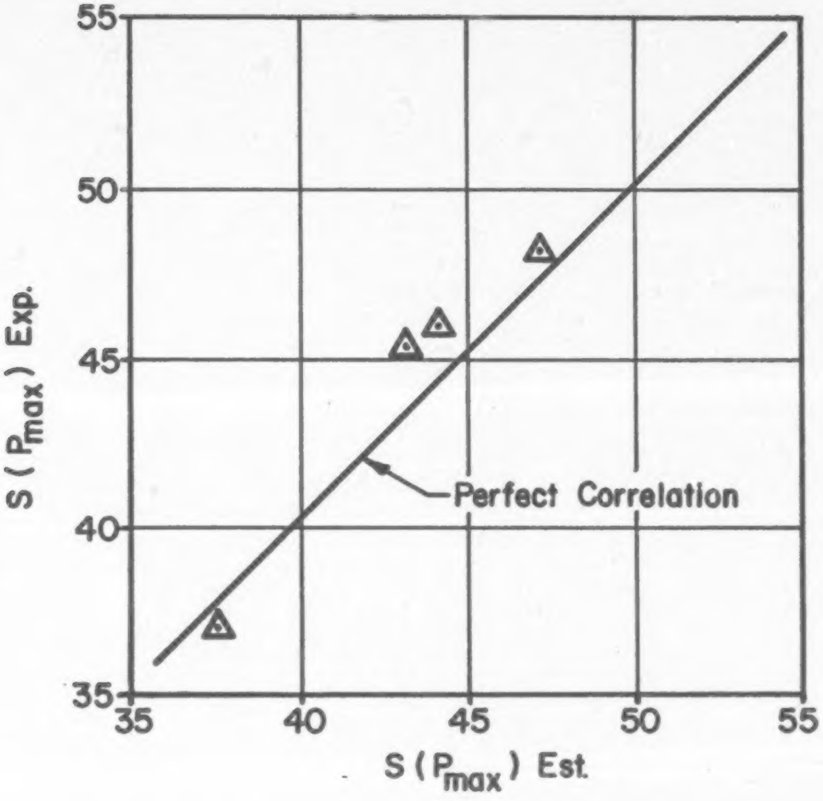

Figure 4.5. Correlation between estimated values of S(P_{max}) and experimentally determined values of S(P_{max})

mass is burned over a crank angle duration that does not vary appreciably from cycle to cycle. The crank angle duration to burn the first 5% of the fuel mass does vary from cycle to cycle and results in C.B.C. variations. Examination of cumulative heat release curves such as Fig. 2.3, offers further evidence. The time or crank travel required to burn approximately the first 5% of the fuel mass will be referred to as the "initial burn duration". The C.B.C. variation of the initial burn duration causes the C.B.C. combustion variations, and a direct indication of the duration's C.B.C. variations must be determined.

Since the $\overline{P}_{max}$ versus $\overline{\theta}(P_{max})$ curve produced by different spark advances is similar to C.B.C. combustion variations, a pressure development characteristic whose average value change is similar to the change in spark advance would be desirable. In this respect, two pressure development characteristics were measured that could provide this relationship, $\theta(P_{max})$ and $\theta(\dot{P}_{max})$. The combustion data indicates that $\theta(P_{max})$ provides this relationship. Figure 4.6 illustrates the relationship between spark advance and $\overline{\theta}(P_{max})$. A five degree change in spark advance produced a five degree change in $\overline{\theta}(P_{max})$. This relationship was valid until the correlation coefficient between $\dot{P}_{max}$ and $\theta(\dot{P}_{max})$ exceeded 0.2. These results indicate $S[\theta(P_{max})]$ can be used to quantitatively measure the C.B.C. variations of the initial burn duration.

The pressure development characteristic directly related to the gas motion variations is the C.B.C. variations of $\theta(P_{max})$. The sample standard deviation, $S[\theta(P_{max})]$, is a measure of the C.B.C. variation in the initial burn duration.

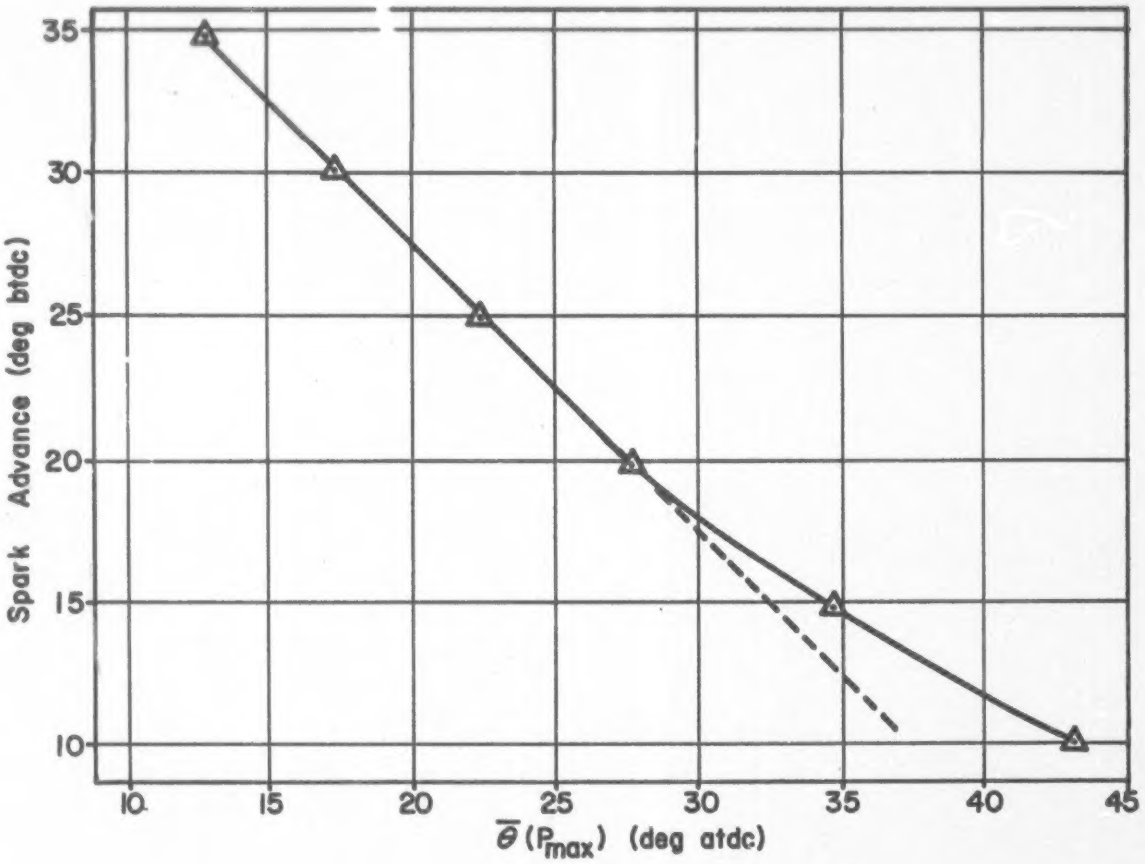

Figure 4.6. Spark advances which produced changes in the average values of the crank angle at which maximum pressure occurred.

4.3 Gas Motion Characteristic

A characteristic of the gas motion which results in variations of the initial burn duration must be identified. In this respect, the air velocity in the combustion chamber was examined for 30 consecutive engine cycles. The velocity for one crank revolution is shown in Fig. 4.7. The sensor location used for all velocity measurements is shown in Fig. 3.15. The C.B.C. velocity variations during the intake process were compared to the C.B.C. velocity variations during compression and attempts were made to correlate characteristics of each. If such a correlation existed, perhaps velocity measurements could be made in the intake manifold and correlated directly with P_{max} or $\theta(P_{max})$ for firing conditions. Such a correlation between intake and compression velocities could not be established. Experimental results did, however, indicate that the large velocity variations in time during the intake persisted into the compression stroke and a qualitative indication of velocity variations was established. Intake velocity variations in time caused velocity variations in the combustion chamber. A conceptual representation of the velocity pattern in the combustion chamber after intake valve closure is shown in Fig. 4.8. Within the cylinder volume there exist local regions of high velocity and low velocity. The intake process causes a heterogeneous space variation of the velocity during the compression stroke. If a region of high velocity is positioned near the spark at ignition, the initial burn duration would be shorter than if a low velocity was so positioned, assuming corresponding levels of small scale turbulence accompany these velocities. Such changes in the gas motion from cycle to cycle could cause the C.B.C. variations of the initial burn duration. The initial

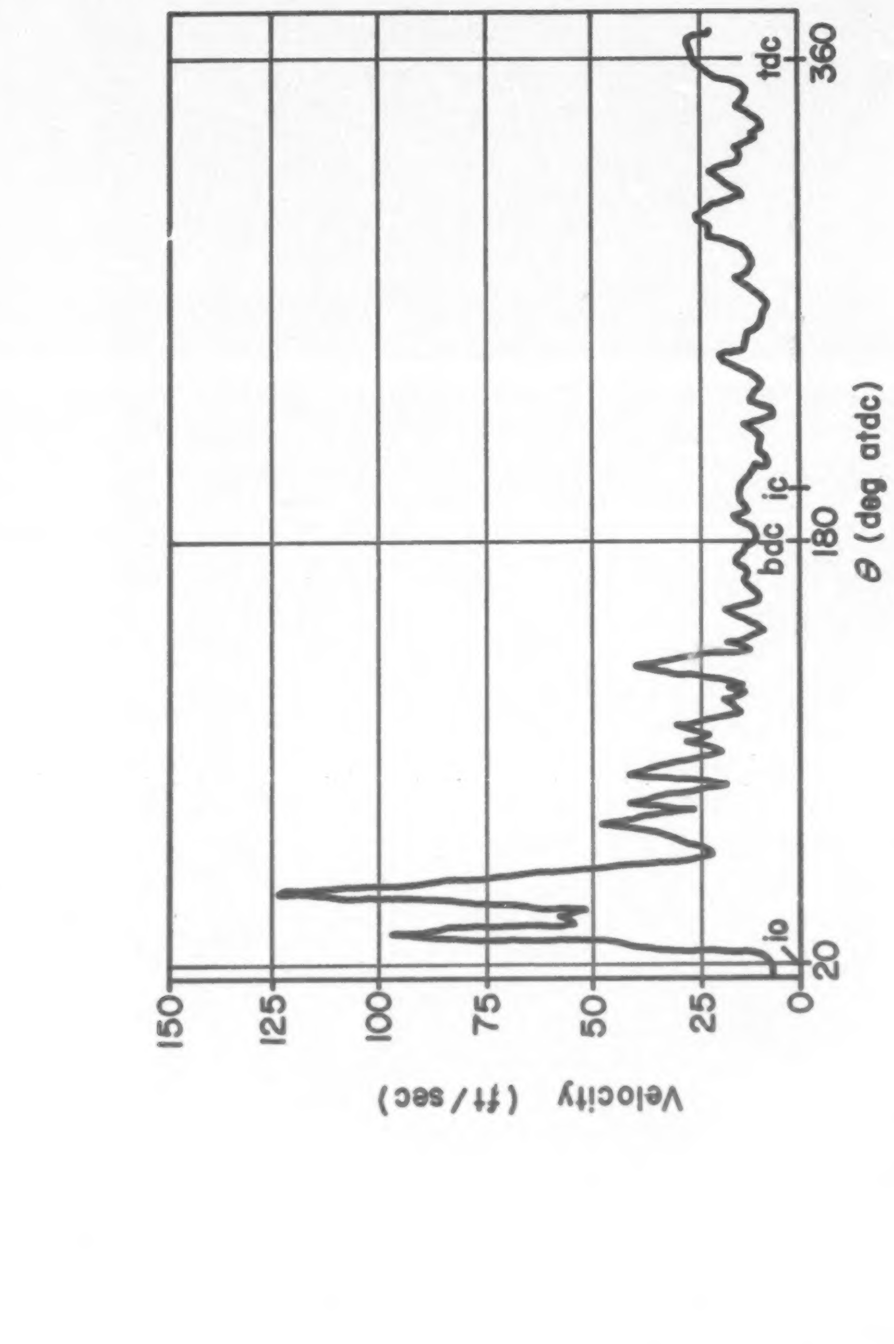

Figure 4.7. Velocity for one revolution of the crank.

H - region of higher than average velocity
M - region of average velocity
L - region of lower than average velocity

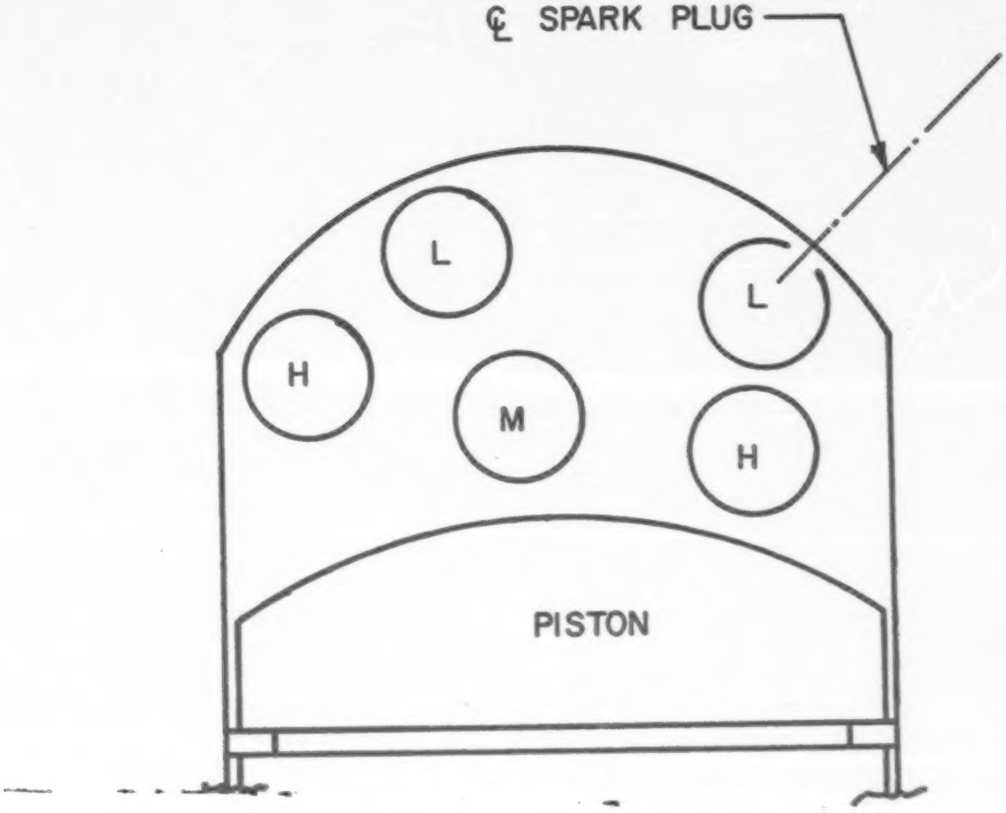

Figure 4.8. Conceptual schematic of velocity pattern in the combustion chamber after intake valve closure.

burn duration is influenced by the small scale turbulence accompanying the local velocity until the flame front area is large enough to intercept the large scale velocity variations which exist in the cylinder. At this time, the flame front then travels across the combustion chamber in a time period which is repeatable or very nearly from cycle to cycle.

Implicit in this reasoning is that the velocity which exists near the spark plug at ignition persists for crank angle intervals corresponding to the initial burn duration. Experimental verification that the velocity magnitude persists for approximately 10 to 15 degrees after ignition is shown in Fig. 4.9. The correlation coefficients between the velocity at crank angles corresponding to ignition and the velocity at crank angles, $\Delta\theta$, away from ignition are shown as a function of $\Delta\theta$ for four engine speeds. The correlation coefficient indicates that if a high or low velocity exists in the vicinity of the spark during a given cycle it remains high or low for approximately 15 degrees of crank travel. The higher the engine speed the larger the crank angle interval for which the velocity persists. Experimental results also indicate that the C.B.C. variations of the initial burn duration increase with engine speed.

The experimental data indicate that C.B.C. variations in the gas velocity in the vicinity of the spark plug result in C.B.C. variations in the initial burn duration. The measure used to indicate the extent of C.B.C. gas motion variations is the sample standard deviation of the velocity at a crank angle corresponding to the spark timing. The C.B.C. variations of the initial burn duration are measured using the sample standard deviation of $\theta(P_{max})$, $S[\theta(P_{max})]$. The velocity and initial burn duration variations will not be measured simultaneously.

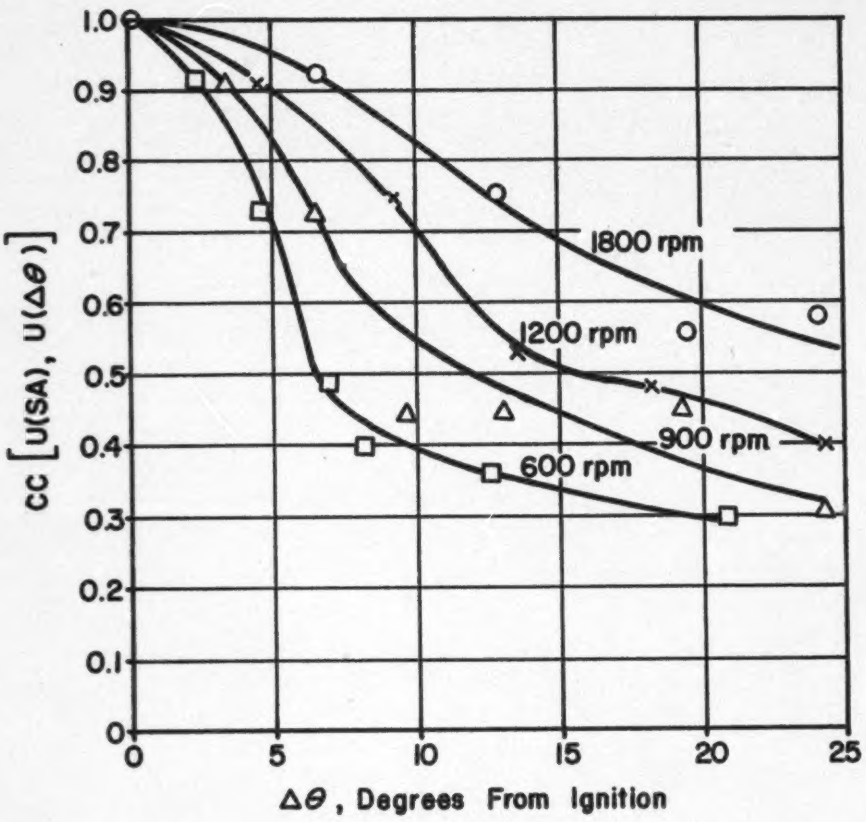

Figure 4.9. Correlation between the velocity at crank angles corresponding to ignition and the velocity occurring Δθ degrees after ignition.

Instead, a model is constructed which relates the sample standard deviations of each variable. Experimental results are then used to verify and test the model. The correlation between the model and experimental results are used to draw conclusions about the hypothesis.

Chapter 5

EMPIRICAL MODELS USED TO CORRELATE CAUSE AND EFFECT OF C.B.C. VARIATIONS

A model, based on experimental evidence, is constructed which relates the C.B.C. variations in the initial burn duration to C.B.C. velocity variations. The last sections in the preceeding chapter establish the measured characteristics used to indicate the extent of each. Different values of the extent of variation are produced by changes in engine variables. The model reflects initial burn duration variations with respect to velocity variations and engine variables. Similarly, a quantitative indication of the effect of initial burn duration variations on $S(P_{max})$ is established. This quantitative indication allows the separation of engine variable effects on the initial burn duration from their effects on the combustion process.

5.1 Model Relating C.B.C. Initial Burn Duration and Velocity Variations

Mixture motion affects the flame front speed as it moves through the cylinder. Evidence presented in Chapter 4 indicates C.B.C. velocity variations in the vicinity of the spark plug at the time of ignition result in C.B.C. variations in the time required to burn approximately, the first 5% of the fuel mass. The dependency of the initial burn duration on velocity are determined using an expression derived from the following model.

Consider that the cylinder volume is divided into two regions, an unburned and burned region as shown in Fig. 5.1. The flame front is positioned at a radius, r_b, at a time, t_b, after the initiation of ignition. The rate of change of the burned volume is given by the

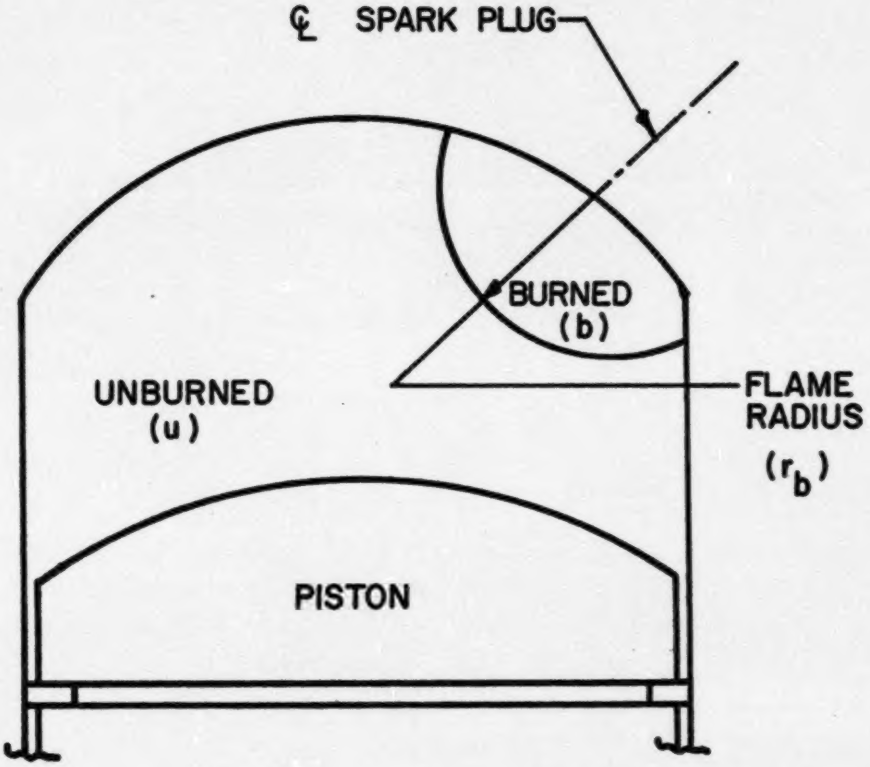
℄ SPARK PLUG
BURNED
(b)
UNBURNED
(u)
FLAME
RADIUS
(r_b)
PISTON

Figure 5.1. Flame front position after ignition used to divide cylinder volume into burned and unburned regions.

following expression (20,29):

$$\frac{dV_b}{dt} = A_b S_b E\ f(U), \tag{5.1}$$

where V_b is the volume of burned gases,

A_b is the area of the flame front,

S_b is the laminar burning velocity,

E is the expansion ratio = $T_b M_u / T_u M_b$,

and f(U) is the increase in S_b as a function of the velocity, U, and is greater than one.

Assuming a hemispheric burning shell of radius r_b, the volume behind the flame front and the flame front area are

$$V_b = \frac{2}{3} \pi r_b^3 \tag{5.2}$$

and

$$A_b = 2 \pi r_b^2. \tag{5.3}$$

Substitution of Eqs. 5.2 and 5.3 into Eq. 5.1 yields the time rate of change of the radius, r_b,

$$\frac{dr_b}{dt} = S_b E\ f(U). \tag{5.4}$$

Only the first few degrees of crank travel after ignition are considered. During this period approximately 2 to 5% of the fuel mass will be burned resulting in a small pressure rise due to combustion. Combustion in constant volume bombs indicate that the expansion ratio, E, is constant for this interval. The effects of increasing pressure and temperature on S_b and E due to piston motion are also small. Heat transfer effects will be neglected, not because they don't have an effect but because from cycle to cycle heat transfer effects appear to be invariant.

Integration of Eq. 5.4, assuming S_b, E and f(U) are constant between the following limits of t,

$$r_b = 0 \quad \text{at } t = 0$$
$$r_b = r_b \text{ at } t = t_b \tag{5.5}$$

yields

$$r_b = S_b E\ f(U)\ t_b. \tag{5.6}$$

The volume burned in time, t_b, using Eqs. 5.2 and 5.6 is

$$V_b = 2/3\pi S_b^3 E^3 f^3(U) t_b^3. \tag{5.7}$$

Equation 5.7 expresses the relationship between the volume burned, V_b, the initial burn duration, t_b, and the increase in the laminar burning velocity due to mixture motion, f(U). The volume burned relative to the cylinder volume at ignition, V_r, is

$$V_r = \frac{V_b}{V_i} = 2/3\ \pi\ S_b^3 E^3 f^3(U) t_b^3/V_i. \tag{5.8}$$

The change in t_b with respect to changes in U can now be stated using the criteria established in Chapter 4. The initial burn duration, t_b, is that time required to burn a small fraction of the total fuel mass. Curry (8) and Obert (30) indicated that for short a period of time after ignition the fuel mass fraction burned and the volume fraction burned are linearly related, i.e.,

$$m_r = \text{constant } (V_r). \tag{5.9}$$

The initial burn duration, t_b, is that critical time in each cycle required to burn the assumed constant mass fraction of fuel or volume fraction that stabilizes the combustion process. The change in t_b with respect to a change in U from equation 5.8 is

$$dV_r = 0 = \frac{\partial V_r}{\partial t_b} dt_b + \frac{\partial V_r}{\partial U} dU \tag{5.10}$$

or

$$\frac{dt_b}{dU} = -(\frac{\partial V_r}{\partial U}/\frac{\partial V_r}{\partial t_b}). \tag{5.11}$$

Evaluating the partial derivatives, $\frac{\partial V_r}{\partial U}$ and $\frac{\partial V_r}{\partial t_b}$, using Eq. 5.8 gives

$$\frac{dt_b}{dU} = - \frac{C_3 V_i^{1/3}}{S_b E} \frac{1}{f^2(U)} \frac{df(U)}{dU} \tag{5.12}$$

where C_3 is an arbitrary constant.

Equation 5.12 is an expression relating changes in t_b to changes in the velocity, U, to burn a constant fraction of the cylinder volume. The derivative, dt_b/dU, can be evaluated in terms of the sample standard deviations assuming the following linear relationship,

$$t_b - \overline{t}_b = CC(t_b,U) \frac{S(t_b)}{S(U)} (U - \overline{U}). \tag{5.13}$$

The derivative, dt_b/dU, is

$$\frac{dt_b}{dU} = CC(t_b,U)\frac{S(t_b)}{S(U)}. \tag{5.14}$$

Since the hypothesis is that t_b and U are related, $CC(t_b,U)$ is taken as one and Eq. 5.14 becomes

$$\frac{dt_b}{dU} = \frac{S(t_b)}{d(u)} . \tag{5.15}$$

Equation 5.15 is with respect to mean values of t_b and U. Using the expression for dt_b/dU in Eq. 5.15, Eq. 5.12 becomes

$$\left[\frac{E\ S_b}{V^{1/3}}\right]_i \frac{S(t_b)}{S(U_i)} = \frac{C_3}{f^2(U)} \frac{df(U)}{dU} = C_3\ g(\overline{U}_i), \qquad (5.16)$$

where the subscript i refers to conditions occurring at ignition. This expression, indicates that, if mixture motion variations are the cause of initial burn duration variations, a high correlation exists between measured values of $S(t_b)/S(U_i)$ multiplied by $\left[\frac{E\ S_b}{V^{1/3}}\right]_i$ and measured values of $\overline{U}_i$.

The expression $[E\ S_b/V^{1/3}]_i$ can be derived from conditions existing at ignition. The cylinder volume at ignition, V_i, is calculated from Eq. B.2 using the crank angle corresponding to ignition. The burning velocity, S_b, is a function of the air-fuel ratio, temperature and pressure existing at ignition. This function is obtained from the experimental data of Garner et al. (31) and Dugger et al. (32) using 2-2-4-trimethylpentane-air mixtures.

$$S_b = C_4 P_i^{-0.4} T_i^{1.4} h(A/F) \qquad (5.17)$$

where

$$h(A/F) = 16.25 - 0.22\ (A/F - 14.35)^2. \qquad (5.18)$$

The expansion ratio, E_i, is a function of the temperatures of the burned and unburned gases and their molecular weights. The chemical reaction consists of complete reaction of isooctane (C_8H_{18}) and air to form the products CO, CO_2, H_2O, O_2, and N_2. The ratio of molecular weights is a function of the mixture air-fuel ratio only. The temperature ratio $(T_b/T_u)_i$ was approximated using the adiabatic flame temperature for T_b. The adiabatic flame temperature was calculated for different air-fuel ratios and mean cylinder gas temperatures at ignition. Pressure effects were found to be negligible. The expansion ratio, E_i, was evaluated over the following air-fuel ratio and temperature ranges using the Hottel Charts (33),

$$\begin{aligned} 1000R < T_i < 1600R, \\ 14.0 \le A/F \le 18.0. \end{aligned} \tag{5.19}$$

The functional dependence of the expansion ratio, E_i, on the temperature at ignition and air-fuel was then approximated using the relationship

$$E_i = \frac{T_b}{T_i}\frac{M_u}{M_b} = \frac{C}{(T_i^{0.66}A/F^{0.33})} . \tag{5.20}$$

Substituting the expressions for E_i and S_b as functions of the air-fuel ratio, temperature and pressure at ignition gives for Eq. 5.16,

$$\frac{P_i^{-0.4}T_i^{0.74}}{V_i^{0.33}} \frac{h(A/F)}{(A/F)^{0.33}} \frac{S(t_b)}{S(U_i)} = C_3\ g(\overline{U}_i) \tag{5.21}$$

The polytropic process expression for the compression stroke up to ignition,

$$P_i V_i^{1.33} = P_{ic} V_{ic}^{1.33}, \tag{5.22}$$

can be used to reduce Eq. 5.21 to an expression involving measured engine operating variables

$$F(O.V.)\ \frac{S(t_b)}{S(U_i)} = C_3\ g(\overline{U}_i), \tag{5.23}$$

where

$$F(O.V.) = \frac{h(A/F)}{\rho_{ic}^{0.4}(A/F)^{0.3}}, \tag{5.24}$$

and ρ_{ic} is the mixture density at intake valve closure.

Confirmation of the model and determining the function $g(\overline{U}_i)$ was achieved using experimental values of $S(t_b)$, $S(U_i)$ and $\overline{U}_i$ for the engine operating variables given in Table 3.7. The value of the sample standard deviation of the initial burn duration, $S(t_b)$, was determined from the following relationship,

$$S(t_b) = \frac{S(\theta(P_{max}))}{6rpm}. \tag{5.25}$$

The experimental values of $F(O.V.)[S(t_b)/S(U_i)]$ versus the average velocity at crank angles corresponding to ignition, $\overline{U}_i$, are shown in Fig. 5.2. The method of least squares linear regression resulted in a correlation of 0.975 between the variables $\log(F(O.V.)[S(t_b)/S(U_i)])$ and $\log(\overline{U}_i)$. The function, $g(\overline{U}_i)$, was found to be

$$g(\overline{U}_i) = (1/\overline{U}_i)^{1.3}. \tag{5.26}$$

This model was tested using engine variables and conditions other than those used to construct it. These testing variables were those of Table 3.7. The model testing results are shown in Fig. 5.3 with the empirical function relating the C.B.C. initial burn duration and gas motion variables.

The experimental correlation of 0.975 between the variables of the model represented by Eq. 5.23 and subsequent verification using independent engine operating conditions confirm the hypothesis. Gas

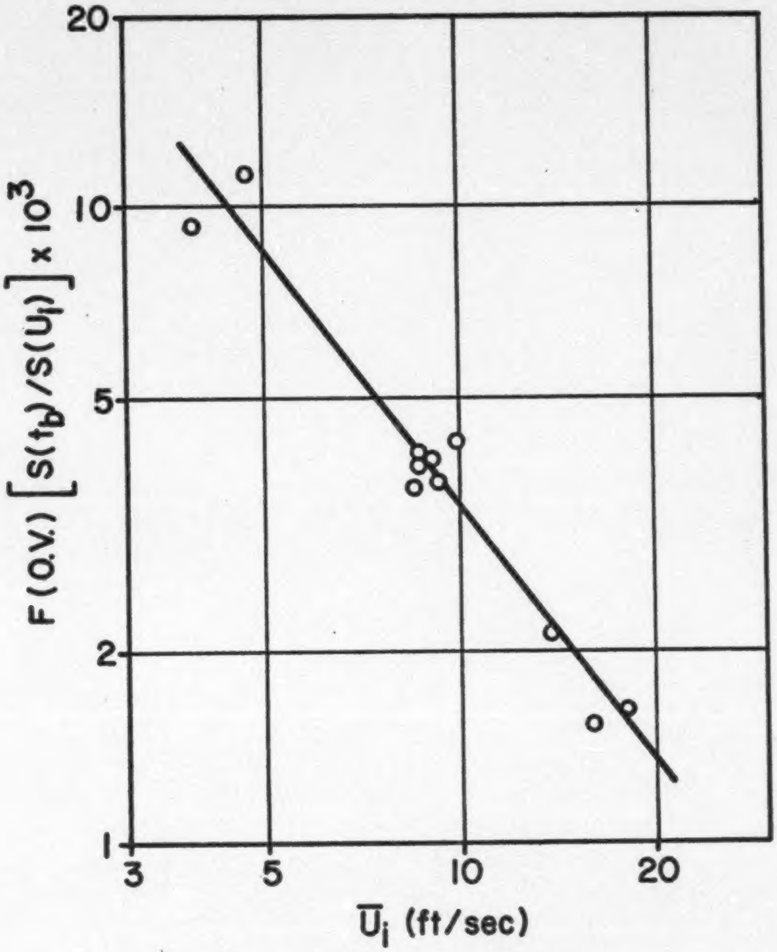

Figure 5.2. Experimental results used to confirm model relating C.B.C. initial burn duration variations to C.B.C. velocity variations at crank angle corresponding to ignition.

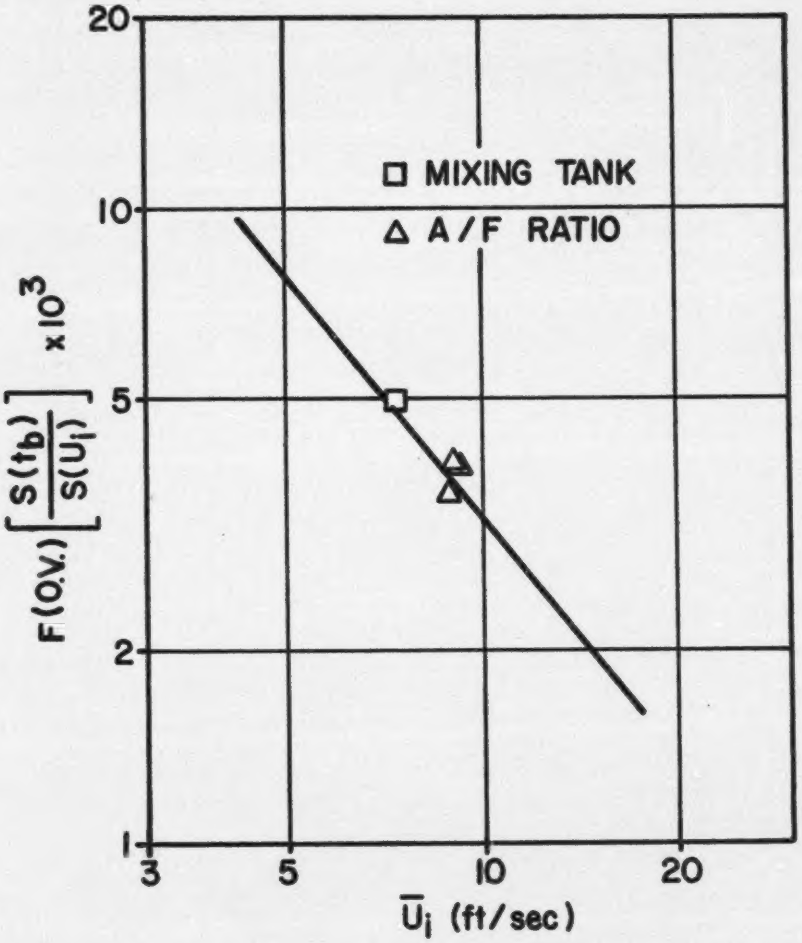

Figure 5.3. Experimental results used to test model.

motion variations from cycle to cycle cause C.B.C. variations in the initial burn duration which result in C.B.C. combustion process variations.

5.2 Maximum Pressure and Torque C.B.C. Variations

The C.B.C. variations of the maximum cylinder pressure for different engine variables are not the same even if the variations in the initial burn duration are equal. The maximum pressure is a function of the initial burn duration and the combustion process up to its occurrence. The C.B.C. variations in maximum pressure are a result of variations of the initial burn duration and the rate at which approximately 85% of the fuel is consumed, the cylinder volume in which the fuel is consumed, the total fuel mass and the piston motion. The combustion process effect on $S(P_{max})$ with respect to engine variables must be separated from effects of the initial burn duration variations.

Assume the relationship between P_{max} and $\theta(P_{max})$ variations to be such that

$$S(P_{max}) = b'S(\theta(P_{max})). \qquad (5.27)$$

The coefficient, b', represents the sensitivity of $S(P_{max})$ to $S(\theta(P_{max}))$. The effect of the combustion process after the initial burn duration is reflected by the value of b'. The experimental data indicate that different quantitative values of b' can be determined for different engine variables and that b' is given by

$$b' = \left|CC(P_{max}, \theta(P_{max})(\frac{S(P_{max})}{S(\theta(P_{max}))}\right| + \left|CC(P_{max}, \dot{P}_{max})CC(\dot{P}_{max}, \theta(\dot{P}_{max})) \right.$$

$$\left. S(P_{max})/S(\theta(\dot{P}_{max}))\right|. \qquad (5.28)$$

The value of b' indicates the effects of the combustion process other than $S(\theta(P_{max}))$ on the variations of maximum pressure. Karim (3) recognized the significance of piston motion, fuel mass, etc., and used the term "phasing" to describe these effects on maximum pressure. The phasing of the combustion process can be thought of as the shape and position of the cumulative energy release curve relative to tdc. Since b' is also an indication of this effect, the effect of b' on combustion variations will be referred to here as the phasing of the combustion process. The higher b' is, the more adverse is the effect of combustion phasing on maximum pressure variations.

An indication of the torque variations relative to the average brake torque, would allow the net effect of combustion process variations to be evaluated. The brake torque C.B.C. variations were approximated by assuming that they are affected only by $S(P_{max})$ and $S(\theta(P_{max}))$. The brake torque variations were calculated by the following relationship,

$$S(T_d) = s_{T_d}(P_{max})\, S(P_{max}) + s_{T_d}(\theta(P_{max}))\, S(\theta(P_{max})). \quad (5.30)$$

The sensitivities, $s_{T_d}(P_{max})$ and $s_{T_d}(\theta(P_{max}))$, were determined from average values of the maximum pressure, the crank angles at which they occur, and the dynamometer scale torque (T_d). These values for 900 rpm, are

$$s_{T_d}(P_{max}) = 0.02 \frac{\text{ft-lbf}}{\text{psi}},$$

$$s_{T_d}(\theta(P_{max})) = 0.03 \frac{\text{ft-lbf}}{\text{deg}} \text{ for 7:1 and 9:1 CR,}$$

$$s_{T_d}(\theta(P_{max})) = 0.20 \frac{\text{ft-lbf}}{\text{deg}} \text{ for 10.5:1 CR.}$$

The ratio, $S(T_d)/\overline{T}_d$, is a quantitative indication of the net effect of C.B.C. variations.

Chapter 6

DISCUSSION OF RESULTS

The effects of the engine variables spark advance, air-fuel ratio, speed and compression ratio on C.B.C. variations are discussed using quantitative measures of the gas motion variations, initial burn duration variations, the phasing of the combustion process, and the coefficient of variation of the brake torque, $CV(T_d)$. The changes in engine variables are relative to the base conditions of 900 rpm, spark advance for maximum brake torque, zero manifold vacuum, 7:1 compression ratio, and approximately 16:1 air-fuel ratio.

6.1 Spark Advance Effects

Spark advance effects on C.B.C. combustion variations are given in Table 6.1.

Table 6.1

Effect of Spark Advance on C.B.C. Variations

SA(btdc)	35°	30°	25°	20°	15°	10°
$S(U_i)/\overline{U}^{1.3}$	0.26	0.264	0.265	0.260	0.261	0.258
F(O.V.)/rpm	0.023	0.023	0.023	0.023	0.023	0.023
$S(\theta(P_{max}))$	3.93	3.44	3.96	4.07	3.89	4.80
b'	9.62	12.1	10.5	9.23	7.72	5.83
$S(P_{max})$	41.8	46.1	48.4	45.3	37.0	32.6
$CV(T_d)$	0.045	0.047	0.052	0.050	0.044	0.045

Retarding the spark from maximum brake torque (30°btdc) causes significant differences in the phasing of the combustion process as indicated by the values of b' in Table 6.1. The parameters associated with velocity variations and initial burn duration variations are not significantly affected. Because b' decreases with spark retardation, the extent of maximum pressure variations also decreases. The reason for this effect, is that as the spark is retarded, the heat release occurs in an increased volume. Thus the volume variation relative to the average volume in which combustion takes place is smaller. The result is a lower sensitivity to initial burn duration variations. The effect of spark advance on $CV(T_d)$ is not significant as both the average and the variations of the brake torque decrease correspondingly.

6.2 Air-Fuel Ratio Effects

The C.B.C. combustion variations as a function of air-fuel ratio at a constant spark advance and manifold vacuum are presented in Table 6.2.

Table 6.2

Effect of Air-Fuel Ratio on C.B.C. Variations

A/F	17.73	16.25	14.50
$S(U_i)/\overline{U}_i^{\,1.3}$	0.265	0.265	0.265
F(O.V.)/rpm	0.018	0.022	0.023
$S(\theta(P_{max}))$	4.6	3.6	3.7
b'	8.0	9.6	9.0
$S(P_{max})$	51.9	41.6	37.5
$CV(T_d)$	0.064	0.045	0.039

Decreasing the air-fuel ratio increases the burning velocity (F(O.V.)) thus decreasing the variations in the initial burn duration. This results in decreasing values of $S(P_{max})$ although the phasing of combustion favors increased variations in the maximum pressure. The net effect of fuel addition is that the average brake torque increases significantly while the torque variations decrease slightly. The result is less engine "surge" as the air-fuel ratio is decreased by fuel addition.

6.3 Speed Effects

Increases in engine speed, at a constant manifold vacuum, increase the velocity during the intake process. The higher velocity causes increases in both small and large scale turbulence. The increase in small scale turbulence with speed is not enough to overcome the large scale velocity variations as evidenced by values of $S(U_i)/\overline{U}_i^{1.3}$ in Table 6.3.

Table 6.3

Effect of Speed on C.B.C. Variations

rpm	600	900	1200	1800
$S(U_i)/\overline{U}_i^{1.3}$	0.31	0.264	0.26	0.25
F(O.V.)/rpm	0.034	0.023	0.018	0.012
$S(\theta(P_{max}))$	2.68	3.44	4.42	5.94
b'	11.9	12.1	11.6	8.43
$S(P_{max})$	35.2	46.1	54.6	72.1

The increases in $S(P_{max})$ with increased speed are a result of gas motion variations. The velocity variations increased in magnitude approximately proportional to the average velocity. The variation in the initial burn duration increased correspondingly, resulting in increased values of $S(P_{max})$ with increasing speed. The values of $S(P_{max})$ did not increase linearly with speed as the quantitative indication of combustion process phasing, b', decreased.

6.4 Compression Ratio Effects

Velocity measurements were not made at compression ratios other than 7.0. Assuming the gas motion effects are primarily a function of speed, the results obtained with varying compression ratio can be examined relative to the phasing of combustion.

Table 6.4

Effect of Compression Ratio on C.B.C. Variations

CR	7.0	9.0	10.5
$S(\theta(P_{max}))$	3.6	3.1	5.1
b'	9.6	8.8	14.2
$S(P_{max})$	41.6	57.2	72.9
$CV(T_d)$	0.045	0.054	0.114

Increases in compression ratio reduce the initial burn duration variations. The phasing of combustion increases accompanying increases in compression ratios caused larger variations in P_{max}. As a result, torque variations become pronounced at the highest compression ratio. In the case of 10.5 compression ratio the value of

$CC(\dot{P}_{max}, \theta(\dot{P}_{max}))$ exceeded a value of 0.2 and caused increases in $S(\theta(P_{max}))$ which are not indicative of the initial burn duration variations. The value of $CC(\dot{P}_{max}, \theta(\dot{P}_{max}))$ does indicate the reason why the phasing of combustion is adversely affected by compression ratio increases. The smaller the clearance volume the greater the volume differences in which the maximum rate of heat release occurs with respect to initial burn duration variations.

The increased C.B.C. combustion variations with respect to increased compression ratio are due to this adverse effect of combustion phasing and result in increased torque variations relative to the average brake torque.

6.5 Relevance of the Results

As was indicated in the first chapter, C.B.C. combustion variations and exhaust emissions are interrelated. Current automotive practice reduces engine emission by retarding the spark from maximum brake torque, lowering the compression ratio and leaning the air-fuel mixture. The results presented in this chapter indicate that engine surge will be reduced or unaffected by all these except leaning the air-fuel mixture. Leaner air-fuel mixtures, however, offer a distinct possibility for exhaust emission reduction. Operation at lean air-fuel mixtures will require reduction of the cause of C.B.C. variations, namely the C.B.C. mixture motion variations in the vicinity of the spark plug at the time of ignition. In other words, the mixture motion will have to be stabilized.

Chapter 7

SUMMARY AND CONCLUSIONS

7.1 Restatement of the Problem

The combustion process of an SI engine exhibits C.B.C. variations which are observed in the cylinder pressure development histories for a number of consecutive engine cycles. The cause of these C.B.C. combustion variations was hypothesized to be C.B.C. variations in the cylinder gas motion. The validity of this hypothesis was to be investigated by experimentally determining the extent of variation of specific pressure development characteristics and the gas motion in the combustion chamber of a CFR engine.

7.2 Conclusions

The conclusions of this investigation with respect to the objectives presented in the first chapter are:

1. The C.B.C. combustion variations are a result of C.B.C. gas velocity variations in the vicinity of the spark plug at the time of ignition.

2. The gas velocity affects the time required to burn approximately the first five percent of the fuel which is defined as the initial burn duration.

3. The sample standard deviation of the crank angle at which maximum pressure occurs is a quantitative measure of the C.B.C. initial burn duration variations.

4. The initial burn duration variations and the phasing of the combustion process determine the maximum pressure C.B.C. variations

and ultimately the torque variations relative to the average brake torque.

5. Qualitatively, the phasing of the combustion process is the shape and position of the cumulative energy release curve relative to tdc of the compression stroke. Quantitatively, the phasing of the combustion process is the absolute sum of the linear regression coefficients between maximum pressure and the crank angles of occurrence of maximum pressure and maximum rate of pressure.

7.3 Recommendations for Future Work

The C.B.C. variations of the gas motion in the vicinity of the spark plug at the time of ignition are the principal cause of C.B.C. combustion variations. The use of shrouded valves (1,7) reduced slightly the combustion variations after careful positioning of the shroud or spark plug. Sonic valves (13) resulted in a very significant reduction of the pressure variations at light loads. However, shrouded valves reduce an engine's breathing capacity (9) and sonic valves are effective only at light loads.

Future work should be directed toward reducing either the gas motion variations in the vicinity of the spark plug at the time of ignition or their influence on the combustion process. Methods which reduce either the velocity variations or the time required to burn the first 5% of the fuel mass should be investigated. These methods could include introduction of a high velocity jet of air-fuel mixture in the vicinity of the spark plug just prior to ignition. The high velocity jet could result in a velocity profile that was repeatable from cycle to cycle and thus stabilize the combustion process. The use of multiple ignition sources (1,9,11) reduced pressure development variations. A single ignition source which ignited a large volume of the mixture could also reduce the combustion variations.

The difficulties in using a high velocity jet would probably limit itsuse to research engines. The most promising area and therefore the area in which most of the future work should be concentrated appears to be the development of a single ignition source which ignites a large volume of the mixture. Such an ignition source would minimize the effects of the velocity variations from cycle to cycle.

The engine variables can be selected to minimize the influence of C.B.C. combustion variations. However, the results presented herein indicate that only small gains are to be made by this approach. The major effort should be directed toward the cause of combustion variations, the gas motion variations in the vicinity of the spark plug at the time of ignition.

REFERENCES

1. Averette, H. S., "A Study of Peak Pressure Variations in the Otto Cycle Engine," S.M. Thesis, Massachusetts Institute of Technology, Cambridge, Massachusetts, June 1964.

2. Harrow, G. A., Orman, P. L., "A Study of Flame Propagation and Cyclic Dispersion in a Spark-Ignition Engine," Proceedings of the Fourth Symposium, ASME, Crenfield, July 1965.

3. Karim, G. A., "An Examination of the Nature of the Random Cyclic Pressure Variations in a Spark-Ignition Engine," Journal of the Institute of Petroleum, Vol. 53, n519, March 1967, pp. 112-122.

4. Barton, R. K., Kenemuth, D. K., Lestz, S. S., Meyer, W. E., "Cycle-by-Cycle Variations of a Spark Ignition Engine - A Statistical Analysis," SAE Paper 700488, May 1970.

5. Kenemuth, D. K., Lestz, S. S., "Charge Conditioning Effects on Cycle-by-Cycle Pressure Development Variations of an SI Engine," Automotive Safety Research Program, Report No. 36, The Pennsylvania State University, March 1970.

6. Land, M. L., "Performance and Operation of Spark-Ignited Gas Engine," Procedings Institution of Mechanical Engineers, Vol. 181, 1966-67, pp. 900-910.

7. Patterson, D. J., "Cylinder Pressure Variations, A Fundamental Combustion Problem," SAE paper 660129, January 1966.

8. Curry, S., "A Three Dimensional Study of Flame Propagation in Spark Ignition Engines," SAE Transactions Vol. 71, 1963, pp. 628-635.

9. Soltau, J. P., "Cylinder Pressure Variations in Petrol Engines," Proceedings of Automotive Division, Institute of Mechanical Engineering, London, England, Vol. 2, 1960-61, pp. 99-115.

10. Troutman, C. L., Lestz, S. S., "Exhaust Emissions and Cycle-to-Cycle Irregularities," Automotive Safety Research Program, Report No. 35, The Pennsylvania State University, June 1969.

11. Vichnievsky, R., "Combustion in Petrol Engines," Proceedings of the Joint Conference on Combustion, The Institute of Mechanical Engineers and The American Society of Mechanical Engineers, 1955, pp. 288-297.

12. Warren, J. A., Hinkamp, J. B., "New Instrumentation for Engine Combustion Studies," SAE Transactions, Vol. 64, 1956, pp. 665-677.

13. Stivender, D. L., "Intake Valve Throttling (IVT) - A Sonic Throttling Intake Valve Engine," SAE paper 680399, May 1968.

14. Peters, B. D., Borman, G. L., "Cyclic Variations and Average Burning Rates in a SI Engine," SAE paper 70064, January 1970.

15. Semenov, E. S., "Studies of Turbulent Gas Flow in Piston Engines," Combustion in Turbulent Flow, L. N. Khitrin, Editor, Proceedings of the Moscow Seminar on Combustion, Translation by The Israel Program for Scientific Translation, Jerusalem, 1963, pp. 122-151.

16. Odashima, S., Meyer, W. E., "A Study of Swirling Air Flow in a Four-Cycle Engine," Automotive Research Program, Report No. 39, The Pennsylvania State University, 1969.

17. Willis, D. A., Meyer, W. E., Birnie, C., Jr., "Mapping of Air Flow in Engines with Induction Swirls," SAE paper 660093, 1966.

18. Muller, G., "Messung des Luftdralles im Zylinder Kines Fremdangetriebenen Dieselmotors Mittels Hitzdrahtonemometer," Institut fur Verbrennungskraftmaschinen und Kraftfahrzeuge, Bericht Nr. 246, Technishne Hoschschule Munchen, September 1966.

19. Weidenmueller, M., "Geschwindigkeiten in Brennraum eines fremdangetrieben Dieselmotor," Motortechnische Zeitschrift, Vol. 31, 1970, pp. 137-144.

20. Lewis, B., Pease, R. N., Taylor, H. S., *Combustion Processes*, I. Princeton University Press, Princeton, New Jersey, 1956, p. 340.

21. Bone, W. A., Townsend, D. T. A., *Flame and Combustion in Gases*, Longmans, Green and Co., LTD., London, England, 1926, p. 244.

22. Winkler, G. L., Lestz, S. S., "An Analog-Digital System for Discriminating Exhaust Gas Sampling," Automotive Safety Research Program, Report No. 28, The Pennsylvania State University, July 1968.

23. *Thermal-System Inc. Bulletin No. 1050*, Thermal System, Inc., St. Paul, Minnesota.

24. Hienz, J. O., *Turbulence*, McGraw-Hill Book Co., Inc., New York, New York, 1959, p. 76.

25. *PDP-9 User Handbook*, F-95, Digital Equipment Corporation, Maynard, Massachusetts.

26. Stone, M. E., "Design and Implementation of a Real-Time Data Acquisition System," M.S. Thesis, Pennsylvania State University, December 1968.

27. Hilsenrath, J., et al., *Tables of the Thermal Properties of Gases*, National Bureau of Standard Circular 564, Washington, D.C., 1955.

28. Cheeseman, R., "Study and Correction of an Ignition Distributor Delivering an Inaccurately Timed Spark," M.E. 401 Research Program, Mechanical Engineering Department, The Pennsylvania State University, 1968.

29. Eschenbach, R. C., Agnew, J. T., "Use of Constant-Volume Bomb Technique for Measuring Burning Velocity," Combustion and Flame, Vol. 2, 1958, pp. 273-285.

30. Obert, E. F., Internal Combustion Engine Analysis and Practice, 3rd edition International Textbook Co., Scranton, Pa., 1968, p. 499.

31. Garner, F. H., Long, R., Ashforth, G. K., "Effect of Pressure on Burning Velocities of Benzene-Air, n-Heptane-Air, and 2,2,4-trimethylpentane-Air Mixtures," Fuel, Vol. 30, 1950, pp. 17-20.

32. Dugger, G. L., Graab, D. D., "Flame Speeds of 2,2,4-trimethyl-Pentane-Oxygen-Nitrogen Mixtures," NACA Tech. Note 2680, January 1952.

33. Hottel, H. C., Williams, G. C., Satterfield, C. N., Thermodynamic Charts for Combustion Processes, Parts 1 and 2, John Wiley & Sons, Inc., New York, New York, 1949.

34. Neville, A. M., Kennedy, B. L., Basic Statistical Methods for Engineers and Scientists, International Textbook Co., Scranton, Pennsylvania, 1964.

35. Spiegel, M. R., Theory and Problems of Statistics, Schaum Publishing Co., New York, New York, 1961.

APPENDIX A

STATISTICAL DEFINITIONS

This Appendix presents the definitions of various statistics (34,35) used to quantify the C.B.C. combustion variations. The sample statistics are the summation over N cycles of engine operation.

1. Mean Value - The sample mean value of the variable x is defined as

$$\overline{x} = \sum_{i=1}^{N} x_i/N.$$

2. Sample Variance (S^2) - The sample variance S^2 of the variable x is defined as

$$S^2(x) = (\sum_{i=1}^{N} x_i^2 - N\overline{x}^2)/N-1.$$

3. Sample standard deviation, (S).

4. Mean Deviation ($\overline{D}$) - The mean deviation, $\overline{D}$, of the variable x is defined as

$$\overline{D}(x) = (\sum_{i=1}^{N} |x_i - \overline{X}|)/N.$$

5. Coefficient of Variation (CV) - The coefficient of variation, CV, for the variable x is defined as

$$CV(x) = S(x)/\overline{x}.$$

6. Index of Variation (IV) - If a normal frequency distribution is assumed the frequency distribution of the variable x is given by

$$f(x) = \frac{1}{\sqrt{2\pi}\,\sigma} \exp\left[-\frac{(x-\mu)^2}{2\sigma^2}\right].$$

where μ is the average and σ^2 is the variance.

The index of variation is defined as the maximum of the normal frequency distribution curve

$$IV(x) = \frac{1}{\sqrt{2\pi}\,\sigma}$$

The index of variation can be determined from experimental data by constructing a histogram. The maximum value of the histogram is an estimated value of the index of variation. The index of variation has the following limits,

$$0.0 < IV(x) \leq 1.0,$$

and the higher the value of IV(x) the less the dispersion.

7. Percentile Range (PR) - The percentile range of a set of data is defined by

$$Pr(x_1 \leq x \leq x_2) = F(x_2) - F(x_1)$$

where $Pr(x_1 \leq x \leq x_2)$ is the probability that the variable x lies between x_1 and x_2 and is numerically equal to the difference in the distribution function F evaluated at x_2 and x_1.

The percentile range is a measure of the dispersion and its notation is

$$PR(x) = x_2 - x_1.$$

8. Sample Range (SR) - The range of a sample population is the difference between the largest and smallest samples. The notation for the range of x is given by

$$SR(x) = x_{max} - x_{min}.$$

9. Coefficient of Skewness (CS) - Skewness is the degree of asymmetry and is defined as

$$CS(x) = \frac{\sum_{i=1}^{N} (x_i - \overline{x})^3}{N-2} / S^3(x).$$

10. Coefficient of Kurtosis (CK) - Kurtosis is the degree of peakedness of a distribution and is defined as

$$CK(x) = \frac{\sum_{i=1}^{N} (x_i - \overline{x})^4}{N-3} / S^4(x).$$

11. Correlation Coefficient

a. Auto Correlation Coefficient (CA) - The auto correlation coefficient, CA, is the correlation of a variable x with other sample values of x. The values of the auto correlation depend on a parameter, k, which for cycle to cycle variations represents the number of cycles between the two values of x that are correlated. The definition for the variable x is

$$CA(x,k) = \frac{S^2(x,k)}{S^2(x)},$$

where $S^2(x,k) = \sum_{i=k+1}^{N} (x_i x_{i-k}) - (N-k)\overline{x}^2 / (N-k-1).$

b. Cross Correlation Coefficient (CC) - The cross correlation coefficient, CC(x,y), is the correlation between two variables x and y. The definition of CC(x,y) for a set of variables

$x_1, \ldots\ldots x_N$, and $y_1, \ldots\ldots y_N$ is

$$CC(x,y) = \frac{S^2(x,y)}{S(x)\ S(y)},$$

where

$$S^2(x,y) = \frac{\sum_{i=1}^{N} (x_i y_i) - N\overline{xy}}{(N-1)}.$$

APPENDIX B

EQUATIONS USED TO CALCULATE VELOCITY

The procedure used to calculate the air velocity from the bridge voltage, cylinder pressure and timing mark are described herein.

The crank angle corresponding to each value of the bridge voltage was determined from the timing marks which indicated tdc of the compression stroke. By counting the number of samples between each indication of tdc, the crank angle travel between each digitized bridge voltage signal was calculated using the following equation:

$$D\theta = 720./NS, \qquad (B.1)$$

where NS is the number of samples between two indications of tdc. The crank angle at which the bridge voltage occurred was then computed from the number of samples between it and tdc and the value of $D\theta$ given by Eq. B.1. The cylinder volume corresponding to each bridge voltage signal was then computed using the following relationship.

$$V(\theta) = VD\left[\frac{1}{CR-1} + \frac{L}{s} + \frac{(1-\cos\theta)}{2} - \frac{1}{2}\sqrt{\left(\frac{2L}{s}\right)^2 - \sin^2\theta}\right], \qquad (B.2)$$

where θ is the crank angle in radians with respect to tdc.

The absolute cylinder pressure, $P(\theta)$, was computed as

$$P(\theta) = P_{ic} + (v(\theta) - v_{ic})\ SFP, \qquad (B.3)$$

where v is the digitized voltage corresponding to the pressure, SFP is the pressure scale factor (psi/volt), and the subscript, ic, refers to intake valve closure.

The pressure, P_{ic}, was calculated using the mass trapped (m_{ic}) in the cylinder volume at intake valve closure. The trapped mass was calculated as the sum of the air mass remaining after exhaust valve closure and the measured air mass inducted each cycle

$$m_{ic} = m_{in} + m_{ec}, \qquad \text{(B.4)}$$

where m_{ec} is calculated by

$$m_{ec} = \frac{P_{ec}\, V_{ec}}{R\, T_{ec}} . \qquad \text{(B.5)}$$

The value of T_{ec} was taken as 575R which corresponds to the water jacket and oil temperatures. The pressure P_{ec} corresponded to the exhaust manifold pressure. The value of P_{ic} was computed using the ideal gas equation of state

$$P_{ic} = \frac{m_{ic}\, RT_{ic}}{V_{ic}}, \qquad \text{(B.6)}$$

where the temperature, T_{ic}, was the intake manifold temperature.

The mean cylinder gas temperature was calculated using the intake manifold temperature and the ideal gas law,

$$T_a(\theta) = T_{md} \text{ for } 20°\text{atdc} \leq \theta \leq 200°\text{atdc}, \qquad \text{(B.7)}$$

and

$$T_a(\theta) = \frac{P(\theta)}{P_{ic}} \frac{V(\theta)}{V_{ic}} T_{md} \text{ for } 200°\text{atdc} < \theta \leq 500°\text{atdc}. \qquad \text{(B.8)}$$

Equation B.8 assumes that no mass was lost from the cylinder volume.

Having calculated the air pressure and temperature at the crank angle at which the bridge voltage occurred, the air properties ρ_a, μ_a, and k_a, were calculated. The equations used to calculate these properties are equation fits of tabulated data (27) and the ideal gas law. These equations are

$$\rho_a(\theta) = 0.075\left(\frac{P(\theta)}{14.7}\right)\left(\frac{530}{T_m(\theta)}\right), \tag{B.9}$$

$$k_a(\theta) = 0.00406\left(\frac{T_m(\theta)}{100}\right)^{0.77}, \tag{B.10}$$

$$\mu_a(\theta) = 0.374 \times 10^{-5}\left(\frac{T_m(\theta)}{100}\right)^{0.71}, \tag{B.11}$$

$$T_m(\theta) = \frac{T_a(\theta) + T_s}{2}. \tag{B.12}$$

The velocity normal to the sensor was then calculated using King's law

$$U(\theta) = \left[\frac{\dfrac{V_B^2(\theta)R_s}{(40+R_s)^2 k_a(\theta)(T_s - T_a(\theta))} - C_1}{C_2}\right]^{1/n} \frac{\mu_a(\theta)}{d_s\ \rho_a(\theta)} \tag{B.13}$$

The constants, C_2 and n depend on the value of the numerator inside the brackets of Eq. B.13. This value was compared to the calibration value and the corresponding values of C_2 and n were used.

APPENDIX C

COMBUSTION DATA

The combustion data used to develop the correlation between C.B.C. velocity and initial burn duration variations are presented in Tables C.1, C.2, and C.3. Combustion data used to discuss the effects of engine variables are also included.

Table C.1

Combustion Data - Average Values of Pressure Development

Speed (rpm)	CR	SA (deg)	A/F	MV (in. Hg)	Torque (ft-lbf)	$\overline{P}_{max}$ (psi)	$\overline{\theta}(P_{max})$ (deg)	$\overline{\dot{P}}_{max}$ ($\frac{psi}{sec}$ x 10^{-3})	$\overline{\theta}(\dot{P}_{max})$ (deg)
					a) Direct Induction				
900	7.0	35	15.9	0.4	21.2	543	12.6	113.0	3.2
900	7.0	30	15.9	0.4	21.4	485	17.0	86.8	5.2
900	7.0	25	15.9	0.4	21.0	430	22.4	65.3	8.5
900	7.0	20	15.9	0.3	20.6	363	27.6	47.5	11.7
900	7.0	15	15.9	0.3	19.6	300	34.7	30.9	14.9
900	7.0	10	15.9	0.2	17.9	240	43.1	19.1	9.4
900	7.0	28	16.9	-4.1	24.9	518	20.7	85.8	8.1
900	7.0	36	16.1	4.2	15.5	372	19.7	59.3	5.2
600	7.0	23	15.4	0.2	23.7	522	21.2	66.5	11.1
1200	7.0	36	16.0	0.4	17.9	422	18.4	90.5	5.3
1800	7.0	52	16.6	0.2	15.5	363	18.2	101.0	2.5
600	7.0	25	16.0	1.3	20.4	435	23.1	48.6	10.0
1200	7.0	38	16.2	-3.4	21.5	522	-	126.0	-
1800	7.0	41	16.2	-3.3	19.4	423	16.8	121.0	2.2

(Concluded on next page)

Table C.1 (Concluded)

Speed (rpm)	CR	SA (deg)	A/F	MV (in. hg)	Torque (ft-lbf)	$\overline{P}_{max}$ (psi)	$\overline{\theta}(P_{max})$ (deg)	$\dot{\overline{P}}_{max}$ ($\frac{psi}{sec}$ x 10^{-3})	$\overline{\theta}(\dot{P}_{max})$ (deg)
900	7.0	25	17.7	0.2	18.5	295	30.0	35.9	8.5
900	7.0	25	16.2	0.2	21.1	420	21.8	69.6	8.1
900	7.0	25	14.5	0.2	22.3	470	17.6	87.5	6.5
900	9.0	23	15.9	0.2	23.0	483	17.4	81.2	0.4
900	10.5	15	15.9	0.2	23.1	478	19.4	72.9	5.4
b) Mixing Tank Induction System									
900	7.0	34	15.3	2.8	20.7	464	19.7	70.7	5.2

Table C.2

Combustion Data - Sample StandardDeviations of Pressure Development

Speed (rpm)	CR	SA (deg)	A/F	MV (in. Hg)	Torque (ft-lbf)	$S(P_{max})$ (psi)	$S(\theta(P_{max}))$ (deg)	$S(\dot{P}_{max})$ $(\frac{psi}{sec} \times 10^{-3})$	$S(\theta(\dot{P}_{max}))$ (deg)
					a) Direct Induction				
900	7.0	35	15.9	0.4	21.2	41.8	3.9	26.2	3.4
900	7.0	30	15.9	0.4	21.4	46.1	3.4	20.6	4.2
900	7.0	25	15.9	0.4	21.0	48.4	3.9	17.8	4.6
900	7.0	20	15.9	0.3	20.6	45.3	4.1	14.5	5.5
900	7.0	15	15.9	0.3	19.6	37.0	3.9	9.9	9.9
900	7.0	10	15.9	0.2	17.9	32.6	4.8	6.3	23.6
900	7.0	28	16.9	-4.1	24.9	55.6	4.2	23.0	4.7
900	7.0	36	16.1	4.2	15.5	52.6	4.4	19.3	4.4
600	7.0	23	15.4	0.2	23.7	35.2	2.7	14.9	4.0
1200	7.0	36	16.0	0.4	17.9	54.6	4.4	25.2	4.0
1800	7.0	52	16.6	0.2	15.5	72.1	5.9	38.7	6.2
600	7.0	25	16.0	1.3	20.4	37.0	3.3	11.2	4.3
1200	7.0	38	16.2	-3.4	21.5	59.9	-	33.9	-
1800	7.0	41	16.2	-3.3	19.4	70.0	8.2	38.6	8.3
900	7.0	25	17.7	0.2	18.5	51.9	4.6	12.9	11.6
900	7.0	25	16.2	0.2	21.1	41.6	3.6	15.6	4.6
900	7.0	25	14.5	0.2	22.3	37.5	3.7	17.4	4.4

(Concluded on next page)

Table C.2 (Concluded)

Speed (rpm)	CR	SA (deg)	A/F	MV (in. Hg)	Torque (ft-lbf)	$S(P_{max}))$ (psi)	$S(\theta(P_{max})$ (deg)	$S(\dot{P}_{max})$ $(\frac{psi}{sec} \times 10^{-3})$	$S(\theta(\dot{P}_{max}))$ (deg)
900	9.0	23	15.9	0.2	23.0	57.2	3.1	16.1	3.7
900	10.5	15	15.9	0.2	23.1	80.1	5.1	32.7	7.1
b) Mixing Tank Induction System									
900	7.0	34	15.1	2.8	20.7	56.9	4.5	21.6	5.5

Table C.3

Combustion Data - Correlation Coefficients of Pressure Development

Speed (rpm)	CR	SA (deg)	A/F	MV (in. Hg)	Torque (ft-lbf)	$CC(P_{max},\dot{P}_{max})$	$CC(P_{max},\theta(P_{max}))$	$CC(\dot{P}_{max},\theta(\dot{P}_{max}))$
					a) Direct Induction			
900	7.0	35	15.9	0.4	21.2	0.92	-0.82	-0.06
900	7.0	30	15.9	0.4	21.4	0.93	-0.90	0.01
900	7.0	25	15.9	0.4	21.0	0.95	-0.82	0.05
900	7.0	20	15.9	0.3	20.6	0.94	-0.74	0.12
900	7.0	15	15.9	0.3	19.6	0.94	-0.69	0.32
900	7.0	10	15.9	0.2	17.9	0.86	-0.76	0.53
900	7.0	28	16.9	-4.1	24.9	0.94	-0.81	-0.01
900	7.0	36	16.1	4.2	15.5	0.93	-0.84	0.03
600	7.0	23	15.4	0.2	23.7	0.90	-0.86	0.06
1200	7.0	36	16.0	0.4	17.9	0.94	-0.87	-0.07
1800	7.0	52	16.6	0.2	15.5	0.96	-0.61	-0.09
600	7.0	25	16.0	1.3	20.4	0.90	-0.81	0.19
1200	7.0	38	16.2	-3.4	21.5	0.94	-	-
1800	7.0	41	16.2	-3.3	19.4	0.96	-0.44	-0.01
900	7.0	25	17.7	0.2	18.5	0.95	-0.54	0.46
900	7.0	25	16.2	0.2	21.1	0.93	-0.83	0.00
900	7.0	25	14.5	0.2	22.3	0.93	-0.82	0.09
900	9.0	23	15.9	0.2	23.0	0.93	-0.37	-0.16
900	10.5	15	15.9	0.2	23.1	0.91	0.43	0.73
					b) Mixing Tank Induction System			
900	7.0	34	15.1	2.8	20.7	0.94	-0.78	0.12

APPENDIX D

The velocity data corresponding to the engine conditions used for the combustion data are shown in Table D.1. Velocity data were taken for a 7:1 compression ratio only. The data are for the averages and standard deviations of the velocity at crank angles corresponding to spark ignition.

Table D.1

Velocity Data - Averages and Sample Standard Deviations

Speed (rpm)	θ_i (deg)	MV (in. Hg)	$\overline{U}_i$ (ft/sec)	$S(U_i)$ (ft/sec)
		a) Direct Induction System		
900	35	0.4	8.74	3.75
900	30	0.4	8.55	3.72
900	25	0.4	8.74	3.85
900	20	0.4	9.01	3.86
900	15	0.4	9.20	4.00
900	10	0.4	10.20	4.52
900	28	-4.1	9.18	4.10
900	36	4.2	9.94	3.80
600	23	0.2	3.87	1.64
1200	36	0.4	13.80	6.50
1800	52	0.2	16.10	7.80
600	25	1.9	4.70	1.66
1200	38	-3.4	14.80	6.72
1800	41	-3.3	18.30	9.67
		b) Mixing Tank Induction System		
900	34	2.8	7.20	3.07

VITA

Mr. Richard K. Barton was born July 31, 1937 in Detroit, Michigan. After serving two years with the U.S. Army, from 1957 to 1959, he graduated from the University of Michigan, Ann Arbor, Michigan, in 1961 with a B.S. in Mechanical Engineering.

Mr. Barton was employed from 1961 to 1964 by the General Electric Co. as a design and development engineer. From 1964 to the present, he has been a Graduate Assistant and Research Assistant in the Department of Mechanical Engineering, The Pennsylvania State University.

Mr. Barton is a member of Pi Tau Sigma and Phi Kappa Phi. He is an associate member of Sigma Xi. He is the co-author of one paper dealing with particulate control equipment and two papers dealing with internal combustion spark ignition engines.